2016-03-01

Extracellular Matrix from Whole Porcine Heart Decellularization for Cardiac Tissue Engineering

Nima Momtahan
Brigham Young University

Extracellular Matrix from Whole Porcine Heart Decellularization for Cardiac Tissue Engineering

Nima Momtahan

A dissertation submitted to the faculty of
Brigham Young University
in partial fulfillment of the requirements for the degree of

Doctor of Philosophy

Alonzo D. Cook, Chair
Jeffery R. Barrow
John D. Hedengren
William G. Pitt
Beverly L. Roeder
Sivaprasad Sukavaneshvar

Department of Chemical Engineering

Brigham Young University

March 2016

ABSTRACT

Extracellular Matrix from Whole Porcine Heart Decellularization for Cardiac Tissue Engineering

Nima Momtahan
Department of Chemical Engineering, BYU
Doctor of Philosophy

Heart failure is one of the leading causes of death in the United States. Every year in the United States, more than 800,000 people are diagnosed with heart failure and more than 375,000 people die from heart disease. Current therapies such as heart transplants and bioartificial hearts are helpful, but not optimal. Decellularization of porcine whole hearts followed by recellularization with patient-specific human cells may provide the ultimate solution for patients with heart failure. Great progress has been made in the development of efficient processes for decellularization, and the design of automated bioreactors. In this study, the decellularization of porcine hearts was accomplished in 24 h with only 6 h of sodium dodecyl sulfate (SDS) exposure and 98% DNA removal. Automatically controlling the pressure during decellularization reduced the detergent exposure time while still completely removing immunogenic cell debris. Stimulation of macrophages was greatly reduced when comparing native tissue samples to the processed ECM. Complete cell removal was confirmed by analysis of DNA content. General collagen and elastin preservation was demonstrated by SEM and histology. The compression elastic modulus of the ECM after decellularization was lower than native at low strains but there was no significant difference at high strains. Polyurethane casts of the vasculature of native and decellularized hearts demonstrated that the microvasculature network was preserved after decellularization. A static blood thrombosis assay using bovine blood was also developed. A perfusion bioreactor was designed and right ventricle of the decellularized hearts were recellularized with human endothelial cells and cardiac fibroblasts. An effective, reliable, and relatively inexpensive assay based on human blood hemolysis was developed for determining the remaining cytotoxicity of the cECM and the results were consistent with a standard live/dead assay using MS1 endothelial cells incubated with the cECM. Samples from the left ventricle of the hearts were prepared with 300 μm thickness, mounted on 10 mm round glass coverslips. Human induced pluripotent stem cells were differentiated into cardiomyocytes (CMs) and 4 days after differentiation, cardiac progenitors were seeded onto the decellularized cardiac slices. After 10 days, the tissues started to beat spontaneously. Immunofluorescence images showed confluent coverage of CMs on the decellularized slices and the effect of the scaffold was evident in the arrangement of the CMs in the direction of fibers. This study demonstrated the biocompatibility of decellularized porcine hearts with human CMs and the potential of these scaffolds for cardiac tissue engineering. Further studies can be directed toward 3D perfusion recellularization of the hearts and improving repopulation of the scaffolds with various cell types as well as adding mechanical and electrical stimulations to obtain more mature CMs.

Keywords: heart, acellular biological matrices, extracellular matrix, automation, cardiomyocytes, induced pluripotent stem cells, differentiation, decellularization, recellularization

ACKNOWLEDGEMENTS

During my time at Brigham Young University, I have had the opportunity to work with some extremely talented and wonderful colleagues. The knowledge that I have gained through my experiences in both classroom and laboratories has been extremely valuable toward my personal and professional growth, and this would not have been possible without help and guidance from a number of people. I would first like to thank Dr. Alonzo D. Cook for accepting me into his lab as his first graduate student and providing me with the guidance, advice, and drive necessary to succeed. I would also like to thank Dr. Martin Tristani-Firouzi and Dr. Scott Cho for their generosity in providing guidance and necessary resources for conducting this research. I would also like to thank my committee members for the time that they have dedicated to meeting with me and advising on specific projects: Dr. William Pitt, Dr. Beverly Roeder, Dr. John Hedengren, Dr. Sivaprasad Sukavaneshvar and Dr. Jeffery Barrow.

I would like to thank everyone that has helped me with my studies. Undergraduate students who devoted a lot of time in the lab and helped me since the beginning of my research: Tanner Smith, Ben Romney, Christopher Russell, Arthur Castleton, Holly Howarth, Makena Ford, Brenden Herrod, Jane Lee ,Whitney King, Blake Swapp, Stefan Gentile, Jeremy Struk, Brielle Woolsey, Brady Vance, Alice Huang, Jordan Eatough, Andrew Priest, Steven Balls, Camille Brantly, Bethany Evans , Michael Stewart, Joey Bloxham, Matthew Zimmerman, Kaitlyn Johnson, Donald Pfeifer, Ryan Goodman, Kole Powell. From the mechanical engineering department I would like to thank Kevin Cole and his student Dan Carpenter who assisted with automation of the decellularization apparatus and Dr. Paul Reynolds from the department of physiology and developmental biology, for his patience and guidance with histology preparation. I would also like to thank past and present members of the chemical

engineering labs, Marjan Javadi, Nafiseh Poornejad, Brent Young and Jeffrey Nielson for all of their help during my time at BYU.

I would also like to thank everyone who helped me outside of the laboratory. Dr. Brad Bundy for giving me the opportunity to be a teaching assistant for heat and mass transfer, as well as for his time and continual career advice. Michael Standing and Dr. Jeffrey Farrer at the Electron Microscopy Facility, for accepting me to the program and providing me with valuable experience and perspective. I would also like to thank BYU graduate studies for honoring me with a graduate research fellowship award that helped fund my research.

I would like to thank my family for their support over the past few years. To my wife, Tayyebeh (Tina) Panahi, for her love, support, and resolute understanding during the long, instable hours and many nights and weekends spent in the lab. To my parents, Soroosh Momtahan and Mina Arjangi, for their love and understanding of my strange schedule, which often caused not being in contact for a long while.

In the end, from the bottom of my heart, I would like to thank The Church of Jesus Christ of Latter Day Saints, which supports BYU financially and spiritually. BYU, throughout the university has provided me the perfect atmosphere for growing spiritually and maturing mentally and I gratefully appreciate that.

TABLE OF CONTENTS

LIST OF FIGURES

LIST OF TABLES

1 LITERATURE REVIEW

Every year more than 600,000 people die of heart disease in the United States and that is 1 in every 4 deaths. Although the annual number of victims varies in different states (Figure 1-1), heart failure is the number one cause of death in the United States.

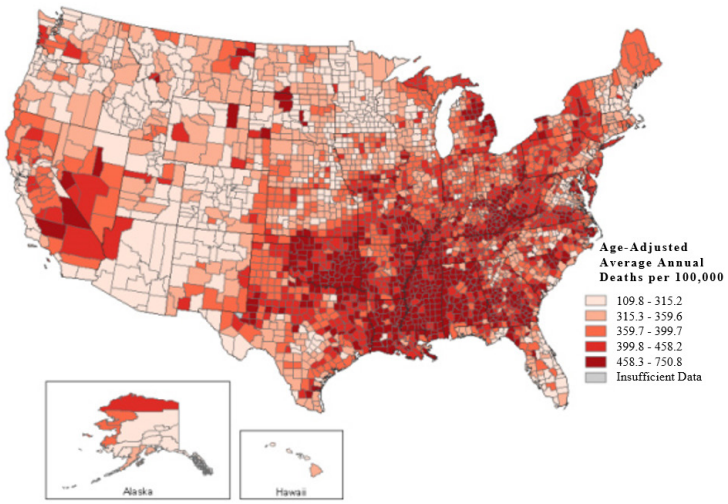

Figure 1-1. Heart disease death rates in adults more than 35 years of age 2007-2009 [1].

End stage heart disease is most commonly associated with severe coronary artery disease (CAD), cardiomyopathy, and cardiac conduction problems causing an irregular heart rhythm that creates a high risk of causing sudden cardiac death. For patients with end stage heart disease the only option is to receive a heart transplant; however, the demand for heart transplants is higher than the supply of suitable hearts. Artificial hearts also have not been able to provide an appropriate solution because of the risk for adverse immune response even with daily immunosuppression medications, and inherent thrombogenicity and blood incompatibility

problems that increase the risk of stroke and hemolytic anemia in patients receiving these hearts. Tissue engineered hearts that are created by decellularization followed by recellularization with the patient's own cells exhibit promising advantages while creating an unlimited source of donor hearts. Also tissue engineered hearts are not immunogenic, meaning they will not be rejected by the recipient's body because the natural scaffold is not immunogenic, and the cells are sourced from the same patient. Advances in research with stem cells, such as the discovery of IPS (induced pluripotent stem) cells have increased the hope to be able to create the ideal tissue engineered heart.

Whole heart recellularization has been accomplished with rat hearts and spontaneous beating of the CMs has been reported [2, 3]. However, the function of these tissue engineered hearts is not appropriate to sustain life and other issues such as thrombosis and immunogenicity are not completely resolved.

If DNA and some membrane proteins from the cells enter the body, it will initiate an immune response; therefore, decellularization is an important step in creating tissue engineered hearts. Ideal decellularization can be achieved by completely removing all cells and cell debris from the heart, while keeping the heart scaffold's vasculature intact and also preserving the important growth factors, glycosaminoglycans (GAGs) and proteins in the extracellular matrix (ECM).

Toward making tissue engineered hearts beneficial for humans, the function of these hearts must be improved and the approach used for rat hearts should be scaled up to human size hearts. Porcine hearts are similar to human hearts in terms of size and anatomy, thus they are useful for this research.

The use of decellularized porcine whole organ scaffolds combined with autologous human patient-specific cells would provide an essentially unlimited supply of organs for transplant. Great progress has been made in culturing patient-specific human cells (*e.g.,* induced pluripotent stem cells [iPSC]) and the promise of constructing a whole human organ from autologous human cells and decellularized porcine organ scaffolds is getting closer to reality [4]. The two steps in this process are decellularization of porcine organs while preserving the extracellular matrix (ECM) and recellularization with a human patient's cells. In order to fully develop this technology, there is a need to optimize decellularization processes and equipment to reliably and safely produce acellular hearts in large quantities for combination with human cells [5]. The processes for recellularization and pre-conditioning the organs in bioreactors prior to implantation also must be optimized. Finally, the organs must be characterized to make sure they are safe and meet all performance requirements.

One of the critical requirements for effective performance of recellularized blood-contacting scaffolds is the prevention of thrombosis. Thrombosis leads to the disruption or blockage of intravascular blood flow and is a consequence of uncontrolled clotting (the formation of fibrin networks) and activation of platelets due to flow disturbances and surface chemistry. The process of thrombus formation includes adhesion of platelets to surfaces, platelet aggregation, and the combination of platelets with fibrin and other cellular components. Thrombi that are released from a surface become thromboemboli, which may lodge in downstream blood vessels and interrupt blood flow to an area of tissue such as the brain, creating a stroke as cells in the brain begin to die. If anticoagulants, antithrombotics, fibrinolytics, and thrombolytics (*e.g.,* coumarins, heparin), or antiplatelet agents (*e.g.*, aspirin) are used during the implantation of recellularized organs to prevent clotting, this may result in uncontrollable hemorrhage.

Developing a reliable method for ameliorating the thrombogenicity of recellularized organs prior to implantation would be a major advance for this technology.

In reviewing the literature, numerous articles exist on the decellularization and recellularization of whole organs. These include eleven review papers on hearts, kidneys, pancreas, lungs, livers and other organs [4-14] totaling 880 citations. Of these citations, 13 papers were identified as most relevant to the design of an automated system for decellularizing whole hearts [2, 3, 15-25]. The types of detergents, concentrations of solutions, flow rates, pressures, incubation temperatures, total number of steps, and organ exposure times were identified as major factors for consideration. These parameters are summarized in Table 1-1. Based on these recommendations, an optimized porcine heart decellularization protocol was conducted with excellent results [26]. Additional papers from the review of the literature identified the best techniques to introduce cells back into the decellularized hearts, growth and differentiation factors required to control cell phenotypes, bioreactor designs, and evaluation methods that have been developed.

The overall purpose of this review chapter is to evaluate and highlight optimal strategies for decellularization, recellularization, growth factor delivery, bioreactor design, evaluation of whole organs, and prevention of thrombosis of blood-contacting porcine whole organ scaffolds. Reviewed papers on decellularization (Table 1.1) were supplemented with articles on cells available for recellularization (Table 1.2), growth factor delivery (Table 1.3), bioreactor design (Table 1.4), evaluation of tissue engineered organs (Table 1.5), and preventing thrombosis (Table 1.6).

1.1 DECELLULARIZATION

The process of decellularization begins with harvesting a heart from a heparinized animal under general anesthesia or from an animal at an abattoir immediately after exsanguination. For the latter, heparinized physiologic saline is used for antegrade coronary arterial perfusion and endothelial lavage to remove blood from the cardiac chambers. Heparinized salt solutions are typically used to remove circulating blood from the heart and to prevent coagulation in the smaller vessels. The heart may be transported at room temperature or on ice, and stored in the refrigerator or freezer for up to a year. Once initiated, the decellularization process is generally continuous, with the exchange of various fluids containing detergents or enzymes to disrupt the cell membranes and detach the cells from their underlying extracellular matrix. The detergents are then removed by washing steps. Hypotonic and hypertonic solutions may be used to further disrupt the cell membranes by osmotic shock. Sterilization may be performed prior to recellularization using antibiotics and acidic solutions. Various processes requiring different solutions, times, number of steps, or order of the reagents have been investigated as summarized in Table 1-1.

During the decellularization process, the cells are disrupted and detached from the basement membrane protein structure, or ECM. Detergents are perfused through the vascular network of the organ to solubilize cell contents and membrane components. Lipids, sugars, soluble proteins and DNA are removed. Insoluble proteins, such as collagen, laminin, fibronectin, and elastin that form the structural features remain, as well as some signaling molecules that are important for guiding tissue regeneration after recellularization. All of these changes result in a tissue construct that is uniquely modified by the process. Standardization of the process, and the use of common assays to confirm the results, are required to create a fully

functional human heart replacement. The reduction of time is a critical factor for optimization in the decellularization process, in order to limit damage to the ECM by exposure to the detergents, reduce the risk of contamination, and minimize material and labor costs.

The first report of perfusion decellularization of whole hearts was by Ott and Taylor *et al.* in 2008 [2]. In their study, they used sodium dodecyl sulfate (SDS) to decellularize rat hearts for 12 h, followed by 15 min of deionized (DI) water, then Triton X-100 for 30 min to remove SDS and renature the ECM. Phosphate buffered saline (PBS) with antibiotics was then perfused through the heart for 124 h. This group demonstrated that a rat heart could be decellularized to form an ECM scaffold that could be re-seeded with a recipient's cells and grown into a functional heart. They also compared different methods for decellularizing rat hearts using SDS, Triton X-100 and polyethylene glycol. They concluded that SDS was most effective in removing cells from the heart, but challenges remained, including removal of excess SDS from the matrix. After decellularization, they recellularized the rat heart with freshly isolated neonatal cardiac cells through intramural injection. Perfused organ culture was maintained for 8–28 days. By day 8 after cell seeding, they reported that the heart constructs showed electrical and contractile responses to stimulations and heart beats were observed.

Since the pioneering work of Ott and Taylor *et al.* [2] to decellularize and recellularize rat hearts, multiple groups have applied decellularization technology to rat (13-17), mouse [19, 20], pig [21-26] and even human hearts [5, 27-29]. For example, Sanchez and Taylor *et al.* reported the decellularization of 23 whole human hearts with SDS for 4-5 days [28]. Guyette and Ott *et al.* also reported the decellularization of porcine and human hearts [27, 29].

Table 1-1. Summary of Decellularization Protocols of Heart Tissues

Species	Pre-Decellularization Solutions	Decellularization Solutions	Post-Decellularization Solutions	Decell time (Days)	Total time (Days)	Ref #
Rat	Heparinized PBS, 10 μM adenosine	1% SDS (w/v)	DI water, 1% TX-100, Antibiotic solution	0.5	6	[2]
	PBS containing 1% Pen/Strep	8mM CHAPS , 1.8mM SDS (in 1M NaCl, and 25mM EDTA, PBS)	12% FBS endothelial growth media	2	4	[15]
	None	1% SDS (w/v)	DI water, 1% TX-100, PBS	0.8	1	[16]
	Heparinized PBS, 10mM adenosine	1% SDS (w/v), 1% SDC (w/v), 0.05% NaN_3 in DI water; 1% Saponin, 0.05% NaN_3 in DI water	20% glycerol, 0.05% NaN_3, 25mM EDTA in 0.9% NaCl, DI water, 200 IU/mL DNase, MgCl in PBS	0.5	1.5	[17]
	Heparinized PBS, chilled PBS	1% SDS (w/v) in PBS	10% DMSO in PBS	1	1	[18]
	PBS	1% SDS (w/v)	DI Water, 1% TX-100, Antibiotic solution, MCDB-131 medium	0.5	1	[3]
Mouse	DI water	1% SDS (w/v)	DI Water, 15 min, 1% TX-100, 5% Penicillin-Streptomycin in PBS, DMEM	0.5	4	[19]
	DI water, PBS, -80°C	0.2% Trypsin/EDTA; 1% SDS (w/v) in NaN_3	Peracetic acid, ethanol, PBS, DI Water	0.03	0.1	[20]
Pig	Water, -80°C	DI water, 2X PBS, 0.02% Trypsin in EDTA and NaN_3, 3% TX-100, 4% SDC, DI water, PBS	0.01% Peracetic acid, 4% ethanol, PBS	0.1	0.33	[21]
	PBS, 2% Pen/Strep, amphotericin-B	1.1% NaCl, 0.7% NaCl, 0.02% EDTA, 0.05% Trypsin, 1% TX-100, 0.1% NH_4OH	Sterile saline, 70% ethanol	3	4	[22]
	DI water, -80°C, 2X PBS	DI water, 2X PBS, 0.2% Trypsin in EDTA and NaN_3, 3% TX-100, 4% SDC, DI water, PBS	0.01% Peracetic acid, 4% ethanol, PBS	0.1	0.5	[23]
	PBS	0.1% SDS (w/v), 0.01% Trypsin, 1 mM PMSF	70% ethanol	2	18	[24]
	PBS, -80°C	0.02% Trypsin, 0.05% EDTA, 3% TX-100	None	7	8	[25]
	DI water, -20°C	DI water, 0.5% (w/v) SDS	None	1	1	[26]

CHAPS: 3- [(3-Cholamidopropyl)dimethylammonio]-1-propanesulfonate; DI: Deionized water; EDTA: ethylenediaminetetraacetic acid; PBS: phosphate buffered saline; PMSF: phenylmethylsulfonylfluoride; SDC: sodium deoxycholate; SDS: sodium dodecyl sulfate; TX-100: Triton X-100

The methods used for decellularizing human hearts were developed based on published protocols by the same authors for decellularizing hearts from rats [2] and pigs [21]. Retrograde perfusion of 1% (wt/vol) SDS through the aorta was performed after perfusing the organs with heparin solution at constant pressure of 60 mm Hg. Triton X-100 and PBS were then perfused through the hearts to complete the decellularization and remove detergents [30]. All steps were performed aseptically to prevent contamination of the organs. The sections below review the key papers that have reported results for decellularizing whole mammalian hearts.

1.2 DEVELOPMENT OF DECELLULARIZATION PROTOCOLS IN RODENT MODELS

Heart models were first developed using rodent models since large numbers are available commercially, and the small size gives better control of the decellularization environment with fewer cells required for recellularization. Fischer F344 [2, 15], LEW/crl [17], Wistar [31, 32] and Sprague Dawley [16, 18] rats, average body weight of 300 g, have been used in these studies as well as mice with average body weight of 30 g [19, 20].

One of the key concerns in the use of decellularized organs has been the recipient immune response to residual proteins, DNA and cell debris remaining in the ECM. Although ECM proteins are considered non-immunogenic for transplantation, DNA residues more than 50 ng per mg of lyophilized tissue and residual cell proteins in tissues can induce negative immune responses in the host body [23, 33]. Gui *et al.* [15] used serum nucleases to remove residual DNA from decellularized tissues. Harvested hearts from Fischer F344 rats were cut along the longitudinal and circumferential axes, then incubated with CHAPS, SDS buffers and endothelial growth media (EGM) containing 2.5 to 12% fetal bovine serum (FBS) for 22, 22, and 48 h, respectively. A significant decrease in the amount of residual DNA was observed in samples treated with FBS. Quantification of β-actin, an indicator of residual cytoplasmic proteins, was

used to evaluate treatment efficacy. From these studies, the use of detergents combined with rinses containing serum nucleases was superior in removing cell debris as indicated by the significantly lower amounts of β-actin remaining in the samples. Additional research will be required to confirm that these steps remove all immunogenic components.

In 2012, Witzenburg *et al.* [16] examined the effect of decellularization on mechanical characteristics of the right ventricles of rat hearts. Hearts were harvested from adult female Sprague Dawley rats (9–13 wks of age) with fresh hearts serving as controls for comparison to decellularized hearts treated with 1% SDS over 20 h. Strain tracking was performed within 48 h of dissection of the heart samples on a biaxial system and Verhoeff's stain was applied to examine the epicardial surface. From these tests, it was concluded that although decellularization produces quantitative differences in modulus, decellularized tissue still provides a useful model of the native tissue extracellular matrix. Further studies will be needed to confirm that decellularization processes will not detrimentally impact the mechanical structure of the porcine hearts that are similar in size and anatomy to human hearts.

Akhyari *et al.* [17] compared three published protocols [2, 21, 34] with a novel protocol developed for whole heart decellularization of LEW/Crl rats. Searching for an ideal protocol for myocardial decellularization, they introduced a protocol using SDS, sodium deoxycholate (SDC), glycerol and saponin as detergents. Examining the decellularized hearts for remaining noncollagenous proteins and residual DNA content, as well as preservation of GAGs and viability of C2C12 myoblasts after reseeding in the ECM, they concluded each protocol had its advantages and disadvantages. Comparing all four protocols it was shown that none of the analyzed protocols produced a biological matrix entirely free of donor cell material and a

scaffold with preserved ECM components. This study demonstrates the need for careful removal of cells to avoid damaging the ECM.

Crawford *et al.* [18] reported successful recellularization of decellularized Sprague Dawley rat hearts after long term cryopreservation, to determine if long intervals between decellularization and reseeding with cells might be a viable option for commercial scales. In their study, hearts were harvested from Sprague Dawley rats, flushed with 2500 units of heparin in PBS, then decellularized with 1% SDS in PBS for 24 h, and cryopreserved at -80°C with 10% DMSO in PBS. After up to 1 yr, the hearts were thawed, treated with 1% Triton-X 100 in DI water, washed with DI water, and incubated in 6.7 U/ml nuclease at 25°C for 1 h. For decontamination, the samples were placed in 0.1% peracetic acid and 4% ethanol for 20 min and soaked in medium with FBS for 1 h to prepare for recellularization. Cell seeding was then performed by injecting 2×10^7 canine endothelial cells with an 18 gauge needle directly through the myocardium at 5 mm spacing. The hearts were incubated under static conditions for 45 min and then moved to the recellularization bioreactor at 37°C and 5% CO_2, then growth medium was pumped through the heart for nine days. No DNA testing was reported for these decellularized samples to ensure complete removal of residual DNA; however, to ensure non-toxicity of the samples, canine peripheral blood progenitor cells were grown in contact with decellularized fragments in culture wells, and when compared with wells without tissue fragments, no differences in cell proliferation were observed, signifying no gross, growth-impeding toxicity. This study is an example of the successful use of cross-species cells and scaffolds. It provides encouragement for the use of porcine hearts with human cells.

Ng *et al.* used the same techniques and decellularized the hearts of 9-12 week old male FVB/N mice [19]. The decellularization was initiated with overnight perfusion of 1% SDS in

distilled water followed by washing the decellularized organ with TX-100 in distilled water for 1.5 h to remove the SDS residue. Disinfection was accomplished by perfusing the decellularized hearts with a solution of 5% penicillin-streptomycin in PBS for 72 h at 4 °C. Then the hearts were reseeded by retrograde aortic injection with 3×10^6 human embryonic stem cells (hESC) and human mesendodermal cells (hMECs) derived from hESCs. After 14 weeks of static culture in H9c2 conditioned cell medium (Dulbecco's Modified Eagle's Medium with 10% fetal bovine serum, 2 mM glutamine and 1% Pen/Strep), the hearts were implanted subcutaneously into severe combined immunodeficiency mice and then the hearts were dissected and characterized after 2, 4 and 6 weeks. They reported that the stem cells expressed cardiac specific markers such as cTnT, Nkx-2.5, Myl2, Myl7, Myh6 and CD31; however the beating function was lacking.

In another use of cross-species ECM and cells, Lu *et al.* reported the use of human iPSC-derived cardiac progenitor cells in mouse hearts [20]. The optimal decellularization procedure was completed in less than 2 h and after 20 days of culture with cardiac multipotent stem cells derived from human iPSC (Y1-iPSCs), the hearts began to beat. Differentiation into cardiac myocytes, smooth muscle and endothelial cells on the ECM was reported and it was shown that ECM stimulates the proliferation of cardiac myocytes for a longer period of time than in 3D environments without ECM. Also the effect of isoproterenol on the beating recellularized hearts was tested and demonstrated an increase in beats per minute by a factor of 2.

In summary, in studies performed in rodent models to date, whole hearts have been successfully decellularized and recellularized with endothelial cells to prevent thrombosis and heart muscle cells to produce contractility. When these hearts are transplanted, however, the pumping force of the implanted heart is not sufficient to sustain life, and the endothelialization is

incomplete, leading to potential thrombosis in the absence of anticoagulants, and the possibility of hemorrhage when anticoagulants are used.

1.3 DEVELOPMENT OF DECELLULARIZATION PROTOCOLS IN PORCINE MODELS

Although Ott and Taylor mentioned in their original report [2] the attempt to decellularize a porcine heart, they did not provide details. Several other groups have subsequently attempted the decellularization of porcine hearts [21-26]. In general, the same concentrations of detergents and solutions used for murine hearts have been used for porcine hearts. Solution volumes have been increased, but exposure times have been optimized to less than 1 day. Summaries of five different protocols for porcine hearts are given below.

In the first report of porcine heart decellularization, Wainwright *et al.* [21] attempted decellularizing a porcine heart with a complex protocol in order to achieve an intact ECM scaffold. In this procedure, the hearts were frozen at -80°C for at least 16 h for convenience of storage and to aid in cell lysis. The hearts were then thawed in type 1 distilled water (containing <0.1 mg/kg solids and <10 colony-forming units of bacteria/mL) at room temperature. The aorta was cannulated with a ½" to ¼" straight barbed reducer and connected to ¼" internal diameter (ID) silicone tubing. Each heart was placed in a 4L beaker containing 3L of hypotonic water that was recirculated using a peristaltic pump for 15 min at 1 L/min. The water was replaced with 2X PBS at 1 L/min for 15 min. Three liters of 0.02% trypsin, 0.05% ethylenediaminetetraacetic acid (EDTA) and 0.05% NaN_3 solution were warmed to 37°C using a digital hotplate and then perfused through the myocardial vasculature at 1 L/min for 2 h. A 3% Triton X-100, 0.05% EDTA and 0.05% NaN_3 solution was then used for perfusion followed by a 4% SDC solution at 1.3 L/min each for 2 h at room temperature. After each chemical solution was used as a

perfusate, type 1 reagent grade water was perfused through the heart for approximately 5 min with no recirculation followed by recirculating 2X PBS for 15 min to aid in cell lysis and removal of cellular debris and chemical residues.

Eitan *et al.* [22] decellularized 3 mm thick ring samples dissected from the left ventricle of hearts harvested from slaughter-weight female pigs. The samples were incubated for 48 h in 1% Triton X-100 + 0.1% NH_4OH in PBS solution followed by washes in sterile saline solution, followed by immersion in 70% ethanol overnight for decontamination. The effects of decellularizing a porcine heart and reseeding with adult sheep cardiac fibroblasts, newborn Sprague Dawley rat cardiac myocytes and mesenchymal stem cells on mechanical properties were examined, and these studies showed the viability and proliferation of cells from various species on decellularized samples. DNA or cell residue assays were not performed on these decellularized tissues to ensure complete removal of DNA and cell debris; however, in order to indicate the biocompatibility of these samples, they measured the stimulation of macrophages *in vitro* using basal nitrite concentration to demonstrate one aspect of their sample's biocompatibility.

Remlinger *et al*. [23] reported a whole porcine heart decellularization based on the protocol of Wainwright *et al*. Their modification was adding cycles of hypotonic/hypertonic solutions with type 1 distilled water and 2X PBS each for 10 min. They also increased the total enzyme and detergent exposure time from 6 h to 8.5 h, and increased total decellularization time after thawing the hearts from less than 8 h to more than 12 h. Using a Pico Green assay, they reported 350 ng DNA per mg of native ventricles and less than 50 ng DNA residues per mg of lyophilized decellularized heart, representing a significant decrease in residual DNA. Although DNA lengths of less than 200 base pairs (bp) and total content less than 50 ng/mg have been

proposed as acceptable threshold levels for DNA residues after decellularization [8, 35], it has not been shown that reductions in DNA levels lead to improvements in recellularization or acceptance by the host. Further work is required to demonstrate the effect of residual DNA on the performance of recellularized hearts.

Wang *et al.* [24] reported the decellularization of sections from porcine hearts in a rotating bioreactor. The bioreactor stimulated decellularized myocardium samples in square shapes both mechanically and electrically, and was used to improve differentiation of stem cells into myocardiac cells and recellularization of samples. They decellularized 20×20×3 mm myocardium sections with 0.1% SDS, 0.01% trypsin, 1 mM phenylmethylsulfonylfluoride (PMSF) as a protease inhibitor, 0.2 ug/ml RNase and 0.2 mg/ml DNase in the presence of 100 U/ml penicillin and streptomycin for 2.5 weeks, renewing the solution every 2 days. Cell viability, histology and immunofluorescence staining were performed to confirm the presence, number and phenotype of cells following reseeding. The differentiated cells expressed myosin heavy chain, cardiac troponin T and sarcomeric α-actinin, indicative of a CMs phenotype. The rotating bioreactor maintained long-term viability of cells in a sterile environment with the ability to provide mechanical and electrical stimulus.

Merna *et al.* [25] reported the use of optical imaging to predict the change in mechanical properties during decellularization of porcine hearts. Each heart was frozen at -80ºC, then thawed and decellularized with 0.02% trypsin and/or 3% Triton X-100 solutions containing 0.05% EDTA and 0.05% NaN_3 for 1 to 7 days. Multiphoton microscopy (MPM) combined with image correlation spectroscopy (ICS) were used to noninvasively characterize the mechanical properties of the hearts. It was found that Triton X-100 preserved the collagen matrix, whereas trypsin weakened the heart structure.

Some important lessons have been learned from the prior work on optimization of decellularization. For example, trypsin or other enzymes are typically used to detach cells from surfaces, including tissue culture polystyrene. In employing the use of enzymes to remove cells from the whole organ extracellular matrix, there is a concern that damage may occur to the ECM or insoluble signaling proteins. The paper by Merna *et al.* [25] showed that trypsin weakened the heart tissue more than Triton X-100. Also, DNAse was used to break up and remove the DNA that could be potentially immunogenic. Several papers have indicated, however, that the removal of DNA by detergents such as SDS and Triton X-100 is sufficient, and the presence of low amounts of DNA is not considered an impediment to recellularization or of concern for immunogenicity [9]. This conclusion was based on the studies by Keane *et al.* [36] that described similar cell behavior on fully decellularized scaffolds compared to those after incomplete decellularization. Additional work is required to verify this conclusion. Overall, while there are various methods that have been successful for decellularization, the combination of SDS and Triton X-100 appears to be the best method reported so far. SDS is a strong ionic detergent that is very effective at removal of cells, but persists in the ECM. Triton X-100 is very effective at removing SDS and remaining cell debris. In my experience, retrograde perfusion with 3 batches of SDS for 2 h each, alternating every 2 h with DI water, and then perfusing with Triton X-100 for 4 hours, followed by extensive rinsing in DI water for at least 4 hours, produces a completely decellularized porcine heart.

1.4 STRATEGIES FOR RECELLULARIZATION

The process of recellularization involves the selection and proliferation of cells, as well as the provision of nutrients, growth factors, gases and waste exchange in a bioreactor. Many cell

types [3, 19, 20, 37-62] from autologous and allogeneic sources have been proposed for use in recellularization (Table 1.2).

It may be necessary to provide co-cultures of multiple cell types, or if a pluripotent cell type is selected, it may be possible for that single cell type to differentiate into all the cell types of the heart. Early attempts to engineer heart valves identified the aortic valve interstitial cells [46], saphenous vein cells, and myofibroblasts [47] as potential cell sources. Cells that have been specifically considered for whole heart engineering include embryonic stem cells [58], skeletal myoblasts, resident adult cardiac stem cells, adipose-derived stem cells, peripheral blood mononuclear cells, bone marrow-derived hematopoietic and mesenchymal stem cells [59] to provide contractility and to produce extracellular matrix proteins during tissue repair and remodeling. CMs are required to populate the thick portions of the heart muscle; fibroblasts are required for generation, maintenance and repair of the extracellular matrix; and endothelial cells are required to line the flow surfaces. In addition, smooth muscle cells that form the walls of blood vessels and pacemaker cells that control the heart rhythm must also be reintroduced. Care must be taken to prevent contamination from bacteria and fungi during recellularization, storage and handling prior to implant. Ideally, the patient's own (autologous) cells would be used, however this would most likely require the isolation and culture expansion of cells in a facility that is capable of simultaneously handling human cells from many patients under strict controls. Alternatively, allogeneic cells could be used, but they would need to be carefully selected or may require surface modification to prevent the cells from initiating an immune response.

Table 1-2. Cell Sources for Regenerative Medicine

Species	Cell type	Comments	Ref(s) #
Murine	Transdifferentiated fibroblasts into cardiomyocytes without inducing pluripotency	Direct reprogramming may be the most promising approach	[37]
	iPSC	Immunosuppression enhances engraftment	[38]
	Transdifferentiated	Inefficient to reprogram	[39]
	iPSC	High quality iPSC differentiate better	[40]
	STAP	Low pH induces pluripotency	[41, 42]
	Cardiac telocytes	Injecting telocytes improved the function of hearts after infarction	[43]
	Neonatal cardiomyocytes, RAEC	Cardiomyocytes were injected into the decellularized scaffold, RAEC were infused through the brachiocephalic artery and vena cava of decellularized rat hearts	(17)
Murine/Human	iPSC	Viral infection and correct stoichiometry of 4 transcription factors affect efficiency	[44]
	hESC, mouse cardiac cells	Combined cells with urinary bladder matrix for cardiac repair	[45]
Porcine	Aortic valve interstitial cells	Primary cells were obtained from porcine leaflet explants and reseeded onto decellularized heart valves	[46]
Human	ESC	ESCs were differentiated into hMEC and cardiac cells in decellularized mouse hearts	[19]
	iPSC	Cells were differentiated into cardiac progenitor cells, EC, SMC and cardiomyocytes in decellularized mouse hearts	[20]
	Saphenous vein endothelial cells and myofibroblasts	Decellularized porcine heart valves were reseeded with human cells	[47]
	Stem cells	Umbilical cord matrix was proposed as a source of stem cells	[48]
	iPSC	Sendai RNA virus is efficient, and doesn't integrate into host	[49]
	iPSC	Progress toward virus-free iPSC	[50]
	iPSC	Need to increase efficiency, reduce risk of teratoma, develop methods for cell delivery	[51]
	iPSC	High purity enrichment by FACS	[52]
	CPC	Genetic modification	[53]
	iPSC	Cardiomyocytes useful for drug screening, toxicity studies	[54]
	Macrophages	Macrophages are a primary responder after myocardial infarction	[55]
	Fibroblasts	Fibroblasts are the most abundant cell in the myocardium	[56]
	Endothelial cells	A functional non-thrombogenic layer of EC on collagen was constructed	[57]
	ASC, BMMNC, MSC, ADSC, HFSC, UCSC, MDSC, EPC	Sources for stem cells	[58]
	ASC, ESC, iPSC, BMMNC, PBMNC	Many cells types are available for potential use in tissue engineering cardiac tissue	[59]
	ESC, BMAPC, MSC, HSC	Differentiation agents for hESC	[60]
	iPSC	Useful for understanding disease mechanisms, screening new drugs and cell replacement therapy	[61]
	ASC, ESC, iPSC	Describes 4 ways to engineer organs	[62]

ADSC: adipose-derived stem cell; ASC: adult stem cells; BMAPC: bone marrow-residing adult progenitor cells; BMMNC: bone marrow mononuclear cells; CPC: cardiac progenitor cells; EC: endothelial cells; EPC: endothelial progenitor cells; ESC: embryonic stem cells; HFSC: hair follicle-derived stem cells; HSC: hematopoietic stem cells; iPSC: induced pluripotent stem cells; MDSC: muscle derived stem cells; MSC: mesenchymal stem cells; PBMNC: peripheral blood mononuclear cells; RAEC: rat aortic endothelial cells

Several articles have highlighted the progress and challenges associated with culturing cells for regenerative medicine [3, 19, 20, 37-54, 58-62]. Five of these papers specifically

reviewed the use of stem cells for cardiovascular engineering [58-62]. Since these reviews were published, multiple papers have addressed the unique issues pertaining to the use of iPSC, which may ultimately be the best solution to provide patient-specific cells, but will require improvements in efficiency of de-differentiation, the elimination of the risk of teratoma formation, improved culture techniques, and novel methods for delivering the cells to the decellularized matrix.

An alternative to the use of iPSC may be the transdifferentiation of fibroblasts directly to CMs without inducing pluripotency. This has been demonstrated by Ieda *et al.* [37], in which 3 developmental transcription factors (Gata4, Mef2c, Tbx5) were found to efficiently (20%) reprogram cardiac fibroblasts into CMs in 3 days without inducing a pluripotent state. However, Chen *et al.* attempted to replicate this method with contrary results [39].

Bajpai *et al*. [58] and Jing *et al*. [60] also have reviewed the potential and challenges of stem cells for repairing damaged heart tissue. Stem cells are unique in that a certain fraction proliferate and retain their "stemness" while others differentiate. Types of stem cells include embryonic, bone-marrow residing adult progenitor cells, side population, cardiac stem cells, skeletal muscle progenitors (satellite cells), and adipose-derived stem cells. Liu *et al.* [62] described four ways to engineer organs: from a single stem cell, injecting stem cells into blastocysts, using a decellularized tissue scaffold plus stem cells, and combining stem cells with synthetic scaffolds.

There are many advantages to the use of iPSC, including the avoidance of political and ethical issues related to embryonic stem cells. The discovery of the Yamanaka transcription factors (Klf4, Sox2, Oct4 and c-Myc) has allowed many labs world-wide to study iPSC. Cell

lines are now available for many diseases and cell types [50]. Some of the challenges of using iPSC are the low efficiency, need for viral infection, and the possibility of teratoma formation [44]. IPSC from various sources demonstrate variable efficiencies. Recent reports have claimed efficiencies in the creation of iPSC of greater than 90% after enrichment through cell sorting [52]. There are also recent reports that a low pH environment may be sufficient to produce pluripotency [41, 42].

Many other investigators have examined various ways to improve the performance of cells on engineered substrates. For example, the culture environment for endothelial cells has been shown to have a major role in whether anti-thrombogenic or pro-coagulation factors are produced [57]. In addition, Le *et al.* [63] described the surface roughness needed to control protein and cell attachment. Higuchi *et al.* [64] demonstrated that heart matrix supports CMs attachment. Tosun and McFetridge [65] proposed the use of gradients to improve cell seeding, and Daly *et al.* [66] discussed the initial binding of cells during recellularization.

Recently, telocytes, a type of interstitial cell that are found in myocardium, epicardium, endocardium and in cardiac stem cell niches, were discovered. Though the functional role of these cells in myocardial tissue is not completely understood, it has been shown that they play an essential role as niche-supporting cells that nurse the cardiac stem cells and angiogenic cells in the myocardium [67, 68]. Zhao *et al.* [43] showed that cardiac telocytes can be identified using CD34 and c-kit markers as well as morphological techniques. They reported that 4 days after myocardial infarction, the number of telocytes in the heart are highly diminished, and injecting them back into the damaged hearts improved the function and reduced the size of scar tissue in the rat hearts.

In order to reduce the thrombogenicity and improve the function of the recellularized hearts, Robertson *et al.* [3] recellularized rat hearts that were decellularized based on the previous protocol described by the same group [2] with rat aortic endothelial cells (RAEC) and neonatal CMs. They infused either 2×10^7 or 4×10^7 cells to the decellularized hearts from the brachiocephalic artery (BA), aorta or inferior vena cava (IVC). During the infusion from the aorta, retrograde perfusion of media was stopped for 1 h. Alternatively, endothelial cells were infused to the heart from the BA without any breakage in the MCDB-131 media perfusion. They reported that cells delivered only via the aorta were not uniformly distributed throughout the heart and the best result was delivering the cells through the IVC and BA simultaneously. Using both BA and IVC they observed that the endocardial surface of the left ventricle was predominantly recellularized with RAECs delivered via the BA, whereas the endocardial surface of the right ventricle was populated with RAECs delivered via the IVC. After 7 days of RAEC culture, they injected 1.3×10^8 rat neonatal cardiac cells into the left ventricular wall in three to four parallel injections. One day afterwards, electrodes were sutured to the apex and base of the hearts in order to stimulate the cardiac function. After 10 days of culture, a microtip pressure catheter was inserted into the left ventricle and the pressure generation by the cells was monitored. They observed that the pressure generated by the heart, at 4 Hz of stimulation was 6 times higher in hearts that were cultured with RAECs prior to recellularization with CMs.

Challenges remain in selecting human cell types for use in cardiac tissue engineering. These include: combining cells with ECM proteins, promoting cell migration and homing to the proper location in the pre-existing ECM, ensuring electromechanical cell coupling for propagation of depolarization potentials, producing a robust and stable contractile function, and proper vascularization of the tissue [59]. Challenges also remain with the use of stem cells due to

the possibility of teratoma formation, the need to culture and maintain large quantities of viable cells, and the necessity to deliver the cells in a manner that is conducive to their survival and integration into the heart. If stem cells are combined with a decellularized matrix, there is also a need for the addition of growth and differentiation factors (Table 1.3), bioreactors designed to properly condition the heart so it is ready for transplant (Table 1.4), evaluation of the heart prior to implant (Table 1.5), and methods to integrate the heart into the body so it can perform its function. Another major challenge is the prevention of thrombus formation (Table 1.6).

1.5 GROWTH AND DIFFERENTIATION FACTORS

Soluble trophic factors may be delivered during the growth of the tissues to promote differentiation or proliferation. Generally fetal bovine serum is added in cell culture, although the elimination of as many unknowns as possible has led multiple researchers to develop xeno-free formulas of cell media. In the case of adding growth factors to the porcine hearts, testing of the combination of factors and possibly their sequence of administration will be necessary to identify potential regeneration factors and eliminate immunogenic factors. Some of the growth and differentiation factors used in tissue engineering [20, 69-77] are listed in Table 1-3.

Critical factors [78] that have been identified for evaluation include basic fibroblast growth factor (bFGF) [20, 69], transforming growth factor beta 1 (TGFβ1) [70, 71], vascular endothelial growth factor (VEGF) [20, 72], hepatocyte growth factor (HGF) [72], platelet-derived growth factor (PDGF) [74, 75], bone morphogenetic protein (BMP) [76], and angiopoietin-1 [77].

Table 1-3. Growth and differentiation factors

Factor	Purpose	Comments	Ref #
BMP-4, Activin A, bFGF, VEGF, DKK1	iPSC-derived cardiac progenitor stem cells, endothelial cells, smooth muscle cells and cardiac myocytes differentiation	Cardiac progenitor stem cells were derived from iPSC in culture flasks and then differentiation into various cardiac cells was done in the accellular ECM of a mouse heart	[20]
bFGF	Induces the proliferation of endothelial cells, fibroblasts, smooth muscle cells, and hepatocytes	bFGF was released from alginate with initial 40% burst followed by sustained delivery, increasing vascularization of alginate scaffold	[69]
TGFβ1	Mediator of inflammatory and fibrotic response	Mediates the cardiomyocyte proliferation and production of ECM by fibroblast	[70, 71]
VEGF	Regulates new vessel growth	PEG scaffolds releasing VEGF were completely remodeled into vascularized tissue	[72]
HGF	Mitogen of hepatocytes, increases proliferation of endothelial cells but not vascular smooth muscle cells	HGF bound by a collagen binding domain from fibronection was released from a collagen sponge, increased vascularization	[73]
PDGF	Multiple roles in growth of fibroblasts, SMC, and glia cells; also implicated in various diseases	PDGF was shown to be effective in periodontal regeneration	[74, 75]
BMP	Critical to development and differentiation of cells to cardiomyocytes	Fibroblasts were found to differentiate into cardiomyocytes by BMP	[76]
Angiopoietin-1	Regulates vascular integrity and quiescence	Provides a connection between quiescient and active endothelial cells	[77]

bFGF: basic fibroblast growth factor; BMP-4: bone morphogenetic protein-4; DKK1: Dickkopf-related protein 1; HGF: hepatocyte growth factor; PDGF: platelet-derived growth factor; TGFβ1: transforming growth factor beta 1; VEGF: vascular endothelial growth factor

The temporal and spatial distribution of the factors is important, and encapsulation or controlled release strategies of the factors may be required. Lee *et al*. [79] found that synthetic

particles that released VEGF in response to mechanical stress could control blood vessel density in newly forming tissue.

Freeman *et al* [80] demonstrated that the release of bFGF from alginate hydrogels doubled the formation of blood vessels, and Harel-Adar *et al.* [80, 81] showed that modulation of cardiac macrophages by phosphatidylserine-presenting liposomes improved infarct repair.

1.6 BIOREACTOR DESIGNS

Pre-conditioning of the organ with a physiologically relevant set of conditions must be performed prior to implant. Bioreactors that can operate in a range of temperatures, from room temperature to 37°C, allow for gas exchange, and provide nutrients during the growth phase have been designed [82]. For hearts, the muscle must be allowed to grow and organize, and then be subjected to flow conditions that mimic normal blood flow dynamics in order to strengthen the muscle until it can perform its function of pumping with the appropriate force. One particular challenge with hearts is incomplete perfusion due to trabeculated atrial appendages that are potentially difficult to perfuse. For example, the left atrial appendage (LAA) has a narrow, sharply pointed shape. It is believed to function as a decompression chamber during left ventricular systole and other periods when left atrial pressure is elevated, and it has endocrine function as the primary source of atrial natriuretic factor (ANF). In contrast, the right atrial appendage is broad-based and less distinct in appearance, with trabeculations (pectinate muscles) that extend toward the tricuspid valve and are not confined to the appendage [83]. Al-Saady *et al.* [84] posited that obliteration or amputation of the LAA may help reduce the risk of thromboembolism in patients with primary cardiac disease, but this may result in undesirable physiological sequelae such as reduced atrial compliance, reduced secretion of ANF in response to pressure and volume overload, and decreased stroke volume and cardiac output that may

promote heart failure. Bioreactor designs must be robust, and potentially may need to include sensors to detect flow rates and pressures to provide a means to compensate for changes related to the presence of atrial appendages, while optimizing flow to help minimize thrombogenesis.

Several investigators have proposed various designs [2, 31, 85-87] for bioreactors (Table 1.4). Bioreactors that are able to create high pressure at the coronary arterial orifices should be used to ensure that the atrial appendages will have sufficient flow in the vessels so that they can be decellularized and recellularized completely.

Decellularization is often performed in a modified Langendorff apparatus [2] with retrograde perfusion preferentially used over antegrade flow. Geeslin *et al.* [86] discussed the bioreactor designs for vascular conduit regeneration, including duel reservoirs for endothelial cells and smooth muscle cells. These were connected in parallel with pumps and oxygenators. The smooth muscle cells were cultured on the exterior of a decellularized matrix, while the endothelial cells were cultured on the lumen. Avci-Adali *et al*. [87] discussed a rotating bioreactor based on ready-to-use medical disposables to re-endothelialize a vascular conduit. Their results demonstrated that ePTFE grafts with albumin and heparin coatings produced the most extensive endothelial cell adhesion and spreading.

Bursac *et al.* [85] discussed rotating bioreactors for culturing CMs in 3D cultures. They found that cells cultured in 3D created better tissue than in 2D monolayers. Huelsmann *et al.* [31] applied the concept of 3D stretching to provide mechanical stimulation to a whole decellularized heart matrix from Wistar rats. Their device included an inflatable latex balloon inserted into the left ventricle and inflated by a syringe pump, and was controlled with a pressure sensor and LabView software. Hearts seeded with C2C12 murine myoblasts were cultured for 24 h in static

culture, and with biomechanical stimulation for another 72 h. Although the results demonstrated lower cell viability, there was an improvement in orientation of cells in the exercised hearts. Further work will be required to optimize the development of bioreactors for whole porcine hearts.

Table 1-4. Bioreactors

Size	Media	Comments	Mechanical Specification	Estimated Cost	Ref #
250 mL (whole rat heart)	Decell: SDS, SDC, NaN_3, Saponin Recell: FCS, DMEM	O_2, CO_2, N_2 in a gas mixer with chamber controlled pH. Mechanical stimulation improves cell alignment.	Left ventricular 3D stretching latex balloon, controlled with pressure and a membrane pump	$10,000	[31]
	Decell: SDS, TX-100 Recell: IMDM, FBS, HS	O_2,CO_2, electrodes for stimulation of cardiomyocytes, recording ECG and pressure	Pulsatile flow from peristaltic pump, Controlled pressure and flow	$70,000	[2]
100 mL (biopsy of porcine heart)	Recell: DMEM, 10% FBS, HS	CO_2, electrical stimulation and ECG recording	Rotating bioreactors were used to culture cardiomyocytes in 3D	$10,000	[85]
40 mL (rat aorta)	2 reservoirs for external media and internal media	Small rotating bioreactor that can be put in CO_2 incubator	Pulsatile flow	$5,000	[86]
1-2 mL (small vascular grafts and stents)	VascuLife EnGS EC culture media	Can be put in CO_2 incubator, not suitable for long cultures because of no media perfusion	Rotated culture at 5 rpm, no perfusion	$3 per device	[87]

DMEM: Dulbecco's Modified Eagle's Medium; EC: endothelial cell; EnGS: endothelial cell growth supplement; FBS: fetal bovine serum; FCS: fetal calf serum; HS: horse serum; IMDM: Iscove's Modified Dulbecco's Medium; SDS: sodium dodecylsulfate; SMC: smooth muscle cells; TX-100: Triton X-100

1.7 EVALUATION OF ORGANS

Each type of recellularized organ (kidney, lung, heart, etc.) will require a different set of tests to evaluate its functional performance prior to implant. For example, the proper performance of kidneys will require that the cells filter blood and create urine. Lungs will require

that the cells exchange oxygen and carbon dioxide with circulating blood. Hearts must be pre-conditioned to pump blood at physiologically relevant pressures and flow rates. Although bioengineered recellularized organs may eventually be able to perform desired endocrine functions, this physiologic property must be secondary, and is expected to be sacrificed during the development of transplantable organs with adequate biomechanical function to sustain life. Nevertheless, across all of these organs, the flow surfaces must be prepared for contact with blood. Endothelial cells naturally perform the function of preventing thrombosis. The logical goal of whole organ recellularization, therefore, is to fully cover every blood-contacting flow surface with endothelial cells. Assuring that the blood-contacting flow surface has been thoroughly re-endothelialized will require the development of strategies to measure endothelial cell viability, coverage and functional performance in prevention of thrombosis, in addition to other analytical tests.

Analytical methods have been identified to detect proteins [15, 17, 18], cellular debris, and DNA content after decellularization [2, 3, 15, 17, 21, 23]. Research has also been done on the evaluation of mechanical characteristics after decellularization and recellularization [2, 15, 16, 21, 22], demonstrating the potential for strengthening the muscles prior to implant. In addition, Jungebluth *et al.* [88] has demonstrated a viability assay for cells prior to transplantation. These strategies are summarized in Table 1-5.

1.8 STRATEGIES FOR PREVENTING THROMBOSIS

During the development of vascular grafts, intracoronary stents, the total artificial heart, and other blood-contacting medical devices, many strategies have been proposed for preventing thrombosis, including delivery of anticoagulants, the attachment of endothelial cells [3, 89-95] [96-98], attachment of heparin [99], the creation of non-fouling surfaces [100-103], and other

approaches. The use of anticoagulants (*e.g.,* heparin) in the systemic circulation can be used to prevent acute thrombosis, but may lead to hemorrhage over the long-term, and are not included in this review. The other strategies are summarized in Table 1-6 and described in detail below.

Table 1-5. Evaluation Methods

Type of Analysis	Method	Criteria for Success	Ref #
Protein	Cytoplasmic protein (*e.g.* β-actin) removal as detected by immunoblotting	Residual cytoplasmic proteins should approach 0%	[15]
	Noncollagenous protein content, including laminin and elastin, detected by histology staining and Western blotting	Less than 7% of native non-collagenous proteins retained	[17]
	Monitor total protein content in the effluent	Approach 0% after 6 hours	[18]
GAG	Total glycosaminoglycan (GAG) content	More than 200-250 μg/g preserved	(15)
DNA	Quant-iT PicoGreen dsDNA assay after using serum nucleases to remove DNA	Residual DNA was 0%	[15]
	DNA labeling with fluorescent markers	Less than 4% remains	[2]
	DNA quantification kit (Qiagen, Hilden, Germany)	Less than 3 μg/g (0.5%) of native DNA remained	[17]
	Quant-iT PicoGreen dsDNA assay	Less than 8% remains	[21]
Mechanical	Burst pressure of human umbilical arteries	No significant difference in burst pressure of blood vessels after decellularization	[15]
	Stress-strain test	Very similar to native	[2]
	Ball burst test	Maximum force endurance the same as native	[21]
Cell Viability	Colorimetric method for testing tissue engineered tracheas prior to implant	Average cell coverage of 40%	[88]
	Live/Dead Assay after 24 culture with C2C12 myoblasts	>95% cell viability	(15)

The process of preventing thrombosis is closely related to strategies for recellularization. If endothelial cell coverage could be perfectly achieved, and inflammation during healing at the anastomoses could be minimized, then theoretically thrombosis could be avoided. Kasimir *et al.* [89] described the decellularization of porcine heart valve matrix with Triton X-100 and SDC

(sodium deoxycholate). The scaffolds were then recellularized with human umbilical vein endothelial cells (HUVEC) and tested with human platelets from volunteers. Platelet adhesion and activation were measured and antibodies to collagen and elastin were used to characterize the material. It was found that the decellularized scaffold was a platelet-activating surface. However, seeding the surface with endothelial cells abolished platelet adhesion and activation. They concluded that endothelial cells are essential to prevent thrombosis. Kasimir *et al*. [90] then tested Synergraft valves (porcine) vs. Triton X-100 decellularized grafts. Important factors that were identified included the α-gal epitope, monocyte migration, calcification of glutaraldehyde cross-linked valves, and the need for complete coverage by endothelial cells to prevent platelet activation, since platelets recruit leukocytes and express chemokines and cytokines that activate monocytes, leading to inflammation. The removal of the α-gal epitope, present on the surface of porcine vascular endothelium, is important since α-gal activates the classical complement pathway, resulting in hyperacute rejection and graft failure. In addition, other glycosaminoglycans (GAGs) can interact with cytokines and chemokines and may also need to be eliminated to avoid an inflammatory or immune response.

Alternatively, GAGs may need to be preserved to properly attach the endothelial cells. The GAGs are part of the local environment surrounding each cell, called the pericellular matrix (PCM). The PCM may need to be reconstituted with the appropriate GAGs and proteins to retain adhesion molecules and insoluble signaling molecules while also removing the immune activating molecules. McLane *et al.* [94] discussed the role of the pericellular matrix on chondrocytes and methods to noninvasively measure the ultrastructure of the hydrated zone that extends 100 to 500 nm from the cell surface. It was concluded that the PCM mediates cell interactions with surrounding tissue, and may influence important processes such as cell

adhesion, mitosis, locomotion, molecular sequestration, and mechanotransduction. In reestablishing the PCM for cardiac cells, care must be taken to first provide a nominally non-thrombogenic or non-fouling surface. The CMs and endothelial cells can then be added. If there is a break in coverage of the endothelial cells, the platelet adhesion and activation may be mitigated by the non-thrombogenic constituents despite the presence of the underlying thrombogenic extracellular matrix. Lichtenberg *et al.* [91] decellularized pulmonary valves using detergents, and DNAse I to remove greater than 95% of the DNA. In the decellularized structures, collagen, elastic fibers, GAGs and basement membrane were all preserved. It was hypothesized that the absence of endothelium may predispose the matrix surface to thrombosis. Adhesion ligands (collagen IV, laminin, and perlecan) in the basement membrane were thought to attract circulating endothelial cells or progenitor cells which covered the pulmonary valves. They provided evidence that preservation of GAGs followed by reendothelialization can prevent thrombosis and hyperplasia of tissue engineered blood-contacting structures.

Another approach has been to reattach specific GAGs to the blood-contacting surface. For example, heparin attached to expanded polytetrafluoroethylene (ePTFE) vascular grafts has been successful in preventing thrombosis [99]. The trade-off between controlling thrombosis with systemic heparin, and preventing the natural healing response at the anastomoses and pseudointimal hyperplasia in the lumen of the implant has always been a challenge for vascular grafts. Propaten® vascular grafts successfully prevent early thrombosis due to the covalent end-point heparin attachment method developed by Carmeda® and the high concentration of heparin attached to the surface. Ye *et al.* [92] proposed the use of a polyelectrolyte multilayer film on decellularized porcine aortic valves to prevent thrombosis. The alternating layers of heparin and chitosan provide another method of attaching heparin to the surface to prevent the initiation of

thrombosis. A non-thrombogenic underlayer could provide a safety factor against thrombosis if the endothelial cell layer is incomplete or disrupted during initial or long-term use.

The use of *in vitro* endothelialization [96] is another proposed way to prevent thrombosis in tissue engineered and synthetic vascular grafts. However, attempts to endothelialize vascular grafts have generally been unsuccessful due to the cost and complexity of maintaining living grafts during shipping and storage. Several strategies have been employed to increase endothelial attachment. For example, fibronectin was added to decellularized aortic grafts to accelerate reendothelialization and prevent thrombosis [97]. Wissink *et al.* developed a new method for collagen crosslinking using N-(3-dimethylaminopropyl)-N'-ethylcarbodiimide (EDC) and N-hydroxysuccinimide(NHS) in order to improve endothelial cell seeding on human umbilical veins [98]. Lord *et al.* [100] proposed the use of perlecan (which is the main heparan sulfate proteoglycan secreted by endothelial cells) to reduce thrombogenicity and demonstrated that perlecan did not permit aggregation of platelets when the heparan sulfate chains attached to perlecan were intact. Elastin has also been proposed as a non-thrombogenic material [101]. Other non-fouling synthetic materials, including polyethylene oxide (PEO), have been proposed [102]. Similarly, Smith *et al.* [103] at Semprus® Biosciences (a division of Teleflex) developed a technology to attach sulfobetaine molecules to the surface of blood-contacting devices that minimizes thrombus formation. The Semprus® technology employed zwitterionic sulfobetaine molecules that coordinate water near the surface of blood-contacting catheters to create a non-fouling surface. Both bacteria and platelets were prevented from attaching. All of these approaches to improve reendothelialization could be considered for adaptation to decellularized organs. Each approach would require further optimization, and may require new chemistry and process conditions to provide benefit without damaging the ECM.

It may also be possible to genetically modify the cells that are used for recellularization to be more thromboresistant. For example, Kader *et al.* demonstrated that overexpression of endothelial nitric oxide synthase (eNOS) by endothelial cells produced anti-thrombotic conditions and decreased platelet aggregation by 46% [95]. Alternatively, some have proposed that it may be possible to implant decellularized tissues into the recipient's body without the need for reendothelization. Assmann *et al.* [32] dissected thoracic aortas from Wistar rats and decellularized them with four 12-h cycles of 0.5% SDS + 0.5% SDC and then rinsed the aortas with distilled water for 24 h to wash off the detergents. The aortas were then rinsed with three 24-h cycles of 1% penicillin/streptomycin in PBS. These engineered grafts were implanted in recipient rats and connected to their circulatory system. After 8 weeks they extracted and examined the samples and reported a confluent luminal cell layer, purportedly from circulating cells in the peripheral blood. Although this approach is promising, it has not been shown that these results can be extrapolated to smaller blood vessels (<4 mm) where artificial grafts have consistently failed due to thrombosis and hyperplasia.

In order for reendothelialization to be effective, the specific attachment of endothelial cells to the surface may be required, while avoiding the attachment of platelets. Insoluble signaling proteins such as fibronectin are believed to be required in order to reestablish correct spatial orientation of cells during recellularization. Specific sequences of amino acids, such as arginine-glycine-aspartic acid (RGD) peptides from fibronectin, are involved in cell attachment, and if disrupted, may not permit proper positioning of the new cells on the matrix. Bellis [93] recently reviewed the use of RGD peptides for directing cell attachment. In the late 1980's on through the 1990's, a number of labs were successful in attaching RGD peptides to a variety of surfaces to promote endothelialization [102, 104-109]. Although the first approach for specificity

in the attachment of endothelial cells to synthetic matrices was based on the use of RGD peptides, these peptides were found to be non-specific and also bound platelets in addition to endothelial cells. In addition, although RGD peptides have been shown to promote the attachment of cells *in vitro*, once a surface is exposed to blood the surface is rapidly remodeled and covered by circulating proteins (Vroman effect). Therefore, combining peptides that promote the adhesion of endothelial cells with non-fouling surfaces or non-thrombogenic molecules may be a more likely way to succeed. The creation of a non-fouling, non-thrombogenic surface followed by RGD, YIGSR, GFOGER, cyclic RGD, REDV, or other specific peptides to attach endothelial cells has been proposed [93]. This approach will require further investigation. To be successful, cells should attach, integrate, promote regeneration, and be interactive and biomimetic. Multiple modification steps with various molecules may be needed to achieve all of these objectives.

It is clear that in order to advance the field of whole organ decellularization and recellularization, there are many possible ways to accelerate the processes, and there are many variables that can be optimized. In the pioneering work of Ott and Taylor [2], an *in vivo* animal model assay was used to test the performance of bioengineered hearts. It would be cost prohibitive to test all the possible combinations of seeding strategies and to compare all of the other variables in animal models. Therefore, rapid, reliable, and relevant *in vitro* assays that are amenable to whole organ testing will be essential tools to investigate the various strategies for recellularization and thrombosis prevention. The multiple modalities, blood components, and conditions that affect thrombus formation on a surface necessitate concomitant sophistication in the test methods to assess this phenomenon. For example, coagulation may be more pronounced in areas of low flow and stagnation (*e.g.,* atrial appendages) while platelet activation, adhesion,

and aggregation may be elevated in regions of high shear (*e.g.,* coronary arteries). Thus, assessment of whole organ performance may require a diverse panel of tests to identify specific problems that will help expedite development of a non-thrombogenic organ. The ISO 10993-4 standard prescribes such a panel of *in vitro* tests for the assessment of blood-contacting device hemocompatibility [110] that may serve as a useful guide when adapted suitably for whole organ thrombosis assessment. Assessments of fluid phase markers of coagulation cascade activation (*e.g.,* thrombin-antithrombin ELISA) and platelet activation (*e.g.,* β-Thromboglobulin ELISA, p-selectin expression by flow cytometry) are some of the recommended tests [111]. Evaluation of surface-bound platelets and thrombus using radiolabeled platelets and scanning electron microscopy are highlighted as important tests [112]. The roles of the complement pathways and leukocytes in thrombosis have also been recognized and associated assays are considered valuable [113].

In addition to the tests outlined in the ISO 10993-4 standard, several other test models have been reported in the literature. Hanson and Sakariassen [114] reviewed the experimental models of thrombosis used to measure antithrombotic drug efficacy. They demonstrated that flow of the blood in a circuit can also activate platelets. Shankarraman*, et al.* [115] have utilized thromboelastography to quantify thrombogenicity of blood-contacting surfaces. *In-vitro* blood flow models have been used to assess thrombosis and thromboembolism associated with artificial hearts and vascular implants such as stents [29, 111, 112, 116, 117]. Ensley and Nerem [118] studied the effects of shear stress on performance of endothelial outgrowth cells. McGuigan and Sefton [57] seeded human umbilical vein endothelial cells (HUVECs) on collagen and developed thrombogenicity assays using whole fresh blood from consenting donors.

They perfused constructs with blood, demonstrating that HUVECs prevented the attachment of platelets.

In the first report of measuring thrombogenicity in decellularized whole organs, Taylor's research group has shown that recellularizing rat hearts with RAECs prior to adding neonatal CMs decreases the thrombogenicity and improves the beating function of the heart [3]. In order to measure the thrombogenicity of the recellularized organs, they examined protein C activation as an indicator for activation of the anticoagulation pathway. After 7 days of RAEC culture they observed a 6 to 8 fold increase in thrombomodulin and protein C activity in recellularized hearts compared to acellular hearts. They also performed a heterotopic transplantation of the re-endothelialized hearts into recipient rats that were on anti-coagulation therapy with 100 IU/kg sodium heparin on the day of transplant and 200 IU/kg sodium heparin subcutaneous for the next two days and daily coumadin (0.25 mg/kg) in the drinking water. After 7 days the hearts were dissected and they reported the observation of fewer blood clots in the aortas and ventricles of the re-endothelialized hearts compared to acellular hearts. They also observed the presence of endothelial cells in acellular hearts that were not recellularized with RAECs before transplantation.

Thrombogenicity of the decellularized and recellularized whole hearts can be assessed using bovine blood with an assay [119] that has become a standard performance measurement for the medical device industry. In this *in vitro* flow model of thrombogenicity, suitably anticoagulated bovine blood is pumped through the heart at a controlled flow rate. The thrombus that forms in the heart is characterized after a period of blood flow by high resolution digital photography and measured by radiolabeled platelets that accumulate in the thrombus. Scanning electron microscopy of select regions is also used to investigate the morphology of thrombi and

to understand their origin and progression on the test surfaces. One of the unique features of studies conducted with advanced *in vitro* flow models is that relevant conditions can be controlled more precisely than is possible in animal and clinical studies [120]. Parameters that significantly influence thrombosis such as hemostatic conditions (*i.e.,* anticoagulation) can be controlled precisely in the *in vitro* setting. Yet another benefit of an *in vitro* setting is the ability to directly quantify thrombosis (*e.g.*, with Indium-labeled platelets). In future studies, the *in vitro* blood flow model can be used to assess thrombogenicity of tissue engineered hearts and test the effect of various decellularization process conditions and cell sources.

For these studies, fresh blood is obtained by inserting a cannula directly into the heart of cows during exsanguination at a local abattoir and collected into a collapsible reservoir containing an anticoagulant (heparin or sodium citrate). The negative controls in these studies are fully decellularized hearts that would be expected to have a very high amount of thrombus formation. The positive controls are freshly harvested hearts prior to decellularization that would be expected to have a low amount of thrombus formation. The test hearts are decellularized under various conditions, modified with non-thrombogenic molecules, and optimally recellularized with endothelial cells. Test hearts are attached to appropriate polymer tubing whose tips are inserted into the blood reservoirs (maintained at 37^{o}C) to complete the flow circuit. Roller pumps control blood flow at a desired flow rate, and this is monitored non-invasively using an ultrasonic flow probe. The blood collected from a single animal is divided into multiple blood reservoirs (as many as there are hearts to compare simultaneously). Incomplete endothelialization may be detected via this *in vitro* assay, as long as contact of blood from one animal with endothelial cells from another animal does not lead to immune-response mediated thrombosis or other confounding adverse responses. Preliminary studies have shown

that this method can distinguish differences between decellularized and freshly harvested porcine hearts [26]. Additional experiments will be needed to test the thrombogenicity of hearts after recellularization.

Studies can also be conducted with recalcified citrated blood flowing through the heart at a lower flow rate (*e.g.,* 1 L/min) for a shorter duration (*e.g.,* < 30 min) to focus the assessment on coagulation. Other studies can be conducted with heparinized blood flowing through the heart at a higher flow rate (*e.g.,* 3 L/min) for a longer duration (*e.g.,* 2-3 h) to focus the assessment more on platelet-mediated thrombosis. Assessment of plasma markers of complement activation, platelet activation, and inflammation can also be conducted with human hearts and human blood. While *in vitro* tests of thrombosis and associated markers are valuable tools, direct extrapolation of *in vitro* results to the *in vivo* setting may not be possible, and the relevance of certain *in vitro* tests is still being debated [120, 121].

1.9 DISCUSSION

One of the goals of tissue engineering research with decellularized whole organs is to adapt the published protocols for decellularization of blood-contacting scaffolds for automation and scaling to whole porcine hearts. Other goals include the development of strategies for recellularization, growth factor delivery, bioreactor design, quality analysis, and measurement of thrombogenicity *in vitro* prior to implantation. The possibility of using decellularized whole porcine hearts combined with human cells to create viable hearts for transplant is getting closer to reality [4]. Porcine hearts are similar to human hearts in size and anatomy, and the use of porcine heart valves in humans has a long history of success [122]. The development of the

decellularization process in rats [2, 29] has been successfully scaled to porcine hearts [21, 123]. Optimizing the decellularization process further will potentially limit damage to the ECM. Since the ECM signals modulate inflammatory and reparative pathways, these signals affect cell survival phenotype and also gene expression [124]. Expediting the decellularization process will also reduce the risk of contamination and reduce the cost of reagents and labor. In reviewing the literature, I found many papers that described decellularization methods, but very few that described the optimization and automation of recellularization and decellularization strategies to prevent thrombosis in whole organs.

This scope of this review chapter covered the progress that has been made to decellularize whole hearts, including rodent, porcine and human hearts, since the first attempt was reported in 2008 [2], as well as the methods for preventing thrombosis in medical devices. Many variables have been studied for the process of decellularizing whole hearts, including various detergents, concentrations, rinses or washes, flow rates, pressures, and times. This review chapter highlights the most important parameters for optimization in future efforts to automate decellularization and recellularization processes, and prevent thrombosis of blood-contacting organs. I also described a method for the assessment of these strategies through the use of an *in vitro* blood flow thrombogenicity assay [119].

In addition to the previous articles that have been reviewed in this chapter, much can be learned from the history of decellularization of porcine heart valves and small intestine submucosa (SIS), which have been approved as commercial products. Several review articles have been written on these products. For example, Badylak *et al.* have reviewed the development of SIS [33, 125-127] and also recently reviewed whole organ decellularization [125] and the use of porcine bladder [128] for use as a matrix. Gilbert *et al.* [6] reviewed the decellularization

process for tissues and organs, focusing primarily on the development of SIS. The use of mechanical agitation, sonication and osmotic shock with hypertonic/hypotonic solutions were discussed. SDS and Triton X-100 were proposed as detergents that could be used. A call was made for the development of assays to determine the extent of decellularization.

Stem cells are a possible strategy for recellularization, since they are pluripotent, and may be guided to differentiate into a variety of cell types. Use of iPSC has been proposed since they could be patient-specific, but still have pluripotency. The efficiency of creating iPSC is improving, and the use of environmental cues may eliminate the need for the viral introduction of transcription factors [41, 42]. Transdifferentiation may be a better strategy than using iPSC, since transdifferentiation may decrease the risk of teratoma formation associated with inducing pluripotency. At the very least, the iPSC must be shown to be terminally differentiated prior to implantation, as has been done by Advanced Cell Technology, Inc. (ACT), in a human clinical trial using terminally differentiated human embryonic stem cells (hESC) for treating dry age-related macular degeneration [129].

Although it was not the focus of this review chapter, other strategies have been proposed for culturing cells into 3D structures without the use of decellularized scaffolds, mimicking embryological development. Although the initial development of organs during embryonic formation does not require the introduction of a separate scaffold, the size of these organs is very small relative to an adult organ. The embryological organs create their own extracellular matrix as they develop. As a child grows and matures into an adult, all of the organs constantly remodel and replace the smaller versions with larger organs. This provides a rationale for growing new hearts using neonatal or adolescent cells.

The source of cells may be autologous or allogeneic. Ideally, the cells will be autologous, but there may be situations in which autologous cells are not preferred. For example, one may not want to use an elderly patient's cells for recellularization, especially if they are diseased. Even patient-specific stem cells may not be good candidates to recellularize a bioengineered heart for transplantation in individuals with systemic disease. As cells age, they lose their youthfulness, purportedly due to telomere shortening [130]. Juvenile cells that have many years of life ahead of them could be a great source for recellularization. It may be preferable to grow a heart with a younger patient's cells, if they are properly immunologically matched. Cells could be isolated from neonatal or young patients whose families agree to donate their organs. In the best case, juvenile, autologous, patient-specific stem cells can potentially be used from tissue banks, if the patient or the patient's parents had the foresight to bank cells at a young age, or retained the umbilical cord-derived stem cells at birth.

During recellularization, the coordination of multiple cell types in the matrix may require extensive engineering of the matrix proteins. Suggestions of adding RGD peptides (a 3 amino acid sequence from fibronection responsible for cell adhesion) to the matrix have been made [93]; however, RGD peptides are not specific in attaching to the cells and can potentially bind to thrombocytes as well. The use of other peptides such as YIGSR, which is a sequence from laminin protein, may be more effective in not attracting the platelets and be more specific in binding to the desired cell types such as endothelial cells.

There are numerous alternative strategies to the use of decellularized scaffolds and patient specific cells for creating new hearts. For example, 3D printing using cells and ECM proteins has been proposed as a possible method for engineering a new tissue. These technologies hold the promise of exciting possibilities and are also worthy of additional research.

In addition, cell sheet technology has been developed by Professor Okano's lab [131] and L'Heureux *et al.* [132] have described the use of cell layers rolled on a mandrel to create a blood vessel.

Other organs have been decellularized and recellularized, including the trachea [133], lungs [66, 134-140], liver [141, 142], pancreas [143], blood vessels [144], and kidneys [141, 145-148]. Many of these papers have outlined the design criteria for bioreactors for decellularization and recellularization. The general principles addressed in this chapter pertaining to the heart also apply to these other organs. Also, much can be learned from the processes used for decellularization and recellularization studies of other organs that can be applied to the heart.

With all of these tissues, there is a need to prevent transmission of disease. Allografts have been used for many years, and procedures are in place to decontaminate donated tissues, including using acids and alcohols. Hodde *et al.* have described a method to evaluate tissues for viral infection [149], the effects of sterilization on ECM composition and architecture [150], and the effects of sterilization on ECM bioactivity and matrix interaction [151]. All of these sterilization techniques will need to be adapted to decellularized whole organs.

The use of endothelial cells for recellularization is the ideal solution for preventing thrombosis. In the case that there is not complete covering of the flow surface with endothelial cells, a modified subendothelial surface would require the use of non-fouling molecules or heparin molecules attached to the surface. However, this approach may prevent reendothelization or alter the Vroman effect of protein adsorption to the surface, and great care must be taken if these strategies are employed.

The current status of this work is that hearts can be optimally decellularized, and success has been obtained with attachment of cells to the scaffold, but full recellularization to provide function while preventing thrombosis has not been achieved. Additional work is required to automate and optimize the decellularization and the recellularization processes. Once the processes for perfusion recellularization of the whole heart is optimized, other remaining issues with the use of porcine hearts will need to be addressed, including the need for culturing large quantities of immunologically-matched, patient-specific cells; the development of aseptic protocols to maintain the organs free from contamination; re-innervation of the heart muscle; shipping and storage protocols; and the development of surgical techniques to implant porcine hearts into humans. It is my hope that these challenges may soon be overcome, and the promise of regenerative medicine may be realized for heart failure patients.

2 APPROACHES AND RESEARCH AIMS

2.1 SPECIFIC AIM 1

To design and create an automated, pressure-controlled process for optimal decellularization of whole porcine hearts in order to improve reliability and replicability of the results.

2.1.1 SUB-AIM

Reducing the total exposure time of SDS detergent solution required in an optimal decellularization process from days to 6 hours and implementing hypotonic shocks to enhance cell removal from the ECM.

2.1.2 RATIONALE

ECM consists of a large variety of components and using strong ionic detergents can cause the decellularized tissue to be detrimental in tissue engineering due to the denaturation of ECM component proteins. An automated system that allows for perfusion decellularization of whole porcine hearts efficiently may improve the outcome.

2.1.3 HYPOTHESIS

Use of SDS as the main detergent solution in the decellularization process has shown promising results in the literature. However SDS is an ionic detergent and can cause denaturation of the ECM components. Creating an apparatus that can automatically control and increase the pressure in the perfusion decellularization process may reduce the required time for optimal

decellularization and especially reduce the necessary SDS concentration and exposure time. In addition, the decellularization of whole porcine hearts will be more replicable by having a computer control the process.

2.2 SPECIFIC AIM 2

To develop a reliable, inexpensive and quick method for measuring the cytotoxicity of the created ECM using hemolysis of human blood.

2.2.1 SUB-AIM

Optimizing the decellularization process for reducing the cytotoxicity by minimizing the required duration of after-wash with water or a nonionic surfactant solution.

2.2.2 RATIONALE

Cytotoxicity of the ECM created through the decellularization process is due to the residual detergents that are detrimental in tissue engineering purposes. An established method for measuring the cytotoxicity level is the use of a live\dead assay protocol on cells cultured with the sample. However this method is time consuming and expensive. Through the hemolysis of human blood, ruptured erythrocytes release hemoglobin that can be detected by absorbance in the visible light bandwidth.

2.2.3 HYPOTHESIS

ECM samples can be incubated in a solution of human erythrocytes separated form blood. The amount of hemoglobin release can be used as a marker for cytotoxicity of the samples. Various after-wash procedures in the decellularization process will be implemented and the hemolysis assay can be used to determine the optimal after-wash procedure that produces the lowest cytotoxicity in the decellularized ECM.

2.3 SPECIFIC AIM 3

To create beating slices of porcine cECM from whole decellularized porcine hearts with the size of 1 cm^2, combined with human cardiomyocytes.

2.3.1 SUB-AIM

To develop a protocol for differentiation of human iPSC into CMs and reseeding the cells onto the porcine cECM.

2.3.2 RATIONALE

Human iPSCs are capable of proliferating indefinitely and can differentiate into cardiac cells. Therefore they can be used to repopulate the cECM and create a human cardiac tissue that can potentially be used for treatment of patients with heart disease. However, due to the complexity and susceptibility of the iPSCs at their pluripotent stage, to date, no group has reported creating beating porcine cECM with human iPSCs.

2.3.3 HYPOTHESIS

Slices of cECM can be made with accurately thicknesses using a cryostat. Human iPSCs can be differentiated into CMs in a stage-wise manner and at the cardiac progenitor stage, the cells can be reseeded onto the cECM and complete differentiation. Cardiac ECM may help the arrangement and can act as a mechanical support of the cells. Due to the native composition of the cECM, it may also aid in preserving the phenotype of differentiated CMs.

3 Automation of Pressure Control for Whole Porcine Heart Decellularization

3.1 INTRODUCTION

Advances in technology, including total artificial heart transplantations, ventricular assist devices [152, 153] and improved treatment techniques [154], have provided some improvement in the treatment of heart disease, and slowed the accelerating need for end-stage organ transplantation, yet alone are insufficient to meet the rising demand. The latest technologies, including stem cell patches [155], 3D printing of tissues and whole organs [156], and tissue engineering using extracellular matrix (ECM) derived biologic scaffolds are currently under development.

The ECM consists of thousands of types of proteins, the concentration of each varying between organs, and the mechanical properties of ECM change based on environment and age [157]. In addition to providing a mechanical scaffold for homing and 3D functioning of the cells, ECM serves as a signaling and communication material between the cells and promotes cell proliferation and differentiation in the body [158]. Synthetic polymer scaffolds lack in advancing complexity of vasculature and essential growth and differentiation factors [156]. The use of decellularized tissue scaffolds has become an attractive solution as heart vasculature, mechanical integrity, and biocompatibility are preserved while the magnitude of the immunogenic response after transplantation is reduced if seeded with terminally differentiated autologous induced pluripotent stem cells (iPSCs) [14, 159] The ECM provides an acellular structure capable of being seeded by iPSCs or progenitor cells [59]. However, in recellularizing an organ, structural

complexity raises issues of oxygenation and nourishing the seeded cells. The more tissues an organ contains, the more structurally complex the organ becomes and that increases the difficulty of effective diffusion throughout the entire vasculature [10]. Less complicated organs, such as the trachea [133] or urinary bladder [160], have less such problems and are already capable of recellularization. The heart provides a unique opportunity because retrograde perfusion through the aorta can facilitate vascular perfusion [29].

Ideally, decellularization is a process in which the cellular components that promote a chronic immune response, such as DNA and GAL epitopes are removed from the ECM, while the ECM non-immunogenic matricellular proteins and growth factors are preserved [158]. A key challenge in decellularization is to avoid chemical damage from overexposure of cell removal reagents such as sodium dodecyl sulfate (SDS). Although SDS is considered one of the most effective detergents for removing cells and immunogenic components from the ECM [2], excess exposure creates a risk of removing glycosaminoglycans (GAGs) and growth factors as well as denaturing ligands and proteins such as collagen, elastin and fibronectin within the structure [6, 161].

Automated systems assist in standardizing the decellularization process [162] and a pressure controlled system can assure effective perfusion through the coronary vessels during the decellularization process [31]. In this study, automated pressure control was used to optimize the decellularization protocol with retrograde perfusion through the aorta in a porcine heart model. Once hearts were decellularized into cardiac ECM (cECM), they were characterized chemically, mechanically and the in-vitro thrombosis potential was investigated. The cECM was partially recellularized using endothelial cells and human cardiac fibroblasts (HCF) to demonstrate the recellularization potential. This work was published in Tissue Engineering Part C [194].

3.2 MATERIALS AND METHODS

3.2.1 HARVESTING

Porcine hearts were harvested from slaughter-weight, 6-month-old, mature female Hampshire, Yorkshire or Spot crossbreed swine at a local abattoir according to approved protocols for safety and animal care. After exsanguination, the chest cavity was opened using a 12" Finochietto retractor and the heart was dissected from the lung while preserving as much of the aorta, pulmonary artery, vein, and caudal and cranial vena cava as possible. Immediately after removing the heart, a pressurized hand action pump filled with a solution of 1X phosphate buffered saline (PBS), heparin (10 Units/mL) and 1X Antibiotic solution (100 U/mL penicillin, 100 µg/mL streptomycin, 25 µg/mL amphotericin B, Anti-Anti, Gibco®, Billings, MT), was used to rinse all the chambers and vessels of the heart via antegrade perfusion through the vena cava and pulmonary vein and retrograde perfusion through the aorta. Hearts were manually massaged while being washed to remove any static blood in the coronary vessels to prevent further thrombosis. The hearts were then transported in cold heparinized (10 units/mL) type 1 distilled water to the lab and frozen at -20°C.

3.2.2 DECELLULARIZATION APPARATUS DESIGN AND AUTOMATION

A Langendorff system based on Radnoti® porcine working heart system (Monrovia, CA) was modified to be used as the decellularization apparatus. The modified apparatus contained a 5 L reservoir for the perfusate solution, a heat exchanger, a bubble trap and the main 5 L decellularization chamber, with the heart submerged in the perfusate solution. A peristaltic pump (Masterflex® HV-07557-00, Vernon Hills, IL) with Tygon L/S 36 tubing (Masterflex® E-3603) was used to produce a pressurized pulsatile flow.

A negative feed-back control system was implemented to maintain critical parameters during the decellularization process. The system consisted of a computer running National Instruments® (Austin, TX) LabView software and contained hardware to collect pressure data while sending control signals to a pump. A proportional-integral-derivative (PID) control algorithm monitored the pressure signal every tenth of a second and adjusted the pump signal to maintain the desired pressure. The program also included functions for running timed experiments, automatically adjusting pressure levels, and switching fluid streams via electrically controlled solenoid valves, as well as a manual control mode. The pressure controller was designed to control the pressure in the bubble trap. The pressure gauge was placed in line of the flow system at the bubble trap, right before the flow entered the heart through the aorta.

A 10 L water bath with controlled temperature was used to maintain the temperature of the decellularization process at a desired temperature (23 °C) by circulating the water through the jackets of the reservoir and the main chamber, as well as the heat exchanger and the bubble trap. Figure 3-1 shows the schematic of the apparatus design and the interface of the LabView program. (The operating apparatus is shown in supplementary Videos 1 and 2, accessible online: https://goo.gl/uX9wxA and https://goo.gl/pPqWua).

3.2.3 DECELLULARIZATION

Decellularization of porcine hearts was performed using SDS and Triton X-100 in the decellularization apparatus. First, the hearts were thawed at 4°C overnight and removed from the 10 U/mL heparinized water. Excess fat was trimmed and the aorta was separated from the pulmonary artery and cut perpendicularly at the brachiocephalic trunk. The aorta was then cannulated with a Radnoti® (Monrovia, CA) ½” male tube and connected to the apparatus. The

heart was submerged in the 1X PBS solution to avoid axial stress on the aorta due to the heart's weight.

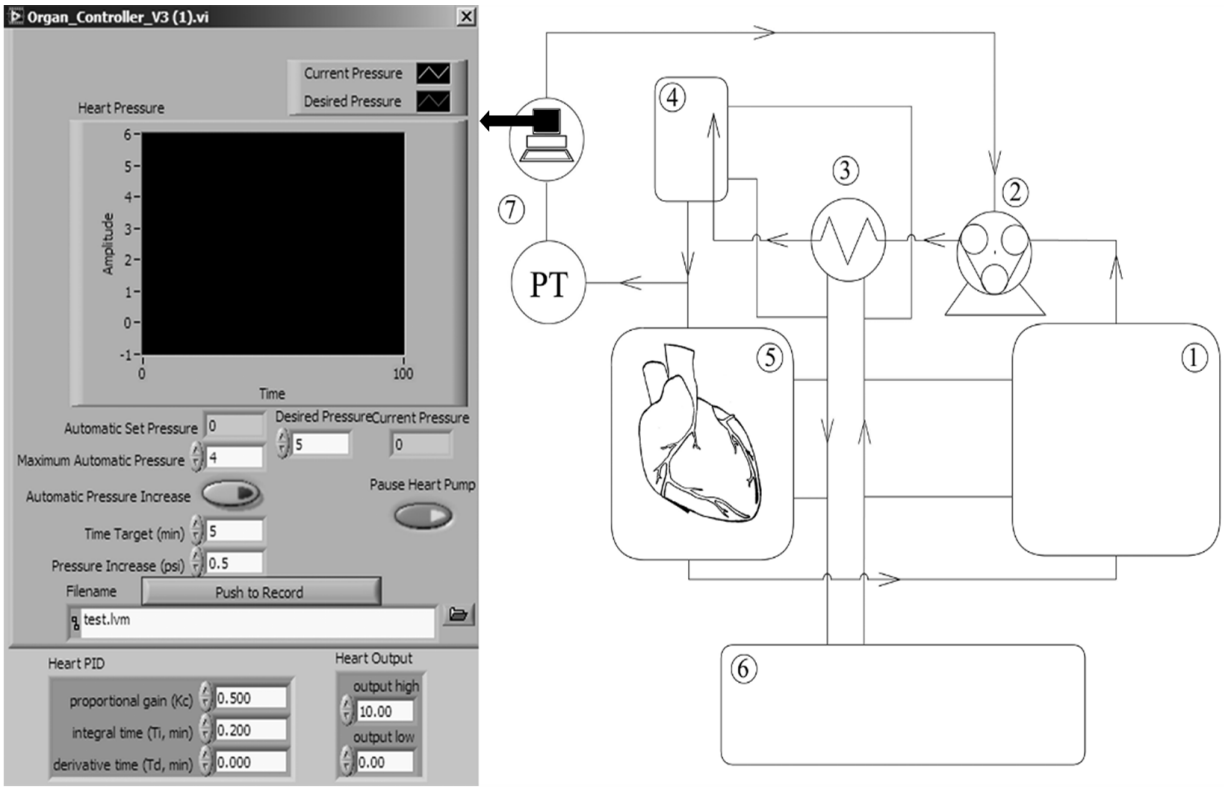

Figure 3-1. Automated controller interface (left) and schematic view of the automated pressure controlled bioreactor for porcine heart decellularization (right). 1: solution reservoir; 2: peristaltic pump; 3: heat exchanger; 4: bubble trap; 5: decellularization chamber; 6: temperature-controlled water bath; 7: control loop.

Care was taken while connecting the heart to attach the connector away from the aortic valve to ensure that the coronary orifices were not covered and the valve could work properly. The decellularization process then started with perfusing 1X PBS through the coronary vessels to remove the blood and thromboemboli followed by an hour of non-recycled perfusion of type 1 distilled water. Alternating between PBS and distilled water resulted in a hypotonic shock to the cells, facilitating decellularization. During the 1 h of PBS perfusion, the pressure was gradually increased to 4 psi using the automated system and distilled water perfusion was performed at 5

psi. The perfusion continued with 3 recirculating 10 L batches of 0.5% (w/v) SDS in distilled water for 2 h, followed by 2 h of non-recirculating distilled water, all performed at controlled pressure of 5 psi. The sixth hour of SDS exposure was followed by 2 h of non-recirculating distilled water at 5 psi and 12 h of overnight perfusion of 10 L recirculating distilled water at 3 psi. The water was then replaced with 10 L 1% (v/v) Triton X-100 and perfusion was conducted while automatically increasing pressure to 5 psi for 2 h to remove remaining SDS and cellular debris. Decellularization was finished with an extensive wash of the heart with distilled water at 5 psi for at least 5 h. The decellularized heart was then dissected and random samples from the left and right atria, ventricles and septum wall were selected for characterization. Samples from the left ventricle were isolated for recellularization or the heart was preserved intact for vascular corrosion casting which is a technique for obtaining the surface area and volume of vasculature in the heart.

3.2.4 DNA, COLLAGEN AND GLYCOSAMINOGLYCANS MEASUREMENTS

To measure the amount of residual DNA fragments, samples were taken from left and right ventricles, left and right atria, and the septa of decellularized and native hearts. Samples were sterilized by immersion in 1X Antibiotic solution in 70% ethyl alcohol for two hours followed by submersion in cell growth medium (DMEM/F-12 with 10% FBS [fetal bovine serum, Gibco®], 100 U/mL penicillin and 100 µg/mL streptomycin [Gibco®]) for 48 h. The samples were then lyophilized and weighed. DNA was extracted from approximately 5 mg of dry samples using Qiagen® DNeasy Blood and Tissue Kit (Valencia, CA). The samples were solubilized with proteinase K overnight and after several centrifugation steps and washing with different buffers, DNA extracts were prepared for quantification. Quant-iT PicoGreen (Invitrogen Corp., Carlsbad, CA) reagent was added to each sample. Samples were excited at

485 nm and fluorescence intensity was measured at 520 nm using a Synergy 2® Multi-Mode Microplate Reader. Gel electrophoresis was performed with DNA extracts loaded on 1% agarose gels to characterize the residual DNA in the structure of the ECM.

To examine the collagen and sulfated glycosaminoglycans (sGAGs) content of the cECM, Sircol® Soluble Collagen Assay Kit (Biocolor Ltd., Newtownabbey, UK) and a Blyscan® sGAG Assay Kit (Biocolor, Ltd), were used, respectively. Approximately 3 mg of dry cECM samples were digested over 3 days using an acid/pepsin solution at 4°C and Sircol® Dye Reagent was added to each sample to form a collagen-dye complex based on the manufacturer's instructions. After solubilizing the dye-reagent complex with an alkali reagent, the absorbance of samples at 555 nm was measured. For sGAGs measurements, each sample was completely solubilized in papain extraction solution for 3 h at 65°C and Blyscan® dye reagent was added to all samples to precipitate the sGAGs-dye complex. The dissociation reagent was then added to dissolve the complex and absorbance was measured at 659 nm.

3.2.5 CELL CULTURE

Murine endothelial cells (MS-1 cell line) labeled with green fluorescent protein (GFP) were thawed and cultured in cell growth medium (DMEM/F-12 with 10% FBS [fetal bovine serum, Gibco®], 100 U/mL penicillin and 100 µg/mL streptomycin [Gibco®]). Human cardiac fibroblast (HCF) cells were cultured in Cardiac Fibroblast Growth Medium (Cell Applications Inc., San Diego, CA). MS-1 and HCF cultures were maintained at 37°C and 5% CO_2 and were both used at early passages. A FLoid® cell imaging station was used to visualize and measure the confluency of the cells as well as for image acquisition.

3.2.6 MACROPHAGE STIMULATION ASSAY

The immunogenic potential of the cECM was measured and compared to fresh heart samples by quantifying the amount of nitric oxide (NO) generated by macrophage cells in contact with specimens. Mouse leukemic monocyte-macrophages (cell line RAW 264.7, Sigma-Aldrich®, St.Louis, MO) were cultured with 3 mL of cell growth medium (10% FBS, DMEM with no phenol red) in 6-well plates until 70% confluent. Lyophilized samples of decellularized (n=6) and native (n=6) hearts were ground to a fine powder using a pestle and mortar filled with liquid nitrogen. Fourteen mg of each specimen were added to a well of 6-well plates. In order to ensure the production of NO by stimulated macrophages, powdered lyophilized *E. coli* bacterial extract was added to wells as positive controls and wells without extract served as negative controls. After 24 h of incubation at 37°C, 5% CO_2, all media were centrifuged at 15,000 g and the amount of NO in the supernatant was quantified as the free stable nitrite form (NO_2^-) using Griess Reagent Kit (Life Technology®, Grand Island, NY) according to the manufacturer's instructions. The concentration of nitrite in the media was then interpolated from a nitrite standard reference curve (0 to 100 µM).

3.2.7 VASCULAR CORROSION CASTING

Corrosion casting was performed on native and decellularized porcine hearts to ensure the integrity of the coronary vessels after decellularization. Two hearts were prepared for casting by surgically suturing the aortic valve closed and placing two 2.5 cm (1") diameter and 1.6 mm (1/16") thick N45 neodymium magnets on either side of the aortic valve. Magnets were positioned carefully not to block the coronary orifices. The aortas were then cannulated with a Radnoti® ½" male tube and connected to a peristaltic pump. A solution of ice cold 2X PBS dyed with trypan blue was slowly pumped into the heart to ensure perfusion through the coronary

vasculature and to hypertonically shrink the native endothelial cells in order to enhance perfusion. Ice cold polyurethane and an epoxy casting resin containing a catalyst (Dowagiac®, Specialty Resin & Chemical LLC, MI) were then mixed at a 35:65 ratio, and immediately perfused through the heart for 5 min. The tubes were then detached and the hearts were allowed to be incubated at room temperature for 1 h to ensure curing was complete. Hearts were then immersed in 3.5 L of 15% NaOH at 37°C to digest the organic tissue. The NaOH solutions were renewed every 3 days or when the solutions became cloudy due to being saturated with the digested tissues. After 10 days, the heart tissues were fully digested and the polymer casts of the internal coronary vasculature were visible. The hearts were placed in 1x PBS overnight, then residual tissue was manually removed.

3.2.8 HISTOLOGY AND SCANNING ELECTRON MICROSCOPY

Decellularized, native, and re-endothelialized cardiac samples from left and right ventricles and atria and the septum wall were dissected and fixed overnight in a solution of 4% paraformaldehyde (PFA; Sigma- Aldrich®) in 1X PBS. The samples were then dehydrated using 30%, 50%, 70%, 95% and 100% ethanol. Afterward, samples were immersed in xylene and embedded in paraffin. Using a microtome, 5 μm slices were made and placed on Fisherbrand® (Pittsburgh, PA) microscope slides. Sectioned samples were then deparaffinized and stained according to the manufacturer's instructions with hematoxylin and eosin (Thermo Scientific®, Pittsburgh, PA), Orcein (O7380; Sigma, St. Louis, MO), or Picro-sirius red (Direct Red 80, #365548, Sigma-Aldrich, Saint Louis, MO) to examine the cellular components, elastin, and general collagen in the native and decellularized samples. Images were acquired using an EVOS® FL Cell Imaging System (Life Technology®, Grand Island, NY).

Scanning electron microscopy (SEM) was performed on decellularized and native heart samples for surface characterization. Specimens were prepared for high vacuum microscopy by fixation in 2% glutaraldehyde in 1X PBS for 24 h at 4°C, dehydration in acetone, and crosslinked with OsO_4. Samples were then dried in a CO_2 critical drier and coated with a 3 nm layer of platinum to enhance conductivity. A Phillips®/FEI XL30 ESEM™ FEG (Hillsboro, OR) Environmental Scanning Electron Microscope was used to acquire images with a field emission gun (FEG) electronic beam at high vacuum.

3.2.9 MECHANICAL PROPERTIES ASSAY

Elastic moduli of the decellularized and native heart samples were calculated by measuring the compression stress as a function of strain in order to evaluate the mechanical stiffness of the decellularized heart samples compared to native hearts kept in PBS at 4 °C for 24h after harvesting. Square shaped, wet samples, approximately 10 mm × 10 mm and 5 mm thick, were longitudinally dissected from the septum and left and right atrium and ventricle walls. An Instron® 3342 Single Column Universal Testing System (Instron, Norwood, MA) was used to perform compression tests. Tissue samples at room temperature were placed flat on the lower metal plate and compressed at a constant rate of 0.07 mm/s until a compressive force of 45N was achieved. Plots of stress vs strain for the specimens were created and the elastic moduli were calculated at the linear portions of the stress/strain curves.

3.2.10 CYTOTOXICITY ASSAY

MS-1 endothelial cells were used to assess cytotoxicity of the decellularized hearts to ensure that the cECM did not adversely affect cell viability. One cm^2 samples were dissected randomly from the endocardium of the left ventricular walls of decellularized porcine hearts and

sterilized by immersion in a solution of 1X Antibiotic solution in 70% ethyl alcohol overnight. Samples were then soaked twice in 1X PBS and incubated in cell growth medium at 37°C, 5% CO_2 for 48 h. Samples of cECM (n=9) in 3 ml of cell growth medium were then placed in wells of 6-well plates, while wells without cECM samples served as controls. MS-1 endothelial cells (1×10^5) were detached from culture flasks using 0.05% Trypsin-EDTA and seeded onto each of the cECM samples and control wells. Cells were labeled with 2 µM calcein AM and 4 µM EthD-III (Biotium® Viability/Cytotoxicity Assay, Hayward, CA) to examine the health and viability of the cells in samples with and without cECM after 1 day and 3 days of culture.

3.2.11 SLICE RECELLULARIZATION

To recellularize cECM samples, MS-1 and HCF cells were labeled with Vybrant® DiO and DiI lipophilic tracers (Life Technologies®, Grand Island, NY), respectively. Labeling was performed by incubating 70% confluent cell layers in T-75 culture flasks with 5 ml of serum-free media and 25 µL of the supplied dye labeling solution at 37°C for 20 minutes. Cells were then detached using Trypsin/EDTA, centrifuged and slowly dispensed, at a concentration of 104 cells/mL, onto 8 mm diameter round, 1 mm thickness cECM samples (n=12) placed in 48 well plates. One mL of medium was renewed every two days. Representative fluorescence images were acquired after 1 week of culture and recellularized samples were fixed in 4% PFA for histology imaging.

3.2.12 PERFUSION RECELLULARIZATION OF RIGHT VENTRICLES

Decellularized right ventricle of the hearts were dissected and trimmed. The sections were then cannulated through the right coronary artery and large open arteries were ligated using a tissue adhesive (3M™ Vetbond, St. Paul, MN). Tissues were then placed in the perfusion

bioreactor and decontaminated by perfusing sterilization solution for 4 hours followed by multiple rinsing and perfusion of sterile 1X PBS to thoroughly remove the sterilization solution. Decellularized right ventricles were perfused with 10 mL/min of growth medium, submerged in 500 mL in a perfusion bioreactor, incubated at 37°C, 5% CO2 for 24 hours. One hundred million (10^8) human umbilical vein endothelial cells (HUVECs) labeled with DIO (green) were perfused into the cECM at a concentration of 10^6 cells/mL and the growth medium perfusion was started after a 4 hour interval to let the cells attach to the cECM. After 10 days the tissue was removed from the bioreactor and 5×10^7 HCFs labeled with DID (red) were needle-injected into ten different areas of the myocardium. The growth medium was renewed and 10 mL/min perfusion of growth medium was restarted 4 hours after injection.

3.2.13 THROMBOSIS ASSAY

A static blood thrombosis assay was developed to qualitatively examine the thrombogenicity of porcine hearts in vitro. Bovine blood was collected at a local abattoir by cannulating the aorta of the heart immediately after slaughter using an 18" long, 1" diameter cannula and collecting the blood in 1 L flasks containing 1500 units of sodium heparin as described by Zhang et *al.* [163].

To develop the assay, in addition to the porcine hearts, 3 bovine hearts were decellularized by aortic perfusion of 10 L of 0.5% SDS for 7 days with renewing the solution every day followed by rinsing with type 1 distilled water after the process. Freshly obtained blood was then perfused through coronary arteries until the chambers of the bovine and porcine heart were filled; the heart vessels were then clamped and the hearts were immersed in a container of blood for 4 h. Native bovine and porcine hearts were used as controls and similarly perfused. After 4 h the hearts were thoroughly rinsed with 1X PBS through all chambers and the

aorta. To evaluate thrombosis, blood clots that could be rinsed out of the heart chambers and vessels were examined visually and the hearts were dissected open to assess platelet adherence to the chamber walls.

3.2.14 STATISTICAL ANALYSIS

Data are shown as average ± standard deviation and the sample size for all of the quantification experiments was n=5 unless stated otherwise. SAS® JMP® 11 (Cary, NC) software was used for statistical analysis of the data. For examining the significance of comparisons, $\alpha=0.05$ was considered as the significance level of p-values. Student's t-test was used for analyzing the data in two groups and the Tukey-Kramer test was performed on the data with multiple groups.

Because of the change in density of the heart after decellularization, the data for quantities of sGAGs and collagen in cECM samples were normalized and reported using the dry mass of the native hearts as the base. For the normalization, the overall weight loss of each of the compartments (right and left atria, ventricular walls, and septum wall) was determined by measuring the ratio of water content to the mass of lyophilized samples in both cECM and native groups and calculating their fraction. The standard deviations of the reported quantities of sGAGs and collagen in cECM samples were determined considering the standard deviations of initial non-normalized values and decellularization weight loss of dried samples.

3.3 RESULTS

3.3.1 WHOLE HEART DECELLULARIZATION

A total of 20 excised porcine hearts were used in these studies, 10 untreated hearts were used as negative controls for various experiments, and 10 hearts were decellularized using the

controlled pressure system (Figure 3-1) with 6 h of ionic detergent wash (SDS) and 2 h of non-ionic detergent (TX-100). Isotonic and hypotonic shocks with PBS and type 1 distilled water, respectively, before and in between steps of the decellularization process, improved the quality of the decellularization and decreased the total decellularization time and detergent exposure. It was observed that the required flow rate to achieve the set point pressure during the SDS perfusion increased from 850 mL/min to 2250 mL/min which is due to cell removal and expansion of the coronary vessels. Figure 3-2 shows a representative porcine heart before (A) and 24 h after decellularization (B). The remaining extracellular matrix was white or translucent due to the disappearance of the red coloration caused by blood and myoglobin proteins. The heart's shape was preserved and the heart valves remained intact and functional. At the time of harvesting, most of the hearts were soft and flexible. At the beginning of decellularization, when they were transferred from the refrigerator to the apparatus, the hearts were rigid and inflexible, which helped the decellularization process by keeping the aortic valve closed, directing the perfusion through coronary artery orifices. During decellularization the cECM became soft and flexible again.

In the H&E staining (Figure 3-2.C,D), the cell cytoplasm was stained with eosin Y (pink color) and the cell nuclei stained with hematoxylin (blue color). The decellularization process removed the cells and cellular components. Sirius general collagen stain (Figure 3-2.E,F) stained collagen protein fibers red, cell cytoplasm yellow, and nuclei black. Comparing the representative images from these different sections of the heart before and after decellularization, the process removed cells and cellular components while the collagen matrix was kept intact. Elastin protein fibers were visualized using Orcein stain represented by the dark brown color as shown in Figure 3-2.G,H.

3.3.2 DNA

DNA can initiate an immune response if it enters a foreign body. However, in addition to DNA, GAL epitope and other membrane proteins and epitopes have been shown to cause an acute immune response that can lead to rejection of a transplanted organ [33]. Since DNA is in the nuclei of the cells, it can be used as a marker for cell removal and decellularization efficacy [35]. Samples of cECM (n=5) from 5 different sections (right and left atria, ventricular walls, and septum wall) of 3 decellularized hearts were prepared for recellularization by sterilization and incubation in cell growth media which contains DNAses that are known to digest residual DNA [15].

The DNA content was extracted using Qiagen™ DNeasy® kit, fluorescent-stained with Quant-iT™ PicoGreen® and the fluorescence was measured. As shown in Figure 3-3.A, the amounts of residual DNA varied in different portions of the heart after decellularization. Samples from the right atrium and left atrium exhibited the highest and lowest DNA removal values (with averages of 99% and 97%, respectively) from 5 different portions of the heart. P-values of less than 0.0001 suggest strong statistical evidence for DNA removal from all portions of the heart after automated, pressure controlled decellularization.

The number of DNA base pairs (bp) in left ventricle samples of native and decellularized hearts was determined via gel electrophoresis. It has been suggested that DNA larger than 200 bp remaining in decellularized ECM can cause a chronic immune response [8]. As shown in Figure 3-3.B, no DNA with more than 200 bp length in cECM samples was detected, while a wide range of DNA sizes was observed in the native heart samples.

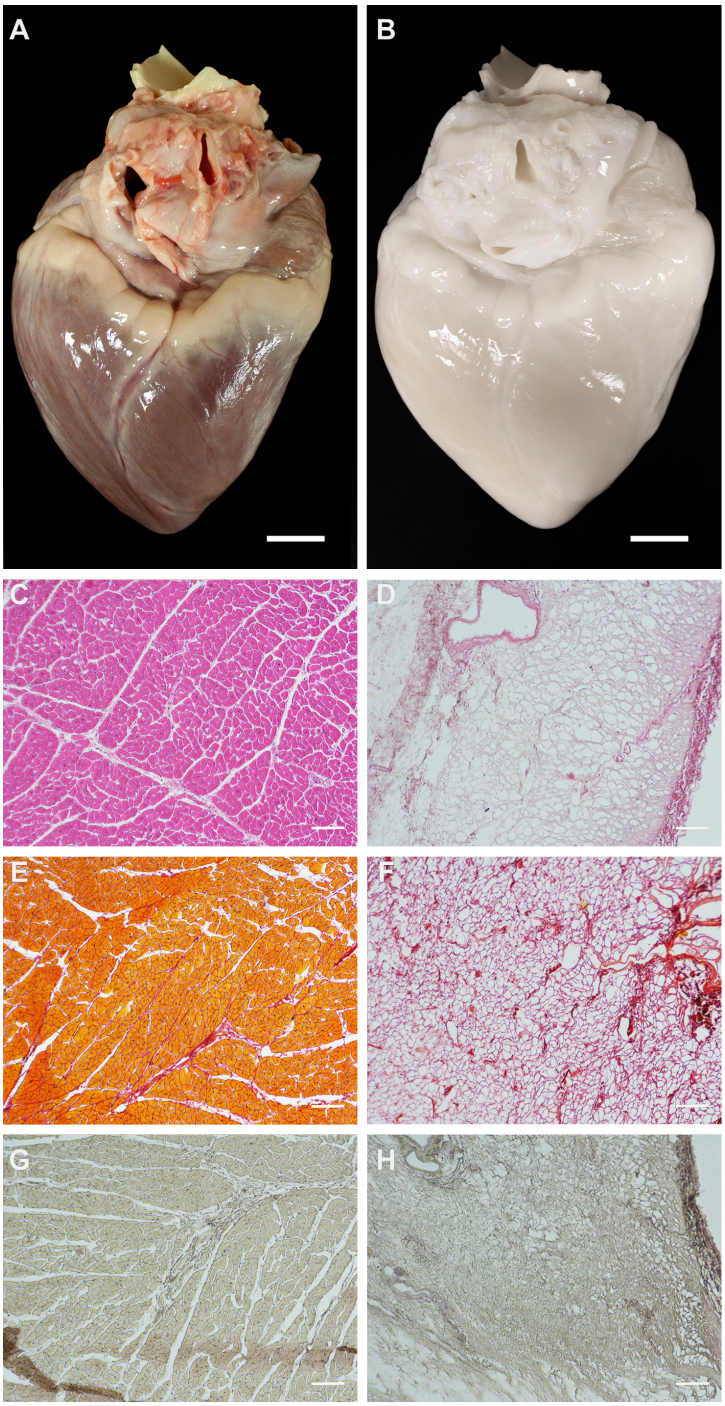

Figure 3-2. A representative porcine heart before (A) and after (B) automated pressure controlled decellularization. Hematoxylin and eosin stained histological images of native (C) and decellularized (D) left ventricular wall samples illustrate complete cell removal. Sirius stained histological images for total collagen in native (E) and decellularized (F) samples illustrate cell removal as well as collagen (red) preservation. Orcein stained histological images for elastin in native (G) and decellularized (H) samples illustrate elastin protein (dark brown) preservation. Scale bars represent 20 mm (A, B) and 100 µm (C-H). 10X magnification lens was used for histology imaging (C-H).

3.3.3 MACROPHAGE STIMULATION

Macrophages are white blood cells that can contribute to stimulating the immune system by encouraging inflammation (M1 phenotype, killer), or moderating the immune response and promoting tissue repair (M2 phenotype, healer). Killer macrophages secrete nitric oxide as they stimulate the immune system [164, 165]. The level of stimulation can be determined by measuring the concentration of produced nitric oxide [22]. The amount of nitric oxide produced by stimulated macrophage cells was quantified as stable nitrite in the medium using Griess Reagent® Kit for decellularized (n=6) and native (n=6) left ventricular samples in the presence of positive and negative controls. As shown in Figure 3-3.C, the concentration of nitrite (μM) formed in the media by macrophage cells exposed to either the negative control or stimulated with decellularized specimens did not produce statistically significant differences (p-value=0.80), while the native and decellularized groups had a 7.27 μM difference in their average of secreted nitrite with high statistical significance (p-value <0.0001). The positive controls showed the highest capacity of nitrite production by the macrophage cells (80.35 μM).

3.3.4 GLYCOSAMINOGLYCAN (GAGS)

In order to characterize cECM and examine the effects of automated, pressure controlled decellularization on the GAGs content of the hearts, 5 random biopsies were obtained from different sections (right and left atria, ventricular walls, and septum wall) of 3 decellularized hearts. Sulfated GAGs were quantified using Blyscan® sGAGs Assay and the normalized results are shown in Figure 3-4.A. Comparing the average amounts of sGAGs between the native and decellularized samples, it was observed that the amounts of sGAGs were not significantly different in various sections of the native heart samples except in the right atrium which had the

highest quantity of sGAGs; however, a statistically significant difference was observed between all groups of cECM samples except the right atrium, right ventricle and septum.

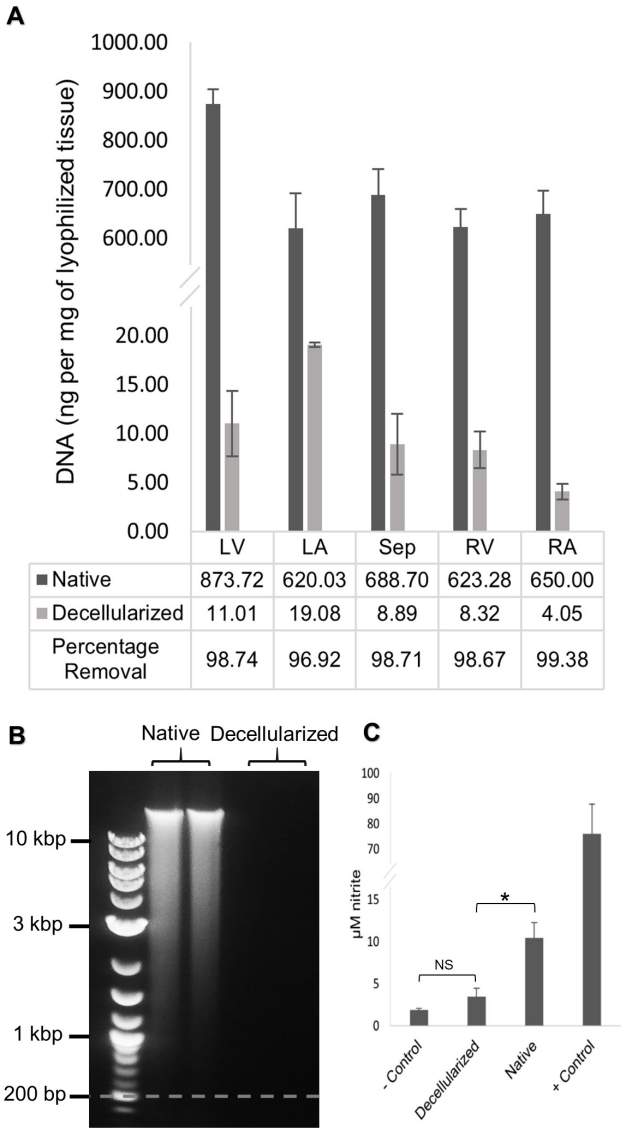

	LV	LA	Sep	RV	RA
Native	873.72	620.03	688.70	623.28	650.00
Decellularized	11.01	19.08	8.89	8.32	4.05
Percentage Removal	98.74	96.92	98.71	98.67	99.38

Figure 3-3. (A) DNA content in different sections of the native and decellularized hearts. (B) Size of the DNA fragments in native and decellularized tissue samples measured using agarose gel electrophoresis. (C) Concentration of nitrite in the macrophage cell media as an indicator for stimulation level. Fine powder of lyophilized native and decellularized hearts were added at equal amounts to the wells of 70% confluent macrophages. Lyophilized Escherichia coli bacterial extract was added to wells as positive controls and wells without extract served as negative controls. LA: left atrium; LV: left ventricle wall; RA: right atrium; RV: right ventricle wall; Sep: septum wall; NS: no significant statistical difference; *: $p < 0.05$.

The highest amount of sGAGs in cECM was in samples from the left atrium, with an average of 40 µg/mg (normalized to weight of lyophilized native tissue) and the lowest was found in the right ventricle samples. The ratio of GAGs in cECM to native samples was 0.17 and 0.18 and 0.32 for right atrium, right ventricle and septum, respectively, while there was no statistically significant deference between cECM and native samples in left atrium and ventricle.

3.3.5 COLLAGEN QUANTIFICATION USING SIRCOL® ASSAY

The amount of soluble collagen was measured in decellularized (n=5) and native (n=5) sample biopsies from different sections of 3 decellularized hearts using Sircol® Soluble Collagen Assay Kit. The normalized amounts of soluble collagen in different sections of the native and decellularized hearts (Figure 3-4.B) showed a decrease in the amount of collagen in the right ventricle, septum, left atrium and left ventricle after decellularization. No statistical significant ($p>0.05$) difference was observed in the right atrium between the decellularized and native hearts. Although not statistically significant in all groups, collagen preservation tended to be higher in the right portion of the heart than the left heart.

3.3.6 VASCULAR CORROSION CASTING AND SEM IMAGING

Casts of the vascular network of native and automated pressure controlled decellularized porcine hearts are shown in Figure 3-5.A,B respectively. The casts were created by retrograde perfusion of polyurethane resin and catalyst through the coronary blood vessels, curing the polymer, and then digesting the heart tissue with NaOH. The resulting cast produced a 3D model of the vascular network that could be used for visual examination of the coronary blood vessels. Care was used when handling the casting during and after processing since the hardened resin

was brittle and the structures contained microvessels. As shown in Figure 3-5.B, the vasculature of the cECM was preserved during the decellularization process.

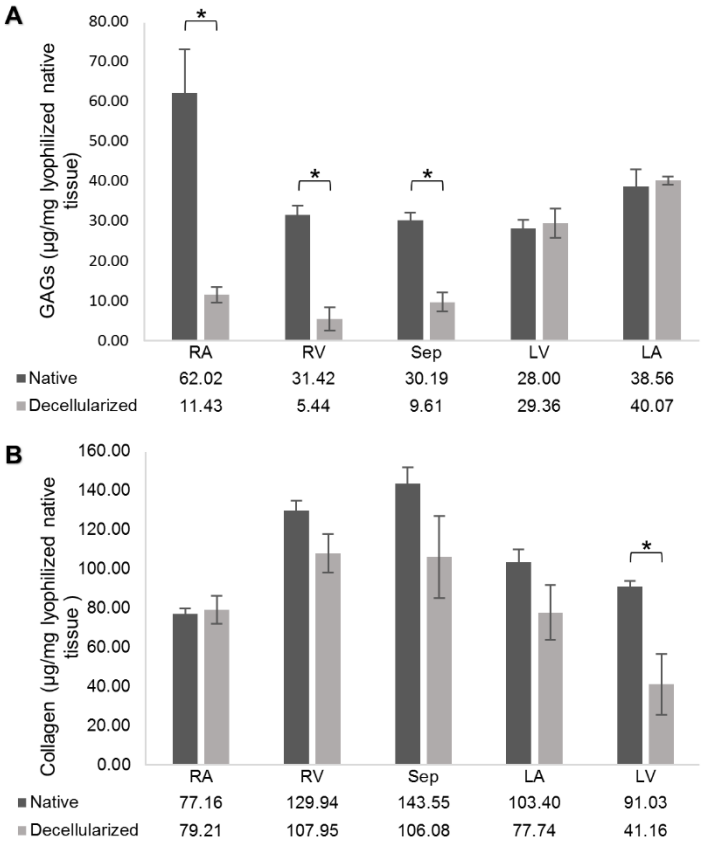

Figure 3-4. (A) Sulfated GAGs content in different sections of the native and decellularized hearts. (B) Soluble collagen content in different sections of the native and decellularized hearts. *: statistical significant difference ($p<0.05$)

SEM imaging was used for microstructural analysis of the cECM and comparison with the native tissue. As shown in Figure 3-5.C-F, the decellularization process increased the porosity of the tissue by removing the cellular components but preserved the protein fibril network. The structure of the cECM was observed to be similar to the native heart samples in both left atrium (Figure 3-5.C,D) and left ventricle (Figure 3-5.E,F) and the coronary blood vessels remained intact.

3.3.7 MECHANICAL PROPERTIES

Young's elastic modulus was determined by plotting compression stress as a function of strain in decellularized and native heart samples and finding the slope of the graph at linear portions at both low and high strains. The results are shown in Figure 3-6.A,B. While the results were not statistically significant in the right and left atria, applying relatively small amounts of pressure tended to result in more deformation in the cECM samples than native hearts (Figure 3-6.A) in all groups. This may be because during decellularization the ECM remained the same relative size as the cellular debris was removed, therefore it became more hollow and easier to deform. Consequently the cECM samples tended to have a smaller Young's elastic modulus than native hearts.

As shown in Figure 3-6.C-G, native samples reached the ultimate resistance force of 45N earlier at lower strain than decellularized cECM samples. Although the elastic moduli demonstrated a more accelerated increase in the native samples, cECM samples showed higher elastic moduli (Figure 3-6.B) under high pressure. This observation might have been caused by not taking into account the Poisson's ratio and assuming the same 1 cm^2 area for the compressed samples which overestimates the pressure at high strains.

3.3.8 MYOCARDIUM SLICE RECELLULARIZATION AND CYTOTOXICITY ASSESSMENT

Culture of MS-1 cells on tissue culture plastic and in the presence of cECM followed by a Live/Dead assay showed no indication of the cECM causing cytotoxicity. Cells seeded with and without cECM reached full confluency in a similar time frame (3 days) and the quantities of healthy and deceased cells were similar in both control and cECM groups (Figure 3-7.A-D).

These results confirmed that MS-1 endothelial cells were able to proliferate in the presence of cECM with comparable results to traditional cell culture conditions.

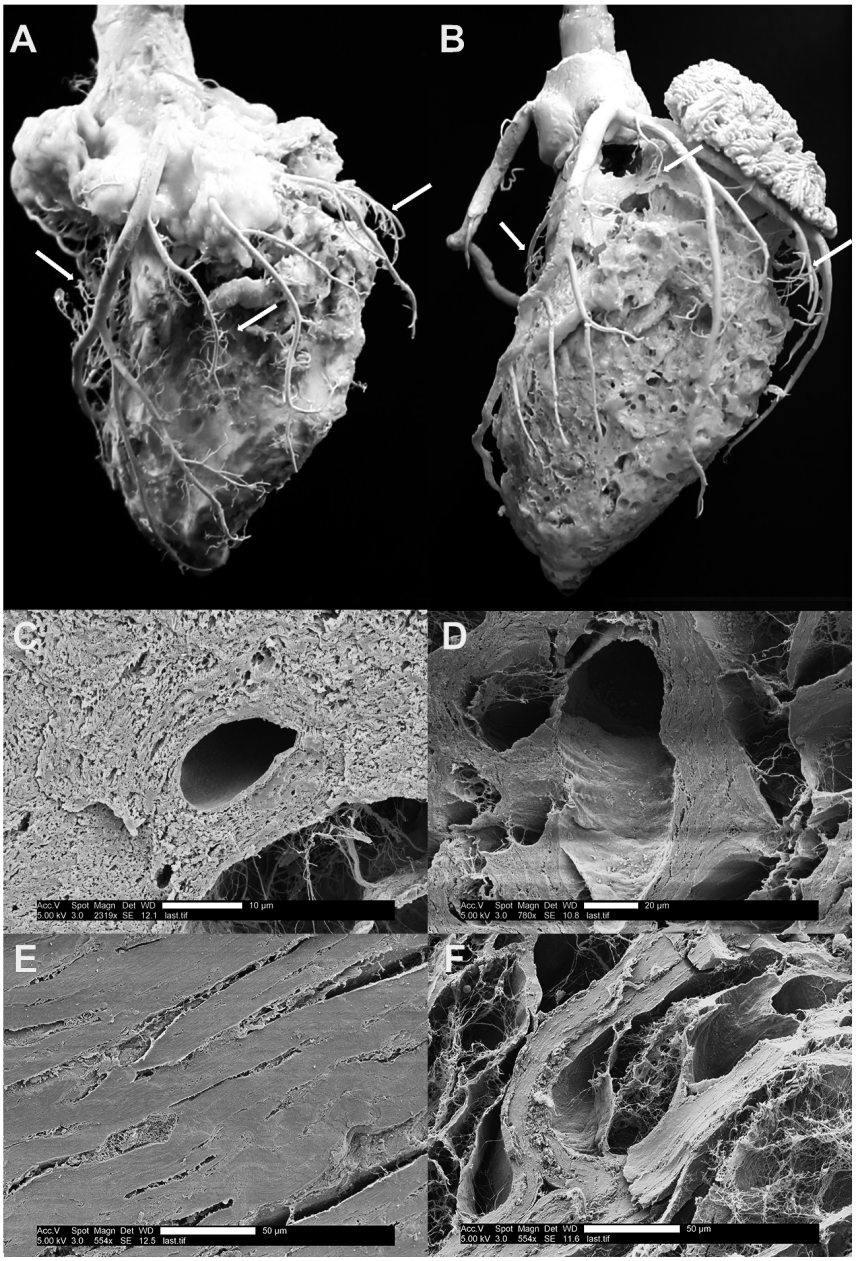

Figure 3-5. Polyurethane vasculature cast of native (A) and automated pressure controlled decellularized (B) hearts. The tissue was digested in 15% NaOH at 37 °C. Arrows point to the preserved microvasculature. SEM images of native (C) and decellularized (D) left atrium and native (E) and decellularized (F) left ventricle illustrate intact blood vessels and porous fibril network after decellularization.

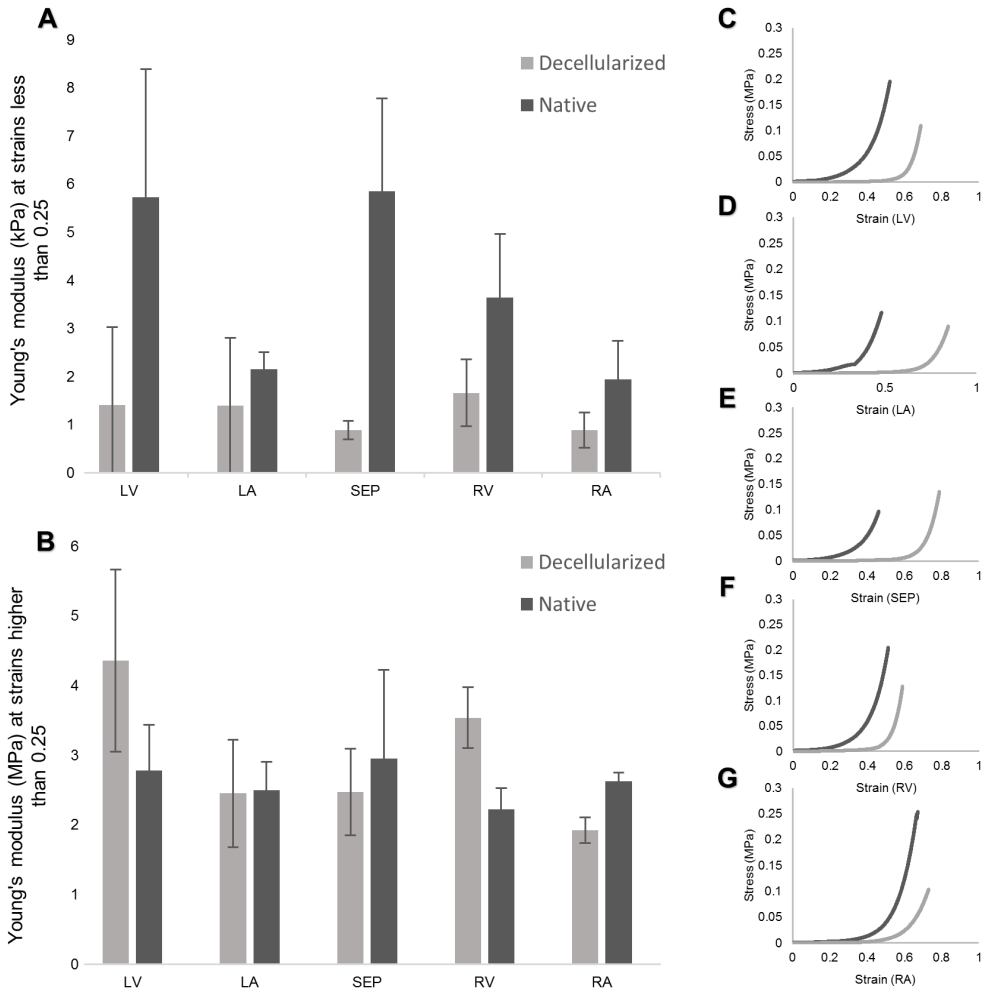

Figure 3-6. Elastic moduli of decellularized and native samples from different section of the heart at low (A) and high (B) strains. Young's modulus was measured by compression tests on an Instron® system up to compressive force of 45N and calculating the tangent line of the stress versus strain at various strains. Stress versus strain results of compression tests for (C) left ventricle, (D) left atrium, (E) septum, (F) right ventricle and (G) right atrium.

3.3.9 RIGHT VENTRICLE RECELLULARIZATION

Polyurethane casts of both decellularized and native porcine hearts were created in order to identify an area in the decellularized heart with an appropriate coronary vessel diameter for cannulation and to map the vasculature network in the decellularized myocardium. These casts (Figure 3-5.A,B) demonstrate that the integrity of blood vessels was preserved after decellularization and were also used for selection of the area for recellularization.

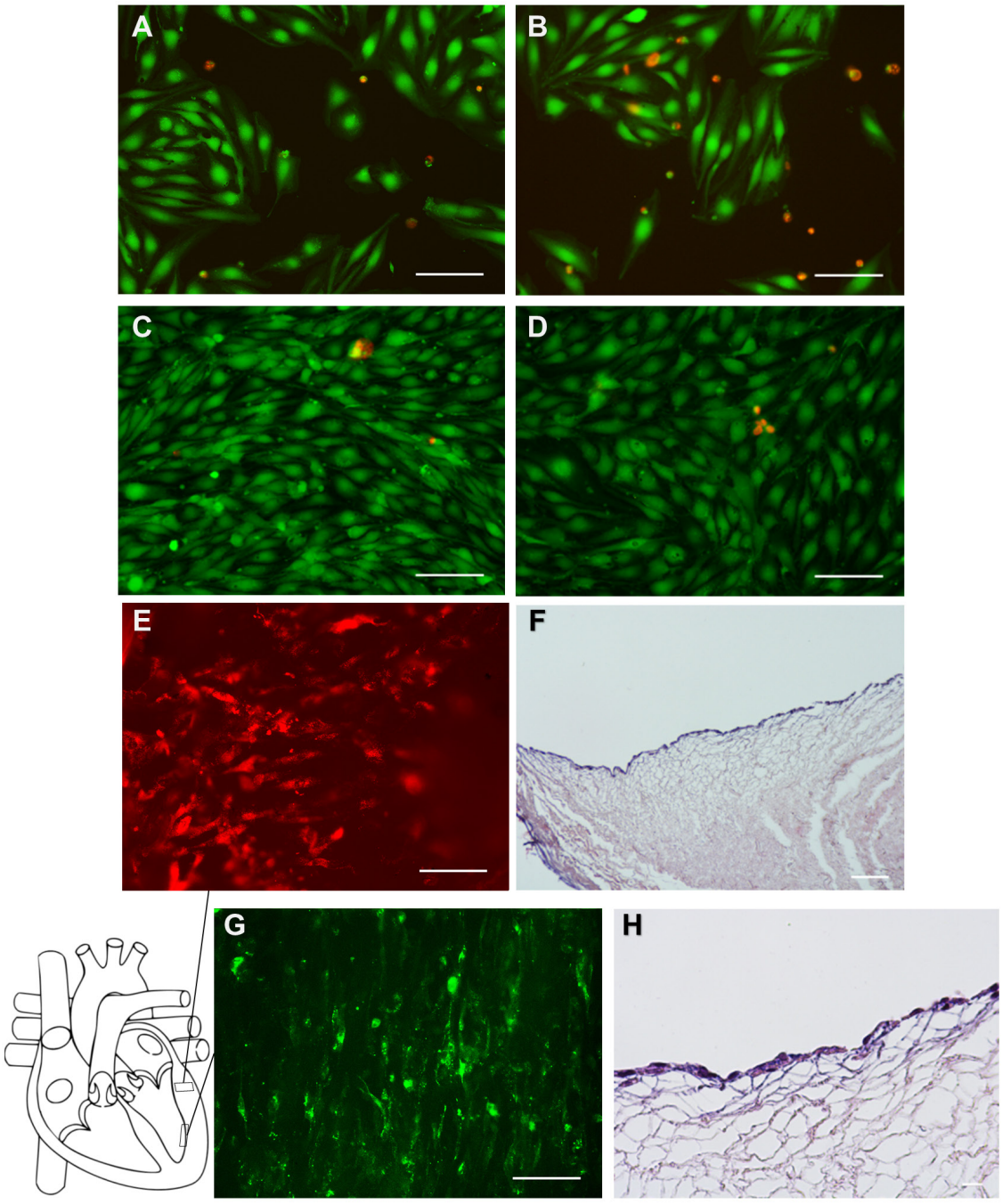

Figure 3-7. (A-D) Cytotoxicity examination of automated pressure controlled decellularized cECM. Viability of the MS1 cells in wells without cECM (A,C) and in wells with cECM (B, D) after 1 day (A,B), and 3 days (C, D) of cell culture was tested with Biotium® Viability/Cytotoxicity assay. (E-H) Representative images of recellularization with HCF and MS1 cells. Fluorescence (E) and H&E stained histological images (F) acquired from DiI labeled HCF seeded on left ventricle myocardium cECM after 7 days of culture. Fluorescence (G) and H&E stained histological images (H) acquired from DiO and GFP labeled MS1 cells seeded on left ventricle endocardium cECM after 7 days of culture. Scale bars represent 100 μm.

The perfusion bioreactors were designed with filters for ventilating the chamber and separate input and outputs for changing the liquid medium and perfusing the tissue (Figure 3-8.A). Separated right ventricle of the hearts were cannulated through the right coronary artery and ligated at the points shown by the red arrows in Figure 3-8.B. Right ventricles were decontaminated (Figure 3-8.C) and recellularized with HUVECs and HCF cells (Figure 3-8.D). After 14 days of recellularization with HCF cells, the tissues were fixed in 4% formaldehyde for 24 hours. Biopsies were taken from random areas of the recellularized tissue and a confocal laser microscope was used in order to acquire 3D images. As shown in Figure 3-8.E-G, HUVECs (green) have attached to the lumen of the blood vessels. Injected fibroblasts created high density clusters around the points of injection and as shown in the images, they demonstrate lower dispersion through the cECM compared to the HUVECs.

3.3.10 THROMBOSIS ASSESSMENT

In vitro static blood thrombosis assays were performed using 1.5 U/mL heparinized fresh bovine blood on native and decellularized porcine and bovine hearts to assure that the cross-species properties of blood and cECM did not interfere with the experimental results. After 4 h of static blood exposure, the hearts were perfused with a 1X PBS solution. Blood clots emerged from the coronary sinus and venous sections of the decellularized hearts, but not from the native hearts. All of the hearts were then dissected and the adherence of platelets to the coronary vessels and inner walls of the heart was visually analyzed as described by Sukavaneshvar *et al.* [166]. Although, no clot formation was observed in any parts of the native hearts (Figure 3-9.A,C,E and G), the coronary sinuses and arteries of the decellularized hearts were clogged with blood clots. Platelets adhered to the inner walls of the right and left portions of the decellularized porcine and bovine hearts as shown in Figure 3-9.B,D,F and H.

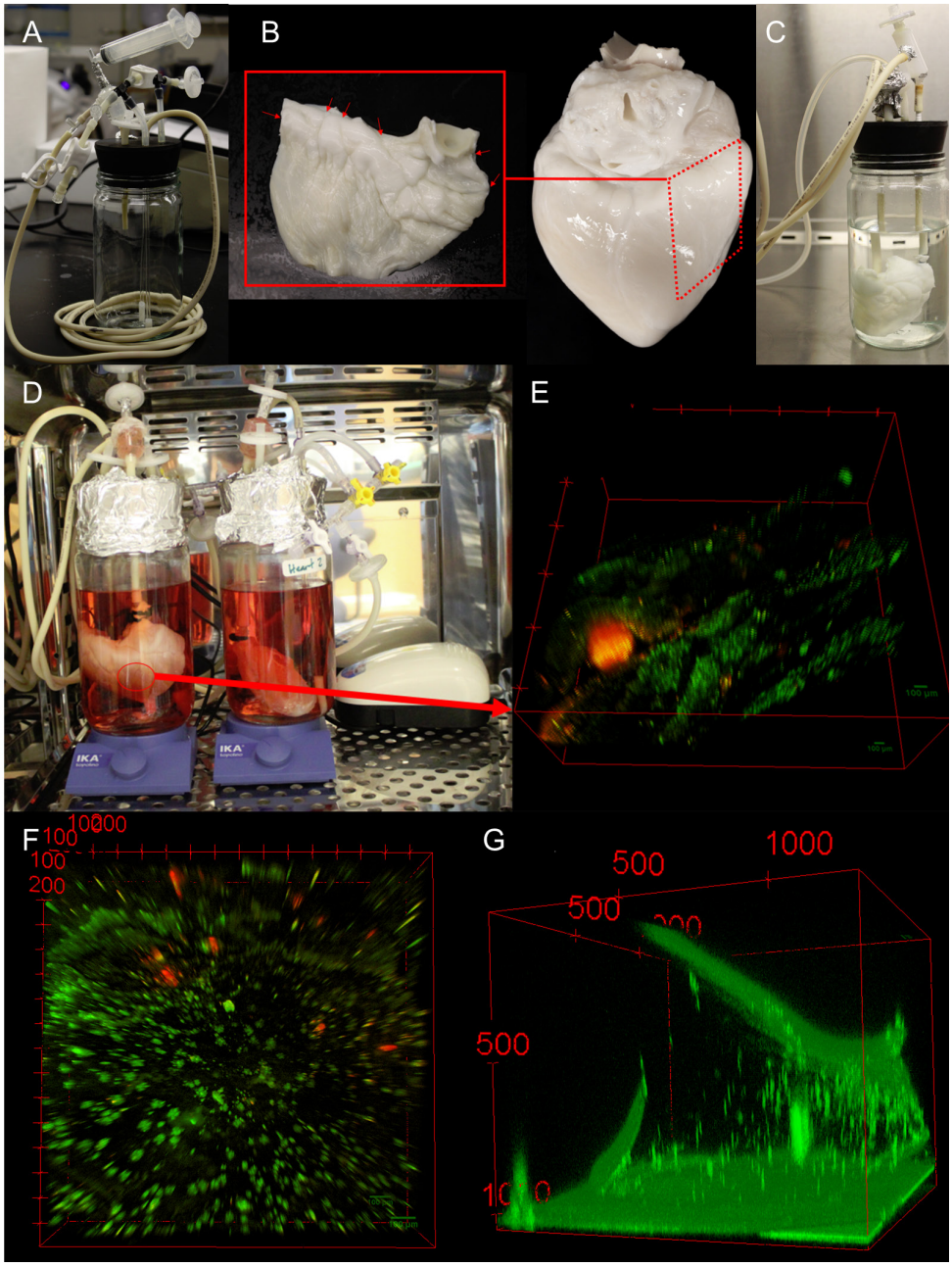

Figure 3-8. Perfusion recellularization bioreactor (A). Dissected right ventricle (B) from the decellularized heart. Arrows show ligated vessels using tissue adhesive. Decontamination of a right ventricle attached to the bioreactor (C). Cannulated decellularized right ventricles in the perfusion bioreactor placed inside an incubator (D) and representative 3D images of recellularized right ventricles, 24 days after HUVECs (Green) perfusion and 14 days after HCFs (Red) were directly injected into the myocardium (E-G). Note the higher distribution of endothelial cells along the vasculature versus the HCFs that are localized to the injected region (E,F) and HUVECs covering the walls of a large (1 mm diameter) branch of the right coronary artery (G).

As shown in Figure 3-9.F and H, significant thrombosis occurred inside the left and right portions of the decellularized bovine hearts and the non-adherent clots had to be removed for visual observation of the platelet adherence to the decellularized tissues.

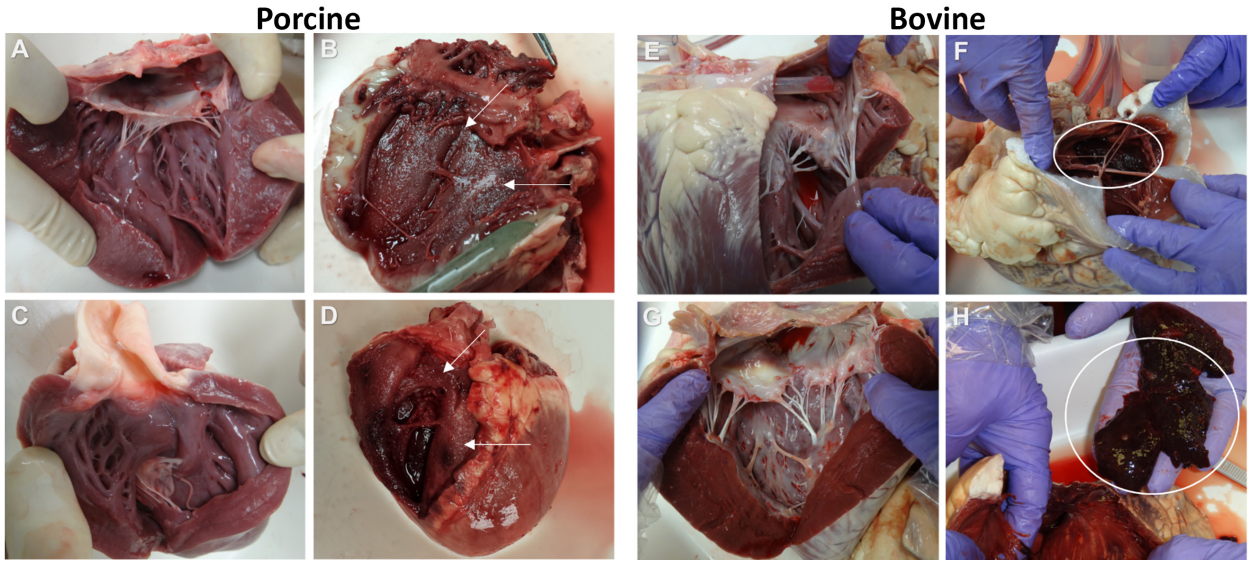

Figure 3-9. Thrombosis assay results on porcine (A-D) and bovine (E-H) hearts. Native hearts did not exhibit thrombogenicity in neither the right (A, E) nor the left (C, G) portions, while activated platelets and thrombosis was observed in the right (B, F) and left (D, H) portions of the decellularized hearts. Arrows point at activated platelets adhered to the ventricular walls (B, D) and circles emphasize on blood clots formed in the ventricle and atrium of the decellularized hearts.

3.4 DISCUSSION

Decellularization of whole porcine hearts was accomplished with 6 h SDS and 2 h Triton X-100 washes. When compared to previous studies, this process included less detergent exposure while preserving the chemical and mechanical integrity of the ECM [2, 3, 29]. It has previously been shown that detergents affect the basement membranes of biologic scaffolds and SDS has the most destructive effect among various ionic and non-ionic detergents [161]. However, to remove cellular material and avoid inflammatory response at the time of transplantation, the use of SDS seems to be an essential step to strip the ECM of any cellular components [3, 167].

Therefore, it was decided to use SDS in an optimized manner to preserve the vital components of the ECM while removing immunogenic cellular materials, resulting in more fully decellularized hearts without the potential for an immunogenic response due to residual cell debris.

DNA content can be used to determine the efficiency of the decellularization process in terms of removing cells and immunogenic factors [35]. It is important to note that the reported amounts of DNA in native tissues varies greatly in the literature, as shown in Table 3-1, which requires reporting the percentage of DNA removal as well as residual DNA content after processing. In this study, more than 98% of DNA was removed using an automated pressure controlled process.

Collagen is responsible for mechanical properties and acts as a signaling molecule for cell differentiation and proliferation [168]. Amongst the various components of the ECM, collagen is the most abundant, with more than 20 types. In a previous study, Naugle *et al*. showed that type VI collagen induced myofibroblast differentiation and type I and III collagen improved proliferation of cardiac fibroblasts [169]. By both collagen quantification (Figure 3-4.C,D) and general collagen staining (Figure 3-2.E,F), our decellularization results demonstrated that collagen was highly preserved.

GAGs are another fundamental component of the ECM that needs to be preserved. GAGs bind growth factors and keep water within the structure of the ECM [168]. It has also been demonstrated that GAGs are susceptible to damage by detergents [19] and dissociating enzymes [170]. Less SDS exposure from our decellularization method increased the preservation of GAGs within the structure of the ECM compared to a previous study [21].

Table 3-1. Summary of DNA content in various perfusion decellularization methods for hearts.

Tissue	Native ng/mg	Decellularized ng/mg	Samples Criteria	DNA Removed (%)	Reference
Porcine heart	8.2	0.82	dry	90.0	[25]
Porcine heart	8.5	0.66	dry	92.2	[21]
Porcine heart	397	35	dry	91.2	[23]
Rat heart	510	16.6	wet	96.8	[2]
Human heart	630	24	wet	96.2	[29]
Porcine heart	691	10	dry	98.5	Figure 3-3.A
Porcine kidney	1,000	13	dry	98.7	[148]
Mouse heart	1,100	33	dry	97.0	[20]
HUV	5,000	100	dry	98.0	[15]
Rat heart	404,000	2400	dry	99.4	[17]

Mechanical properties of the heart, as a continuously beating organ, are crucial for proper function. Maintaining the mechanical strength and stiffness of the cardiac ECM is one of the end goals of whole heart decellularization. However, the stiffness of the ECM can also dictate differentiation of stem cells [171, 172]. Pek *et al*. showed ECMs with elastic moduli ranging from 0.1 kPa to 34 kPa changed the differentiation of mesenchymal stem cells from a neural phenotype to an osteogenic phenotype [173]. Previous decellularization reports of rat [2, 174] and porcine [175-177] hearts demonstrated an increase in the stiffness (i.e. elastic modulus) of decellularized scaffolds compared to their native controls from tensile tests that stretched the scaffolds in various directions. This increase in the stiffness was believed to be due to the denser and more compact matrix that is a result of decellularization [176]. In our study compression tests were performed and it was shown that at low compression strains native tissues demonstrated higher stiffness; however, under high compression strains elastic moduli of the cECM samples were higher or equal to the native hearts, which is similar to previous reports.

It is known that decellularized porcine heart valve matrices induce human platelet activation and cause thrombosis and inflammatory problems [90]. In our work, whole

decellularized porcine and bovine hearts were shown to induce platelet activation and adhesion while native hearts were found to be highly resistant to thrombus formation (Figure 8). This is likely due to the presence of the endothelial cell layer on the inner surface of the endocardium. As previously described by Robertson *et al.* [3] re-endothelialization of the decellularized rat heart with rat neonatal cardiomyocytes diminished the thrombogenicity of the scaffolds in-vitro and in-vivo as well as increasing the beating function of recellularized hearts. Therefore, recellularization with endothelial cells attached to the blood contacting surfaces of the ECM is crucial for whole organ engineering and further studies need to be performed to reduce the thrombosis and inflammatory stimulation of decellularized organs.

The use of decelluarized organs has been proposed by several groups for whole organ engineering. For example, in 2008, Ott *et al*. succeeded to create functional beating rat hearts by decellularization of native hearts with 12 h retrograde perfusion of 1% SDS and recellularization with neonatal cardiomyocytes and endothelial cells [2]. A report on recellularization of decellularized mouse hearts with human iPSCs by Lu *et al.* [20] included a modified retrograde perfusion decellularization method in less than 2 h using enzymatic solutions, 1% SDS, 3% TX-100, followed by 4% sodium deoxycholate (SDC). The hearts were recellularized with multipotential cardiovascular progenitors derived from Y1-iPSCs and after 20 days of culture and differentiation, beating whole mouse hearts were achieved. An optimized, automated method was reported by Akhyari *et al.* [17] and Aubin *et al.* [178] for decellularization of rat hearts using 1% SDS (w/v), 1% SDC (w/v), 0.05% NaN_3 in DI water; 1% saponin, 0.05% NaN_3 solutions and implementing a computer pressure control system through negative-feedback and engineo GmbH software (www.engineo.com) maintaining 77.5 mmHg (1.5 PSI) pressure throughout the process.

The first report of porcine heart decellularization was in 2010 by Wainwright *et al.* [21] in which porcine hearts were decellularized using 2X PBS, 0.02% Trypsin in EDTA and NaN_3, 3% TX-100, and 4% SDC in 8 hours resulted in 92.2% DNA removal. It was reported that the amounts of elastin and GAGs per 1 mg of lyophilized sample were not different than those measured in the native hearts. However, because of the change in density of the samples through decellularization, elastin and GAGs were lost at a ratio similar to the overall loss in dry weight. Remlinger *et at.* [23] in 2012 used the same decellularization method while gradually increasing the flow rate and implementing a maximum of 2200 mL/min flow rate. In our experiments, the pressure increase was also automated and controlled by the computer to a maximum flow rate of 2250 mL/min to maintain the set point pressure.

Ultimately, the use of stem cells or iPSCs would be desirable for recellularization. Therefore, retaining fundamental molecules to signal cell proliferation and differentiation will be required to mimic the function of healthy hearts. A gentle decellularization method is a promising process to obtain intact ECM ready for repopulation with stem cells. Further studies need to be performed to demonstrate the differentiating capacity of these cECM prototypes for human stem cells.

4 USING HEMOLYSIS AS A NOVEL METHOD FOR ASSESSMENT OF CYTOTOXICITY AND BLOOD COMPATIBILITY OF DECELLULARIZED HEART TISSUES

4.1 INTRODUCTION

In order to use cECM made with a decellularization process in tissue engineering purposes, it is necessary to obtain very pure cECM samples that are able to support cell growth without any cytotoxic effects. Due to the use of surfactants in the automated decellularization process which was described in the previous chapter, it is necessary to remove harmful chemical residues that could cause cells to become apoptotic, decrease in function, or cause thrombosis in cardiac tissue samples [179]. Sodium dodecyl sulfate (SDS), a strong detergent that was used to remove cellular material, was the primary concern for causing cytotoxicity in the experiments described in this chapter.

This study examined the utility of a hemolysis assay, the lysing of red blood cells [180], as a novel method to measure cytotoxicity in cECM samples. In order to test this method, porcine hearts were harvested and then decellularized using the automated bioreactor described in chapter 3. After decellularization, samples were taken from the left ventricle and rinsed in phosphate buffered saline (PBS). At various time points, samples were removed from the washes and tested for cytotoxicity. Human blood was purchased from a local blood bank and tested for quality and suitability. Erythrocytes from this blood were then added to the samples of washed cECM and percent hemolysis was calculated. This was done by calculating the percentage of ruptured erythrocytes in each sample by detecting and measuring the amount of hemoglobin

present via spectrophotometry [181]. In order to further assess cytotoxicity, mouse endothelial cells (MS1) were seeded onto the cECM samples. With the assistance of cell staining, it was possible to visualize the healthy and apoptotic cells on each sample. In addition to increased cytotoxicity, another negative side effect of prolonged SDS exposure is the degradation of collagen and other proteins in the cECM. Collagen is an abundant protein in cardiac tissue and is essential for providing structure to the heart [169]. The amino acid hydroxyproline was used as a marker to measure the amount of collagen contained within each sample [182]. Once the amount of collagen was quantified, it was compared against a standard curve of known collagen concentrations to determine the amount of collagen preserved after decellularization.

4.2 MATERIALS AND METHODS

4.2.1 HARVESTING AND DECELLULARIZATION

The harvesting and initial decellularization protocol was similar to sections 3.2.1, 3.2.2 and 3.2.3. Two different protocols for decellularization were used as described in Table 4-1.

Table 4-1. Decellularization protocols for SDS and TX-100 groups

SDS Group	1X PBS 1 h	DW 1 h	0.5% SDS 2 h	DW 1 h	0.5% SDS 2 h	DW 1 h	0.5% SDS 2 h		
TX-100 Group	1X PBS 1 h	DW 1 h	0.5% SDS 2 h	DW 1 h	0.5% SDS 2 h	DW 1 h	0.5% SDS 2 h	DW overnight	1% TX-100 2 h

SDS: sodium dodecyl sulfate; DW: distilled water; TX-100: Triton X-100

In the SDS group, decellularization was done similar to section 3.2.3 but without the rinses after the last 2 hours of SDS solution perfusion. In the Triton X-100 (TX-100) group, hearts were perfused with similar solutions to the SDS group for similar amounts of time and in

the same order. After the last 2 h wash with SDS solution, the hearts were perfused with 10 L of distilled water, recycled for 8 h overnight, followed by 2 h of 1% (v/v) TX-100 perfusion

Subsequent to the final detergent perfusion with either SDS or TX-100 in both groups, the hearts were removed from the decellularization apparatus and the left ventricles were dissected. Samples of decellularized myocardial cECM from the left ventricular wall were obtained, minced and mesh-standardized specimens of $2 \times 2 \times 2$ mm were made from each heart and placed in a beaker filled with 4 L of 1X PBS that was continuously stirred at 60 rpm with a 5 cm stir bar. The left ventricle wall is the thickest portion of the heart and is highly vascularized, therefore it is most probable that the majority of cytotoxicity would be found in the left ventricle. Three liters of the 1X PBS solution were renewed every 24 h. Ten samples were removed from the solution at various time points (approximately every 5 h) with a maximum interval of 10 h between each time point, then stored at 4 °C to be used for hemolysis assay, cell proliferation and cytotoxicity assays, collagen and residual SDS content measurements or structural analysis by scanning electron microscopy.

4.2.2 HUMAN BLOOD TEST: FRAGILITY OF THE ERYTHROCYTES

One to three months post expiration date, anonymous human blood bags were purchased from the MountainStar Health® (Ogden, UT) blood bank. In order to assure the quality of the blood and suitability for hemolysis experiments, the fragility of the erythrocytes were measured using a method based on a study by Parpart *et al.* [183]. For the fragility assay, 4 sets of 0%, 20%, 40%, 60%, 80% and 100% dilutions of 1X PBS with osmolality of 300 mOsm/L in type one distilled water (DW) were made. Fifty µL of blood were added to 1 mL of 1X PBS dilutions in microcentrifuge tubes and mixed gently by manual inversion. After 10 min the tubes were

centrifuged for 3 min at 3,000 ×g, the supernatant removed, and absorbance measured at 540 nm to calculate the percentage of hemolysis using the formula in equation below:

$$\%Hemolysis = \frac{A - A_0}{A_{100} - A_0} \times 100$$

Where:

A = Absorbance of supernatant of erythrocyte suspension with sample solution

A_0 = Absorbance of supernatant of erythrocyte suspension with 100% 1X PBS

A_{100} = Absorbance of supernatant of erythrocyte suspension with 0% 1X PBS

4.2.3 HUMAN BLOOD TEST: HEMOLYSIS ASSAY

Erythrocytes were separated from human blood by centrifugation at 2,000 ×g for 10 minutes and the supernatant was extracted. Erythrocytes were then diluted in 1X PBS to create an erythrocyte suspension (ES) with 2×10^9 cells per mL. A Moxi® Z mini automated cell counter kit (Ketchum, ID) was used to assure the accuracy of the erythrocyte concentration in the ES. Specimens from each of the time points for the SDS and TX-100 groups were placed in 20 mL glass vials with 5 mL of ES. The vials were then placed on an orbital shaker with 125 rpm and maintained at room temperature. Vials without any specimens were used as negative controls and vials with 25 mg of SDS added to the ES were used as positive controls. After 60 min, 1 ml of ES was removed from each vial, centrifuged for 3 min at 3,000 ×g and absorbance of the supernatant was measured at 540 nm. Percentages of hemolysis were calculated using the same equation for percentage of hemolysis with the positive control absorption as A_{100} and negative control as A_0.

4.2.4 CYTOTOXICITY ASSESSMENT AND CELL PROLIFERATION

One of the main advantages of the cECM is its ability to support mammalian cells mechanically and chemically to function and proliferate. Chemicals used during the process of obtaining acellular scaffolds through decellularization can affect the scaffold's supportive properties drastically and cause the cells to become apoptotic or not function well [6]. In order to assess the cytotoxicity of the cECM and investigate the proliferative properties of mammalian cells in contact with the cECM, mouse endothelial cells (MS1) were cultured in T-75 cell culture flasks using a 5% CO_2 incubator at 37 °C with 10 mL of growth medium [10% fetal bovine serum (FBS), 100 U/mL penicillin,100 µg/mL streptomycin] renewed every 2 days. The cells were detached from the flasks at 80% confluence using 0.05% Trypsin-EDTA and 10^5 cells were seeded in each well of 6-well plates. Specimens from various time points of both SDS and TX-100 groups were decontaminated by soaking in a sterilization solution of 100 U/mL penicillin, 100 µg/mL streptomycin and 25 µg/mL amphotericin B (Gibco®, Gaithersburg, MD) in 75% ethanol for 10 min followed by rinsing twice with sterile 1X PBS. The specimens were added to the 6-well plates 2 days after seeding with MS1 cells and the plates were incubated at 37 °C in a 5% CO_2 incubator for 4 h. Wells without any specimen were used as positive controls. The cells were then labeled using 2 µM calcein AM and 4 µM EthD-III (Biotium® Viability/Cytotoxicity Assay, Hayward, CA) in order to assess the cytotoxicity of the cECM specimens and a FLoid® cell imaging station was used to visualize the green and red fluorescence corresponding to healthy and apoptotic cells, respectively.

4.2.5 COLLAGEN QUANTIFICATION USING HYDROXYPROLINE ASSAY

Collagen is the most abundant protein in the extracellular matrix of mammalian tissues, and collagens constitute a large family of proteins that each have at least one triple-helical

domain. Fibrillar collagens consist of three α chains that have 3 polyproline II helices (left-handed) twisted in a triple helix (right-handed) staggered by one residue between adjacent α chains. Interchain hydrogen bonds, electrostatic interactions involving lysine and aspartate, and the high content of proline and hydroxyproline are the factors that influence the stabilization of the triple helix [182]. Because hydroxyproline is found mainly in collagen and rarely in other proteins [184], hydroxyproline content can be used as a marker to measure the amount of collagen.

To prepare cECM samples for quantification of hydroxyproline, decellularized specimens from various time points from both the SDS and TX100 groups were collected and then lyophilized for 2 days. Samples were tested for the presence of hydroxyproline using BioVision's Hydroxyproline Assay kit (BioVision™, San Francisco, CA) based on the manufacturer's protocol. First, 5 mg of the lyophilized samples were homogenized in 500 ml distilled water. Then the samples were digested in 500 ml of 12 N HCl at 60°C for one day. Chloramine T and 4-(Dimethylamino)benzaldehyde (DMAB) reagents from the assay were added to each sample in a 96 well plate, incubated for 30 min at 60 °C and then the absorbance of the samples was measured at 560 nm. A standard curve was prepared with a known hydroxyproline solution to determine the amount of collagen in each sample.

4.2.6 STRUCTURAL ANALYSIS WITH SCANNING ELECTRON MICROSCOPY

The decellularization process makes the cECM porous by removing cellular components from the tissue; however, over-processing or soaking the cECM in PBS for too long, in order to remove detergent residues, can alter the porosity. Scanning electron microscopy (SEM) was used to analyze the porosity and protein conformation of the cECM samples at different time points from both the SDS and TX-100 groups. Biological sample preparation for SEM can also alter the

structure of the sample [185, 186]. In order to avoid significant alteration, samples were minimally processed by soaking the specimens in 50% ethanol (v/v) followed by flash freezing the specimens by placing them in 1L of 100% ethanol, cooled down to about -150 °C using liquid nitrogen. Frozen specimens were immediately placed in a lyophilizer and dried for 5 days. Specimens were then attached to SEM stubs using carbon tape, coated with 3 nm of platinum and placed in a Helios NanoLab™ 600 Focused Ion Beam/SEM (FEI™, Hillsboro, OR) for image acquisition.

4.2.7 SDS MEASUREMENT USING A COLORIMETRIC METHOD

As previously reported by *Jurado et al. Rosconi et al.* [187, 188] amounts of SDS in hydrophilic solutions can be quantified using colorimetric methods. In this study, specimens from both SDS and TX-100 groups, collected at different time points, were placed in 1 mL DW on a shaker for 24 hours at room temperature. Standards solutions of 0 to 10 mg/L SDS in distilled water were created for calibration. A 50 mM buffer solution of sodium tetraborate ($Na_2B_4O_7$, by Sigma-Aldrich®) was prepared and the pH was adjusted to 10.5 by using a dilute solution of sodium hydroxide. To color the SDS, 0.1 g of methylene blue reagent was dissolved in 100 mL of borate buffer solution (10 mM) with adjusted pH 5-6. The methylene blue solution was kept in a topaz-colored flask. In a glass test tube 10 µL of phenolphthalein was added to 5 mL of diluted SDS sample or standard solutions. The solution were alkalinized with addition of 200 µL of sodium tetraborate at pH 10.5 to the color change of phenolphthalein. Next, 100 µL of stabilized methylene blue solution and 4 mL chloroform ($CHCl_3$, Sigma-Aldrich™) were added to the SDS solutions. Before each measurement, the glass test tube was stirred vigorously for 30 s and allowed to rest for 10 min. The chloroform phase was used for colorimetric measurements with UV-vis quartz cuvettes at 650 nm against pure chloroform.

4.2.8 STATISTICAL ANALYSIS

Statistical analysis of the results from the experiments described in this chapter was similar to section 3.2.14. Student's standard t-test was used for analyzing the data in two groups of SDS and TX-100. In the cytotoxicity assay, ImageJ v1.49, which is available in the public domain, was used to calculate the percentages of live and dead cells in random acquired images.

4.3 RESULTS

4.3.1 WHOLE HEART DECELLULARIZATION

A total of 10 hearts were processed for this study. Five hearts were processed for the SDS group and 5 for the TX-100 group based on the protocol shown in Table 4-1. Figure 4-1 shows a processed heart from the TX-100 group after 2 h of TX-100 perfusion. After processing, all hearts were dissected open and the left ventricles were minced to obtain at least 200 specimens of 2 × 2 × 2 as shown in Figure 4-1.

4.3.2 ERYTHROCYTE FRAGILITY

In order to assure the quality of blood used in the hemolysis experiments, erythrocyte fragility was determined by suspending the blood in different osmotic solutions. Blood samples (n=6) were incubated in the various solutions for 10 min and the percentage of hemolysis was recorded using light absorption at 540 nm.As shown in Figure 4-2, solutions of 40%, 60% and 80% 1X PBS (120, 180 and 240 mOsm/L) produced hemolysis percentages of 97.57% ± 4.23, 58.74% ± 8.82 and 6.94 ± 5.96, respectively. A representative image of the supernatant color obtained after centrifugation with the various 1X PBS solutions with respect to the percentage of hemolysis produced is also shown in Figure 4-2. To assure the quality of the results from this assay, the data were compared to an established fragility standard curve for verification[9].

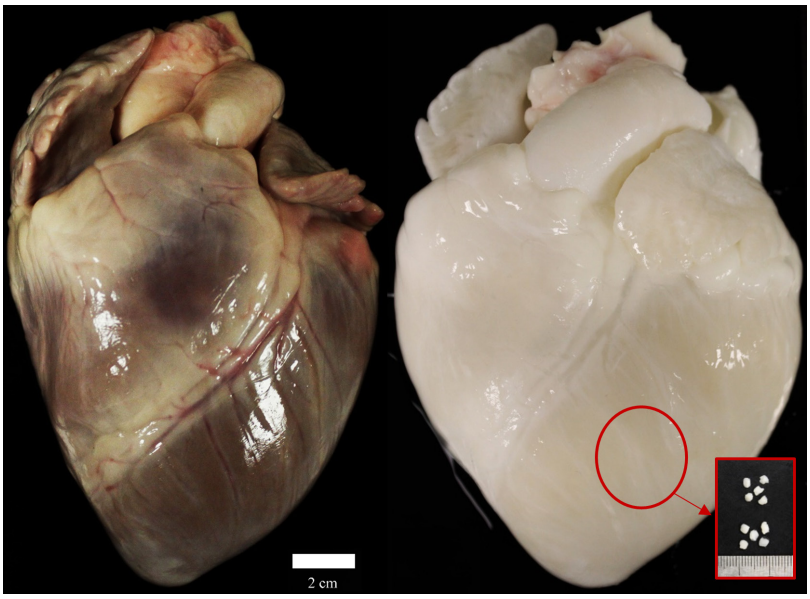

Figure 4-1. Representative native (left) and decellularized (right) porcine hearts after TX-100 treatment. The hearts were decellularized in an automated apparatus through retrograde aortic perfusion. Hearts from the SDS group were taken out of the bioreactor after 6 hours of SDS exposure while hearts from the TX-100 group were perfused with an additional 2 hours of TX-100. Subsequently, hearts were dissected and 2 mm minced samples from left ventricle walls were obtained (shown by the arrow).

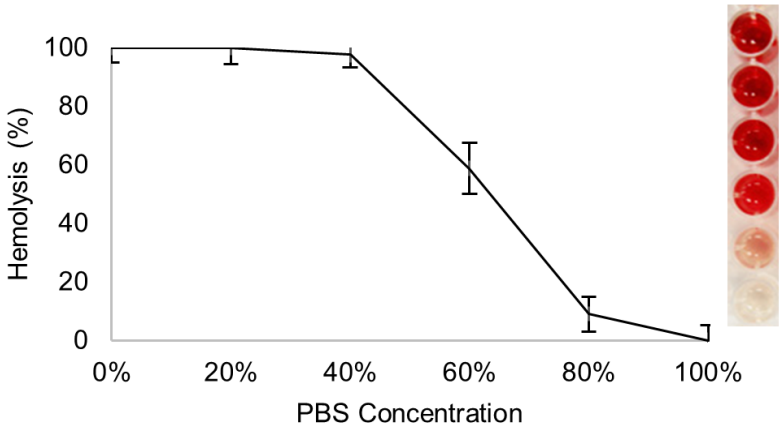

Figure 4-2. Fragility test of human blood. Human erythrocytes were suspended at different concentrations of 1X PBS (300 mOsm/L) in distilled water for 10 minutes. Hemolysis percentages were calculated using 540 nm light absorption of the supernatant solutions after centrifuging. Color bar on the right represents the supernatant after centrifuge with respect to the percentage of hemolysis.

4.3.3 HEMOLYSIS ASSAY

Various chemicals used in the process of decellularization can have different effects on the tissue ultrastructure, mechanical behavior and the biochemical composition, which may affect the subsequent host response to the material. Chemicals are specifically chosen for use in the process due to their inherent potential to damage cell membranes. Thus, if they remain in the cECM after the decellularization process, it is likely that the cECM will be cytotoxic [6, 8]. In order to assess the cytotoxicity of the cECM in this study, specimens (n=6) collected at different time points from both the SDS and TX-100 groups were placed on an orbital shaker at 125 rpm in glass vials containing 5 ml of ES at room temperature for 1 h. It was observed that shorter periods than 60 min led to unreliable results due to incomplete reactions between the residual surfactants and erythrocytes. This observation was also reported by Krzyzaniak and Yalkowsky [189].

As shown in Figure 4-3.A-B, both SDS and TX-100 samples with no wash time produced greater than 90% hemolysis (90.16 ± 25.66 and 91.42 ± 13.84, respectively). No statistically significant difference between the SDS and TX-100 groups ($p > 0.05$) was observed until the 5 h time point, at which point the SDS group produced 72.38% ± 10.37 hemolysis while the TX-100 group produced 25.61% ± 16.12 hemolysis. The statistical difference between the SDS and TX-100 groups continued to be significant until the 40 h time point at which time the specimens in the SDS group produced 8.19% ± 4.31 hemolysis. It was observed that the minimum amount of required wash to reach no statistical significant difference with the negative control was 10 h for the TX-100 and 40 h for the SDS group. For the modeling of the cytotoxicity dilution, decaying exponential functions were fitted to the data. As shown in Figure 4-3.C models based on the functions of $\%Hemolysis = 90.16 \times e^{-0.06t}$ and $\%Hemolysis = 91.42 \times e^{-0.25t}$ can represent

the data for the SDS and TX-100 groups respectively. The models show that the TX-100 samples have a 4.17 times smaller time constant than the SDS samples which means that the Hemolysis percentage drops 4.17 times faster in the TX-100 samples compared to the SDS samples.

4.3.4 CYTOTOXICITY ASSESSMENT

Cytotoxicity of the cECM was measured by counting the number of dead versus live cells using the Biotium® Viability/Cytotoxicity assay. The polyanionic dye calcein provided in the assay is absorbed by live cells and produces a uniform green fluorescence. The EthD-III enters cells with damaged membranes and after binding to mammalian cell nucleic acids, the fluorescence intensity increases by 40-fold and produces a red fluorescence in dead cells. SDS and TX-100 chemicals used for decellularization in this study are inherently able to damage the cell membranes and cause toxicity, thus the Viability/Cytotoxicity assay can be used to determine the level of cytotoxicity.

Although the FBS used in growth medium is known to have neutralizing inhibitors and digestive capacities [15], it was observed that specimens (n=4) from both SDS and TX-100 groups at 0 hour produced 97.35% ± 1.52 and 94.75% ± 3.42 dead cells, respectively, as shown in Figure 4-4.A-B.

A statistically significant difference between SDS and TX-100 groups was observed at the 10 h time point with the SDS group producing 51.94% ± 10.46 dead cells while the TX-100 group produced 7.86% ± 2.53 dead cells. The percentage of dead cells was observed to be higher for the SDS group until the 40 h time point when no statistically significant difference was observed between the SDS and TX-100 groups (p value > 0.05). For the TX-100 group after 10 h, no statistically significant difference was observed compared to the negative control (p value <

0.05), whereas the time point at which there was no statistically significant difference was 40 h for the SDS group. Representative images of the cells in contact with the specimens from both groups, labeled with Viability/Cytotoxicity assay are shown in Figure 4-4.C-J.

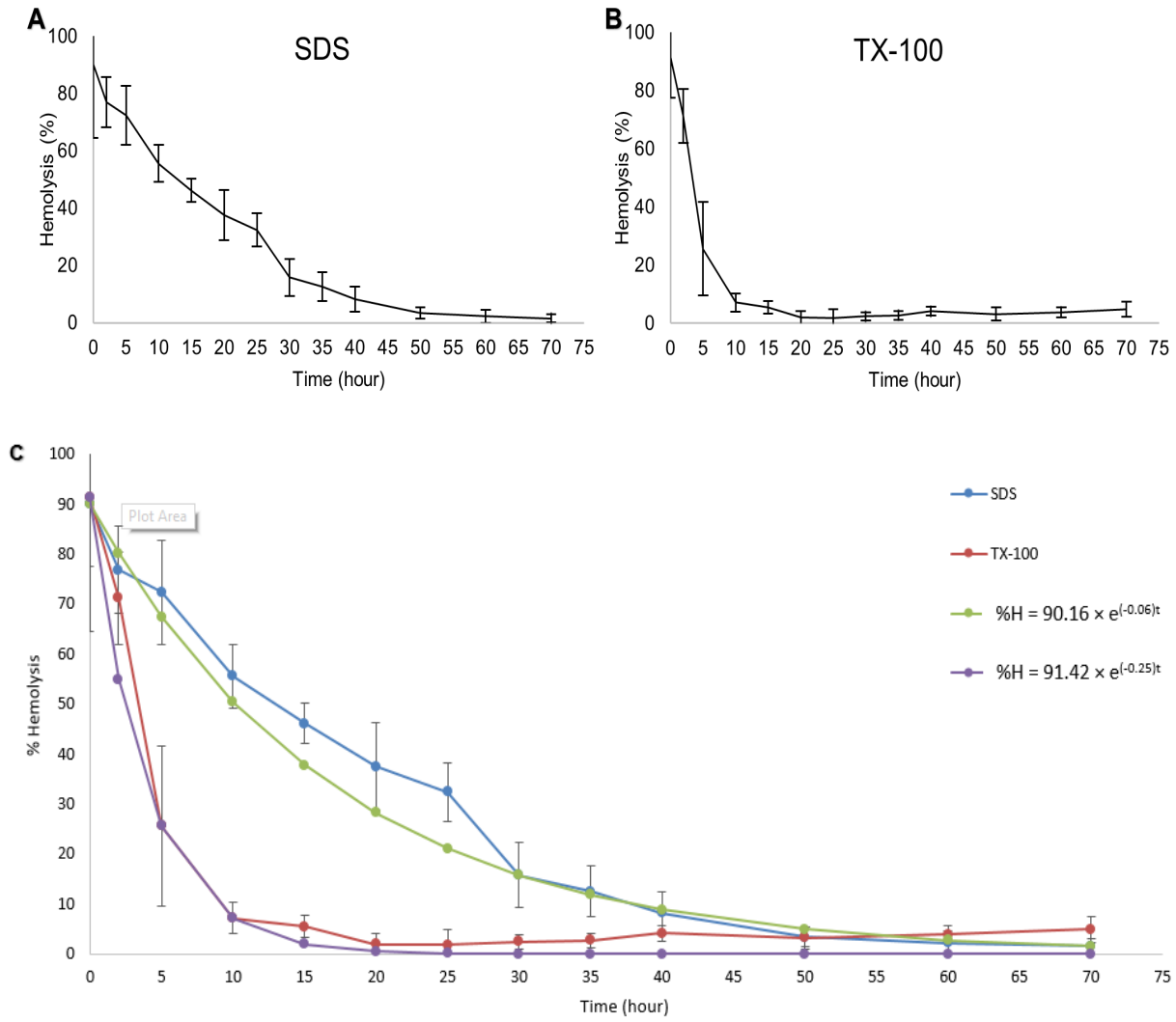

Figure 4-3. Hemolysis percentages of ES in contact with decellularized specimens from SDS (A) and TX-100 (B) groups at various time points. Decaying exponential functions fitted to the data for SDS and TX-100 groups (C). Time axis represents the amount of time in which the specimens were washed with 1X PBS in order to remove residual cytotoxic detergents from the decellularization process and the hemolysis axis represents the percentage of red blood cells that were ruptured due to contact with the specimens.

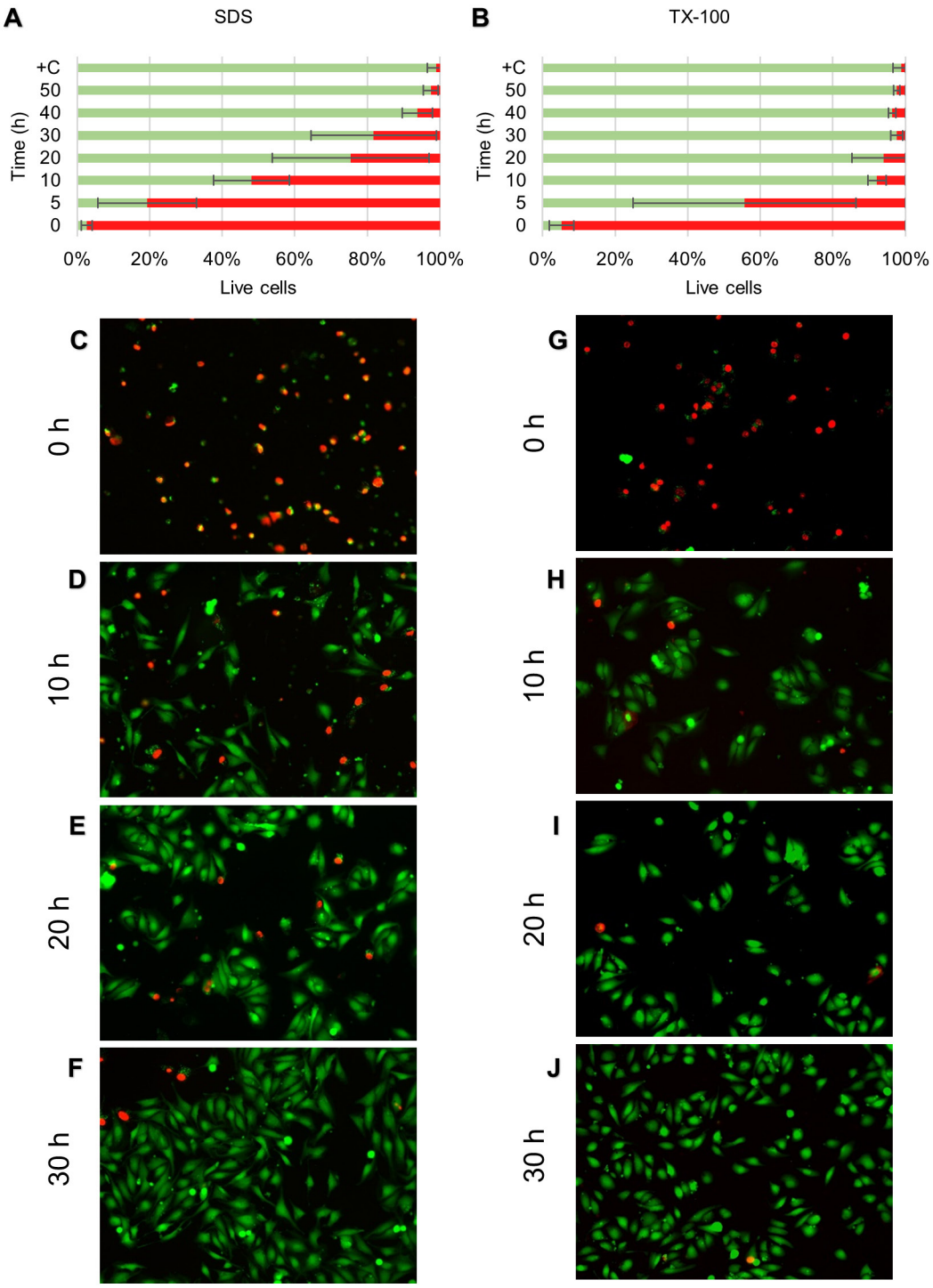

Figure 4-4. Cytotoxicity/viability assay on MS1 cells incubated for 4 hours with specimens from both SDS and TX-100 groups collected at various time points. Quantified percentages of live cells are shown in green bars (A, B). Representative fluorescence images of MS1 cells labeled with cytotoxicity/viability assay after 4 hours of incubation with specimen from the SDS (C-F) and TX-100 (G-J) groups

4.3.5 COLLAGEN QUANTIFICATION USING HYDROXYPROLINE ASSAY

Stabilization of the triple helix in collagen is primarily due to interchain hydrogen bonds, electrostatic interactions involving lysine and aspartate, and the high content of proline and hydroxyproline [182]. Soaking the cECM in PBS for too long, in order to remove detergent residues, can potentially deteriorate the factors involved in the stabilization of the collagen and solubilize this protein. In order to investigate the changes in the amounts of collagen, hydroxyproline content in specimens (n=3) at different time points were measured per milligram of dried tissue in both SDS and TX-100 groups. Although the averages of hydroxyproline content in both of the SDS and TX-100 groups declined over 110 and 75 hours, respectively, the statistical difference was not significant (p-value > 0.05). As shown in Figure 4-5, the contents of hyroxyproline in the SDS group started at (0 hour) 24.16 ± 6.93 µg/mg of lyophilized tissue and reduced to 18.88 ± 8.33 µg/mg of lyophilized tissue after 110 h. In the TX-100 group the contents were observed to start at 23.84 ± 7.39 µg/mg of lyophilized tissue and after 75 h decreased to 20.43 ± 2.19 µg/mg of lyophilized tissue.

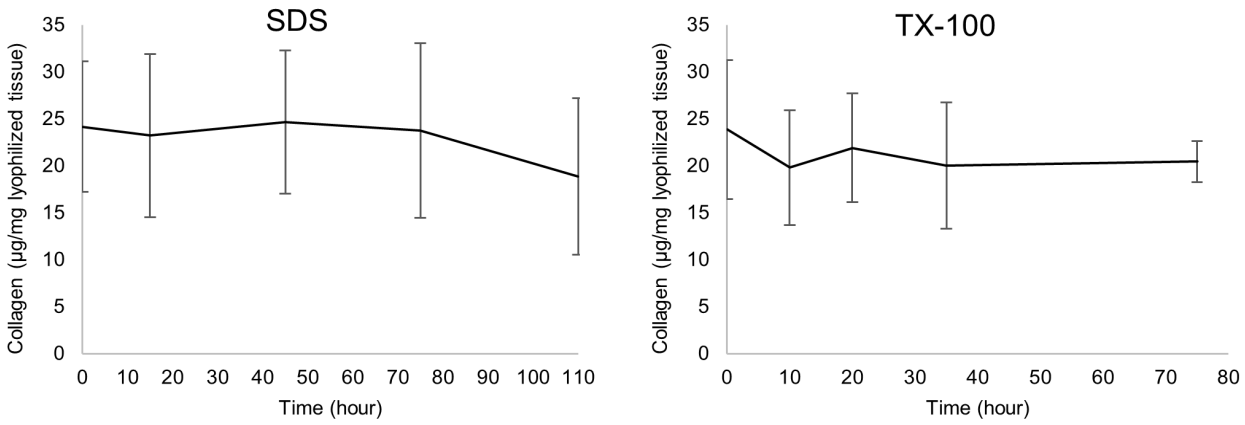

Figure 4-5. Quantified amounts of hydroxyproline as a marker for collagen in the SDS (left) and TX-100 (right) groups as a function of wash time in 1X PBS

4.3.6 SCANNING ELECTRON MICROSCOPY STRUCTURAL ANALYSIS

As previously reported [20, 190, 191], surface structural analysis can be performed using SEM techniques to assess the alignment of collagen fibers. In this study, samples at various time points were flash frozen, lyophilized for 5 days and coated with 3 nm of platinum. Representative SEM images acquired from samples at different time points are shown in Figure 4-6. In both of the SDS and TX-100 groups, samples with longer wash times demonstrated more dissociation and disruption of fiber alignment.

4.3.7 SDS COLORIMETRIC ASSAY

The colorimetric assay with UV-vis detector was used to measure the amount of SDS in different samples. To obtain the linear range of SDS solutions, the correlation between absorbance and concentration was identified. A calibration curve was prepared for different SDS amounts in the range of 0-20 mg/L. The adjusted regression of 0.996 showed a linear correlation between the absorbance and different SDS concentrations and consequently the precision of the applied procedure. Soluble SDS content in the specimens were then calculated using the calibration curve as shown in Figure 4-7.

As shown, the concentration of SDS in the specimens started at 894.32 ± 55.45 and 753.81 ± 48.57 µg/mL in the SDS and TX-100 groups respectively. In the TX-100 group the concentration decreased to 6.99± 0.57 µg/mL after 21 hours, while at a similar time point in the SDS group, the concentration was observed to be 98.06 ± 6.08 µg/mL. After 50 hours, SDS contents in the SDS and TX-100 groups did not demonstrate a statistically significant difference and the concentration was 5.09 ± 0.57 µg/mL in the TX-100 group.

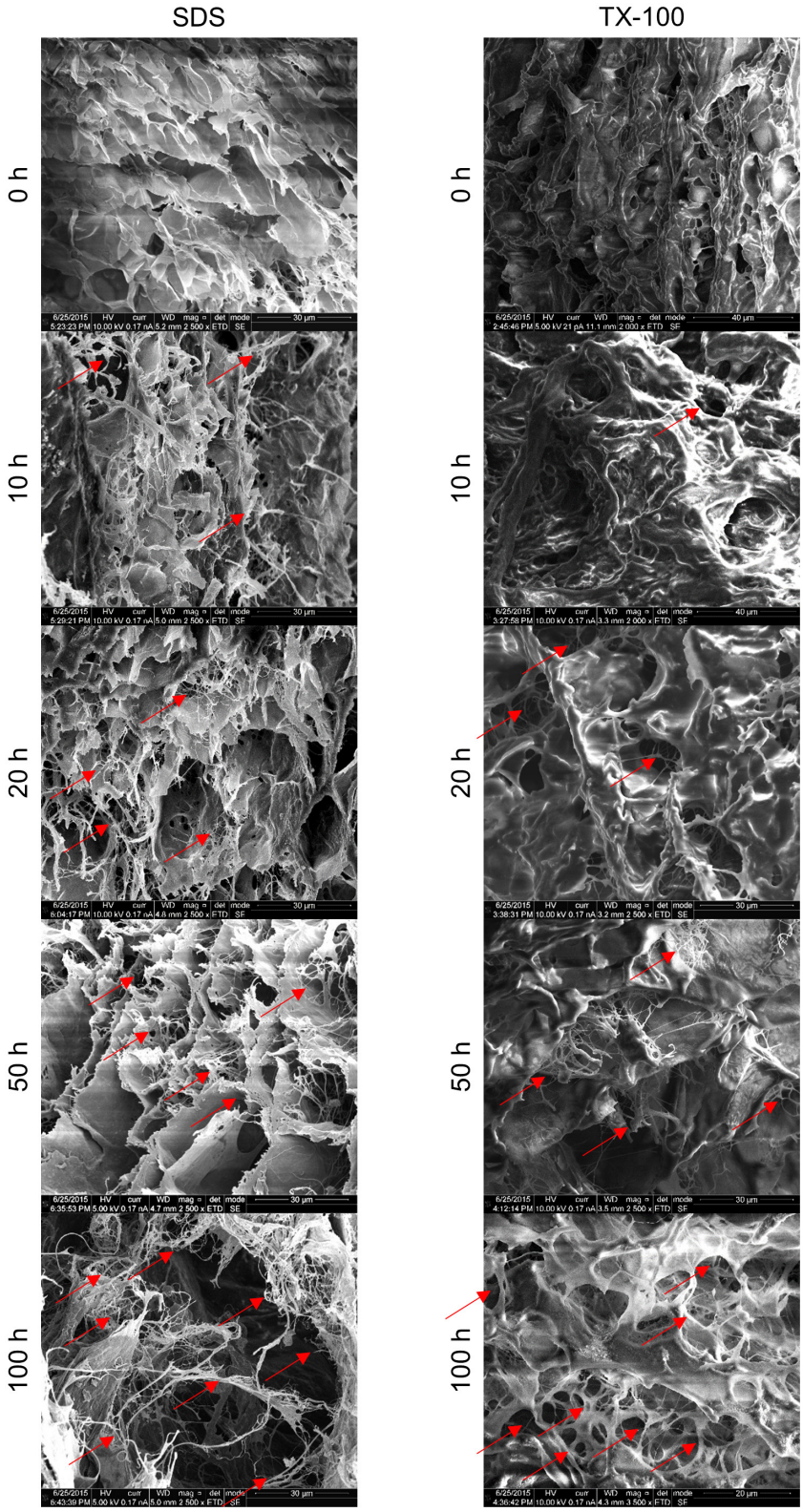

Figure 4-6. SEM images acquired from cECM samples at different time points from the SDS and TX-100 groups. Arrows show dissociated collagen fibers with disrupted alignment

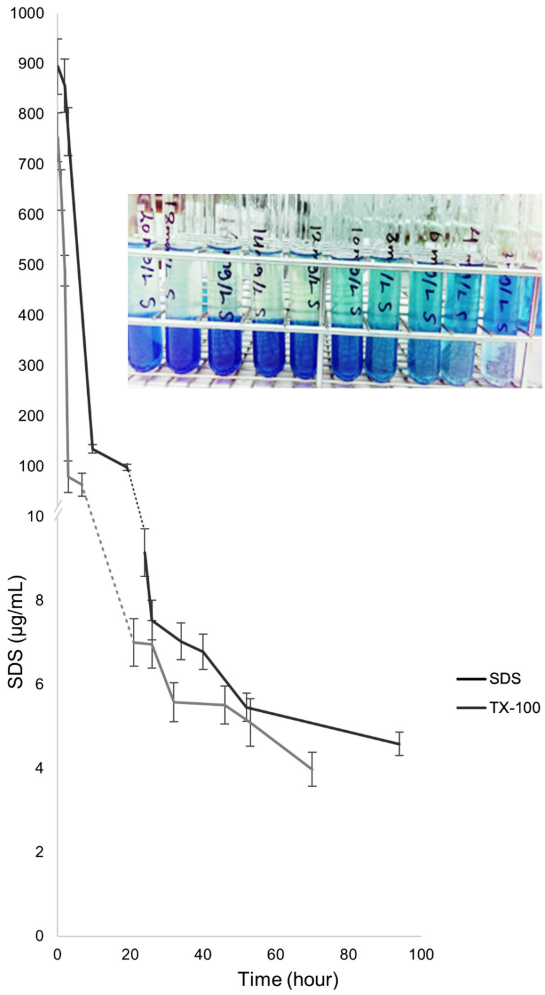

Figure 4-7. Concentration of SDS in 1 mL distilled water incubated for 24 hours with specimens from both SDS and TX-100 groups collected at various time points. Concentrations were measured using a colorimetric assay containing methylene blue and chloroform. The image on the graph shows the test tubes containing standard solutions of SDS in two hydrophilic (top) and hydrophobic (bottom) phases. Note the more saturated blue colors in test tubes containing higher concentration of SDS standard solutions

4.4 DISCUSSION

Natural extracellular matrices have been shown to be promising scaffolds with tissue-specific potential to support cell growth and differentiation [192-194]. They can be obtained by decellularization of native tissue either by perfusing detergent solutions through the vasculature or diffusion of this solution through pieces of tissue [158]. This procedure removes any cellular materials from the matrix that might cause immune reaction after transplantation. Sodium

dodecyl sulfate is by far the most preferred agent for removing cell debris [3, 195]. However, as a strong ionic detergent, SDS can denature proteins [196, 197] and damage phospholipid membranes [198] leading to cell necrosis [199]. Accordingly, one should take sufficient care to remove residual SDS after the decellularization process. This critical issue increases the need for a standard method to evaluate cECM cytotoxicity after decellularization.

In this chapter, a novel, covenient, and rapid method to examine cytotoxicity of acellular cECM was developed. There were several previous chemical methods for quantification of residual SDS [187, 188, 200], but there was still a need to determine a threshold for SDS concentration leading to cell toxicity. Disruption of red blood cells due to SDS contact is a relevant indicator that I used to measure cytotoxicity of cECM. This hemolysis assay is a practical method that directly measures cell death caused by SDS presence that can also be applied to any other tissue or scaffold. Data shown in Figures 4-3 and Figure 4-4 suggest that the hemolysis assay results are generally consistent with the cell viability assay results on acellular tissue (e.g. samples with <20% hemolysis also show <20% dead cells), which is a critical factor in preparation of cECM.

Our data also support the use of Triton X-100 to extract retained SDS trapped in the structure of cECM as suggested by previous researchers [3, 201]. SDS is a relatively small ionic molecule that can diffuse through the collagenous fibers and get trapped there because of its ionic nature [202]. As shown in Figure 4-6, relying just on PBS washes to remove SDS would result in dissociated collagen fibers that not only affects the mechanical strength of cardiac tissue but also might change the seeded cell proliferation and gene expression patterns. TX-100 is a non-ionic detergent that can bind to SDS and facilitate its removal from the cECM, as previously reported [30].

To summarize, in this chapter the hemolysis assay was introduced as a rapid colorimetric method that can be used to examine certain aspects of cytotoxicity of a tissue or scaffold due to residual detergents. More studies need to be performed to see if this assay can be used for other cytotoxic agents such as peracetic acid or ethanol, which are common sterilizing chemicals in biomedical applications. Additional optimization of the hemolysis assay (e.g. ratio of tissue to red cells, contact time) would improve the utility and versatility of the assay.

5 CULTURE OF HUMAN INDUCED PLURIPOTENT STEM CELL-DERIVED CARDIOMYOCYTES ON ACELLULAR ECM SLICES FROM WHOLE DECELLULARIZED PORCINE HEARTS

5.1 INTRODUCTION

Since the emergence of tissue engineering [203] the field has encountered paradigm shifts such as the introduction of human induced pluripotent stem cells [204] and using whole organ decellularization technology. The heart has very limited regeneration capability and an infarction causes loss of about one billion cardiomyocytes, diminishing the pumping function of the heart [155]. The purpose of cardiac tissue engineering is to repair or replace the damaged portion of the heart by generating biocompatible tissues that are fully functional and durable, capable to grow with the recipient [174]. As previously discussed in the first chapter, Table 1-2, various cell types have been introduced for the regenerative medicine purposes. Fetal cardiomyocytes, fibroblasts, smooth muscle cells and various types of stem cells such as embryonic, bone marrow, hematopoietic and induced pluripotent have been studied in cardiac tissue engineering and they have demonstrated varying levels of success in myocardial regeneration [205].

Induced pluripotent stem cells have unlimited self-renewal capability while retaining differentiation potential [206]. Through optimized staged differentiation protocols, these cells can be implemented for cardiac differentiation with high efficiency [207, 208]. Variability of differentiation efficiency, heterogeneity in the differentiated cardiac cell population, scale-up difficulties and immaturity of the differentiated cardiac cells are the challenges that currently

exist. One of the effective tissue engineering approaches for overcoming these issues is designing systems based on biomaterial scaffolds [206].

In this chapter, the effectiveness of porcine cardiac extracellular matrix (cECM) as a supporting scaffold for cardiomyocytes (CMs) differentiated from human induced pluripotent stem cells (iPSCs) was demonstrated. Acellular cECM was produced in an automated, pressure-controlled whole heart decellularization apparatus (as described in Chapter 3) and human iPSCs generated from peripheral blood monocytes (according to the study by *Riedel et al.* [209]) were used for CM differentiation. Differentiated CMs on cECM exhibited improved phenotype maintenance, elongation, arrangement and beating function compared to regular cell culture plates.

5.2 MATERIALS AND METHODS

5.2.1 DECELLULARIZATION AND SAMPLE PREPARATION

The procedures for harvesting and decellularization are described in sections 3.2.1, 3.2.2 and 3.2.3. After the final TX-100 perfusion, the hearts were perfused with non-recycled water for a minimum of 4 h followed by perfusion of 5% ethanol for 30 min. Perfusing the heart with 5% ethanol makes the frozen cECM less brittle at -21 °C which is helpful for slicing with a cryostat machine. Decellularized hearts were then removed from the apparatus, dissected open and the left ventricles were separated. A cryostat machine (HM525 NX, Thermo Scientific®, Pittsburgh, PA) was used to make 300 µm slices and a 12 mm biopsy punch (Acuderm® Inc., Fort Lauderdale, FL) was used to make round cuts. The slices were mounted on 10 mm round coverslip (Ted Pella®, Redding, CA) with the corners hooked to the other side of the glass by pressing them with another coverslip. Coverslip-mounted samples were placed in 48-well plates

and 1 mL of an antibiotic solution containing 100 U/mL penicillin, 100 µg/mL streptomycin, 25 µg/mL amphotericin B in 75% ethanol was added to each well. The samples were incubated for 2 h at room temperature on a rotary shaker. Each well was then washed 3 times with sterile PBS and the plates were centrifuged at 1500 ×g to remove trapped air bubbles from the wells. Each well was then filled with 500 µL of Dulbecco's Modified Eagle Medium (DMEM, Gibco™), pre-warmed to 37 °C and the 48-well plates were stored at 4 °C for up to 2 weeks. Warming the DMEM is advantageous in deaeration of the medium and preventing bubbles forming on the cECM.

5.2.2 CHARACTERIZATION OF THE CECM

In order to demonstrate the acellularity of the cECM slices, amounts of residual DNA in the cECM were measured and compared to the native heart samples without decellularization. DNA content measurement was performed using the protocol described in section 3.2.4.

For surface characterization and porosity analysis of the decellularized cECM, 5 mm × 5 mm × 5 mm samples were prepared for SEM with sample preparation and image acquisition protocols similar to section 4.2.6.

5.2.3 CELL CULTURE AND DIFFERENTIATION

Human iPSCs generated from peripheral blood monocytes (PBMCs) as previously described by *Riedel et* al [209], cryopreserved at -190°C were used in this study. The cells were thawed and seeded in 6-well plates, coated with vitronectin (VTN-N, Gibco™) based on the manufacturer's protocol. Growing and expansion of human iPSCs was performed in Essential 8™ medium (Gibco™) and StemPro® Accutase® (Gibco™) was used as a cell dissociation reagent to detach the iPSCs from plates when passaging at 85% confluence. Cell suspensions

were centrifuged at 160 ×g for 3 mins and the dilution of passaging was optimized to achieve 85% confluency in 3 to 4 days. Rho-associated protein kinase (ROCK) inhibitor (RevitaCell™, Gibco™) was added to the cell suspensions for the first 24 h after each passage to improve the survival rate.

Cardiomyocyte (CM) differentiation of iPSCs was performed on monolayer cultures and the process was controlled visually. The differentiation process included stage-specific application of growth factors and small molecules and was based on the embryo's cardiac developmental program. Three stages of differentiation consisted of a mesodermal differentiation (Stage-1) followed by cardiac progenitor cell differentiation (Stage-2) and finally, differentiation into cardiomyocytes (Stage-3). Starting on day 0, differentiation was started on 90% confluent iPSCs by replacing the Essential 8™ medium with a DMEM/F12 medium supplemented with B-27® without insulin (Gibco™) and Activin A (50 ng/mL). On day 1, the medium was replaced with fresh DMEM/F12 medium supplemented with B-27® without insulin, plus basic fibroblast growth factor (bFGF) and bone morphogenetic protein 4 (BMP4), 10 ng/mL each. On day 3, DMEM/F12 medium supplemented with B-27® without insulin, but supplemented with a WNT signaling pathway inhibitor (C59) was given to the cells. On day 5, the medium was replaced with complete cardiomyocyte medium (B-27®-supplemented RPMI based) and renewed every 3 days.

5.2.4 RECELLULARIZATION OF THE CECM SAMPLES

On day 4 of the differentiation process, the cells were dissociated using 1 mL of TrypLE™ (Gibco™) enzyme. After centrifugation at 160 ×g for 3 mins, the cells were resuspended in complete cardiomyocyte medium. A Moxi Z™ (Orflo™, Ketchum, ID) automatic cell counter was used to count the cells and the cell suspensions were diluted to a

concentration of 2×10^6 cells/mL. ROCK inhibitor was added to the cell suspensions and 500 µL was then pipetted to each well of the 48-well plates including the coverslip-mounted cECM. Plates were then placed in a 37 °C incubator with 5% CO_2 and the media was renewed every other day. CellTracker™ Green CMFDA Dye (Molecular Probes™) was used according to the manufacturer's instructions in order to label the cells reseeded on the cECM. From the stock 1000X dye, 0.5 µL were added to 500 µL of media and the cells were incubated for 30 mins in 37 °C incubator with 5% CO_2. Media was then replaced with complete cardiomyocyte media and an EVOS™ FLoid™ Cell Imaging Station (Thermo Fisher Scientific®) was used to visualize the cells adhered to the cECM.

5.2.5 VIABILITY ASSAY

Assessment of cell viability and cytotoxicity of the experiments was performed using a resazurin-based reagent (Molecular Probes™, Carlsbad, CA) with a protocol modified for human iPSCs. Immediately after renewing the complete cardiomyocyte medium in 48-well plates, 2.5 µL of the stock 100X reagent was added to each well and the plates were incubated in a 37 °C incubator with 5% CO_2. After 15 mins, 200 µL of the assay media were transferred into black 96-well plates and the fluorescence intensities were measured with an excitation wavelength at 560 nm and emission at 590 nm in a microplate reader (Synergy 2®). Fluorescence intensities of samples from the 48-well plates containing the cECM were compared to vitronectin-coated 48-well plates, without cECM, containing known amounts of cells.

5.2.6 HISTOLOGY AND IMMUNOFLUORESCENCE IMAGING

Histology characterizations of the cECM samples were performed with a similar method to which is described in section 3.2.8.

Recellularized cECM samples and undifferentiated iPSCs on vitronectin-coated coverslips were fixed in 4% paraformaldehyde (Sigma- Aldrich®) in PBS for 1 h. The samples were then washed with PBS and incubated in membrane blocking solution (Life Technologies™) at 4 °C overnight. Primary antibodies for cardiac troponin T (cTNT), wheat germ agglutinin (WGA), SOX2, OCT4, CDH1 (E-cadherin), CDH2 (N-cadherin), all purchased from Life Technologies™ were diluted 1:100 in the blocking solution and the samples were incubated for 2 h at room temperature. The samples were then washed with PBS and incubated in anti-mouse and anti-rabbit secondary antibodies (Life Technologies™) diluted 1:100 in the blocking solution for 1 h at room temperature. NucBlue® reagent (Molecular Probes™) diluted in PBS was then used to stain the nucleus of the cells. The samples were then mounted on microscope slides with coverslips using SlowFade® Gold Antifade mountant (Molecular Probes™) and imaged using an Olympus™ FluoView FV1000 (Center Valley, PA) laser scanning confocal microscope.

5.3 RESULTS

5.3.1 DECELLULARIZATION

Porcine hearts were harvested (n=10) from slaughter size female swine. Decellularization was accomplished with total SDS exposure of 6 hours in a pressure-controlled apparatus with an automated pressure increasing function. It was observed that during the first 2 hours of PBS and distilled water washes, outlet fluids from the vena cava were red, indicating removal of residual blood and thromboemboli. After the first hour of PBS perfusion, alternating to hypotonic distilled water, the flowrate was significantly reduced in order to maintain the controlled

pressure, suggesting an increase in the coronary vessels internal resistance due to the enlargement of the cells and reduction of coronary vessel sizes.

The hearts were decellularized with similar results to section 3.3.1. Figure 5-1 shows the results for decellularization performed for the recellularization studies which contains similar data to Figure 3-2 and 3-3.A. Figure 5-1.A represents a native heart and Figure 5-1.B shows a heart after the 5% ethanol perfusion in the decellularization process. H&E staining of native (Figure 5-1.C) and decellularized (Figure 5-1.D) cECM show complete removal of cytoplasm and nucleus.

Comparing native sirius (Figure 5-1,E) and orcein (Figure 5-1.G) stains to cECM sirius (Figure 5-1.F) and orcein (Figure 5-1.H) demonstrate retention of general collagen and elastin fibers after the decellularization process.

Images acquired with SEM show porosity of the decellularized cECM and available strings of collagenous fibers for cells to attach at 2500X (Figure 5-1.I) and 12000X (Figure 5-1.J) magnifications. The results from the PicoGreen® assay showed more than 98% decrease in the amount of DNA after decellularization in the cECM samples. As shown in Figure 5-1.K the average amount of DNA in the samples from left ventricle of native hearts (n=5) was 691 ng/mg of lyophilized tissue and decreased to 11 ng/ mg of lyophilized tissue in the decellularized samples (n=5).

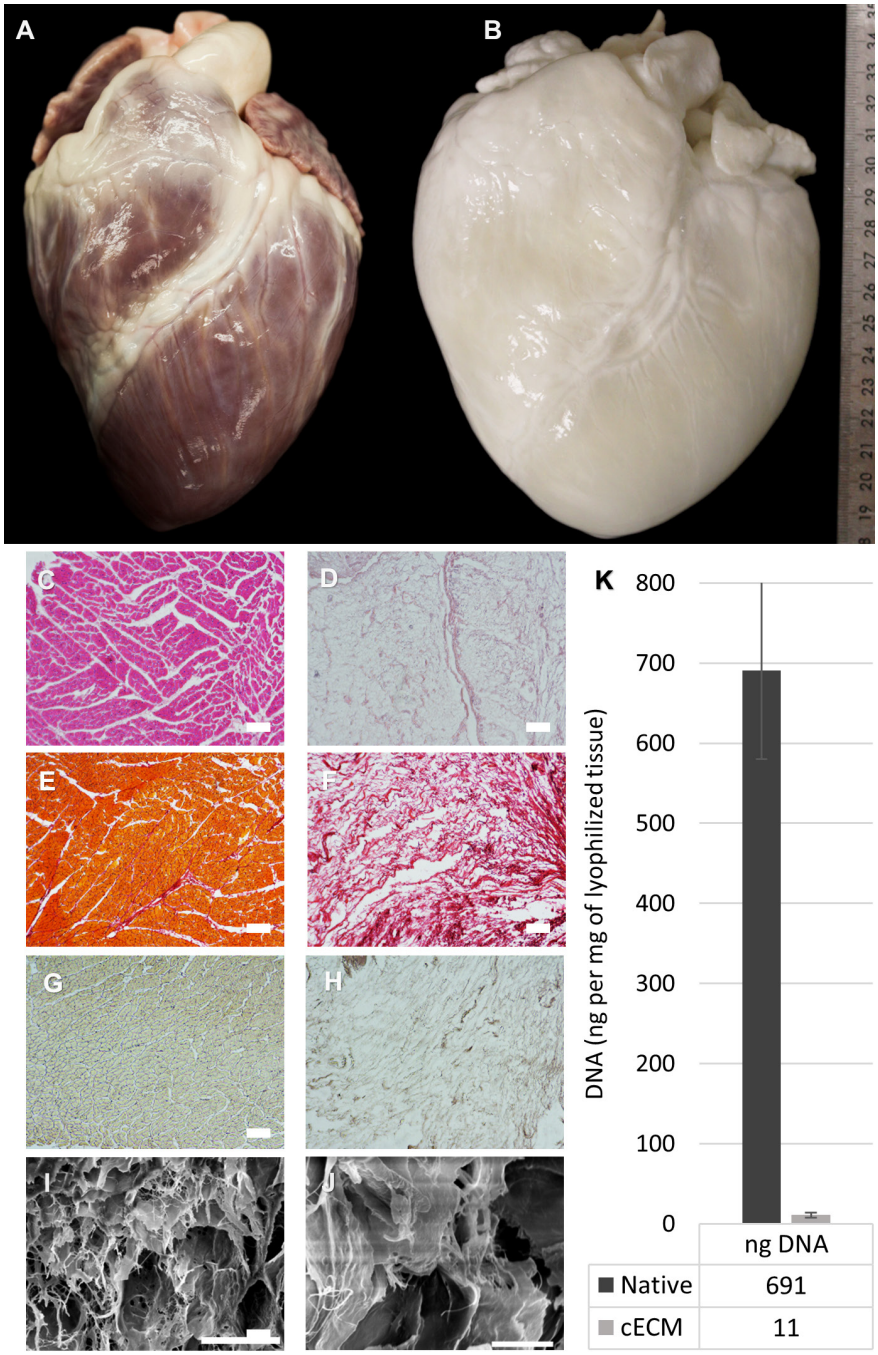

Figure 5-1. Representative native (A) and decellularized (B) porcine hearts. H&E staining of native (C) and decellularized (D) samples show removal of cells and debris. Sirius and orcein staining of native (E,G) cECM compared to decellularized cECM (F,H) demonstrate retention of general collagen (E,F) and elastin fibers (G,H) after the decellularization process. SEM images (I,J) show porosity of the decellularized cECM and strings of collagenous fibers. DNA contents (ng/mg lyophilized tissue) of native and decellularized samples demonstrate more than 98% DNA removal in the decellularization process. Histology images were acquired using 10X optical lens and the scale bars represent 100 µm. SEM images have scale bars for 30 µm (I) and 5 µm (J).

5.3.2 CELL CULTURE AND DIFFERENTIATION

The healthiest iPSCs with least self-differentiated colonies were observed on the third and fourth passages after thawing. Figure 5-2.A shows the pathway for CM differentiation of iPSCs with 3 differentiated stages of mesodermal multipotent stem cells, cardiac progenitors and CMs. At the cardiac progenitor stage, which was achieved by day 4, the cells were reseeded on the cECM. Figure 5-2.B shows a slice of cECM mounted on a 10 mm round glass coverslip.

Before initiating the CM differentiation, self-renewal function and pluripotency of the cells were verified by immuno-staining for OCT4 and SOX2 as represented in Figure 5-2.C-D with green and red colors respectively. It was observed that by day 2, OCT4 and SOX2 could not be detected in the stage-1 and stage-2 differentiated cells, as shown in Figure 5-2.E-H. Staining for N-cadherin and E-cadherin in the differentiating iPSCs at day 0, day 2 and day 4 demonstrated the presence of CDH1 and absence of CDH2 on day 0, which was reversed by absence of CDH1 and presence of CDH2 on day 2. By day 4, neither E-cadherin nor N-cadherin could be detected as shown in Figure 5-2.I-N. DAPI blue staining was used in represented images (Figure 5-2.C-N) for the cell nuclei. Visual appearance of the differentiating cells in 6-well plates were examined by light microscopy and the transition of the iPSCs into CMs is shown in Figure 5-3. Note that the cells elongate and become more opaque during the transition.

5.3.3 RECELLULARIZATION OF THE DECELLULARIZED SAMPLES

One million cells on day 4 were reseeded on coverslip-mounted cECM in 48-well plates and negative control samples were not reseeded with any cells. It was observed that cECM slices which were not strongly hooked to the coverslips curled up and became ball-shaped, not suitable for micro-imaging or video recording. This phenomenon was not observed in any of the negative control samples. Cells that were adhered to the cECM samples were fluorescence labeled with

CMFDA followed by fixation and DAPI nuclei staining 24 h after reseeding. Figure 5-4.A shows a representative stitched image from a recellularized sample with a scale bar of 1 mm.

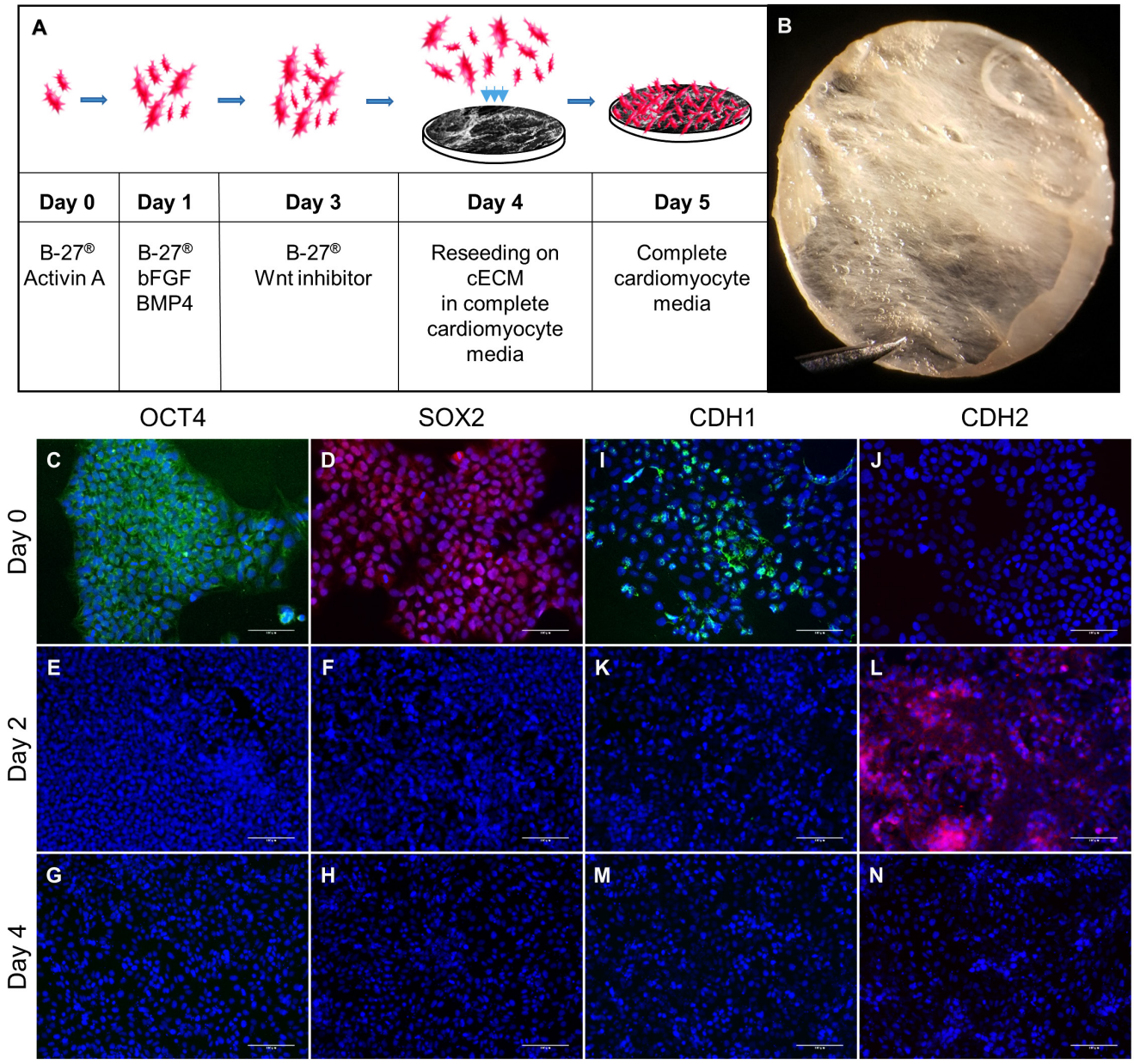

Figure 5-2. Differentiation of human iPSCs into CMs and recellularization of the cECM slices. Diagram of the differentiation pathway (A) and a representative image of a slice of cECM mounted on a 10 mm diameter coverslip (B). Fluorescence immunostaining images for OCT4, SOX2, e-cadherin (CDH1) and n-cadherin (CDH2) of cells at different stages of differentiation (C-N) indicates pluripotent, mesodermal and cardiac progenitor cells. DAPI blue was used in all fluorescence images for staining of the nuclei. All scale bars represent 100 µm.

Figure 5-4.B presents a 10 times higher magnification on the same sample, illustrating a confluent presence of reseeded cells on the cECM. After 10 days of culture, various areas of the cECM started to beat simultaneously and 7 days afterwards, the beating function was improved by becoming stronger and more synchronized throughout the samples. Figure 5-4.C shows a stitched image acquired with cTNT immunostaining of a representative beating cECM. Figure 5-4.D shows a portion of the beating cECM from the same samples on a light transmitted microscope with relaxed and contracted phases of a representative zone, marked with a blue and a red line respectively.

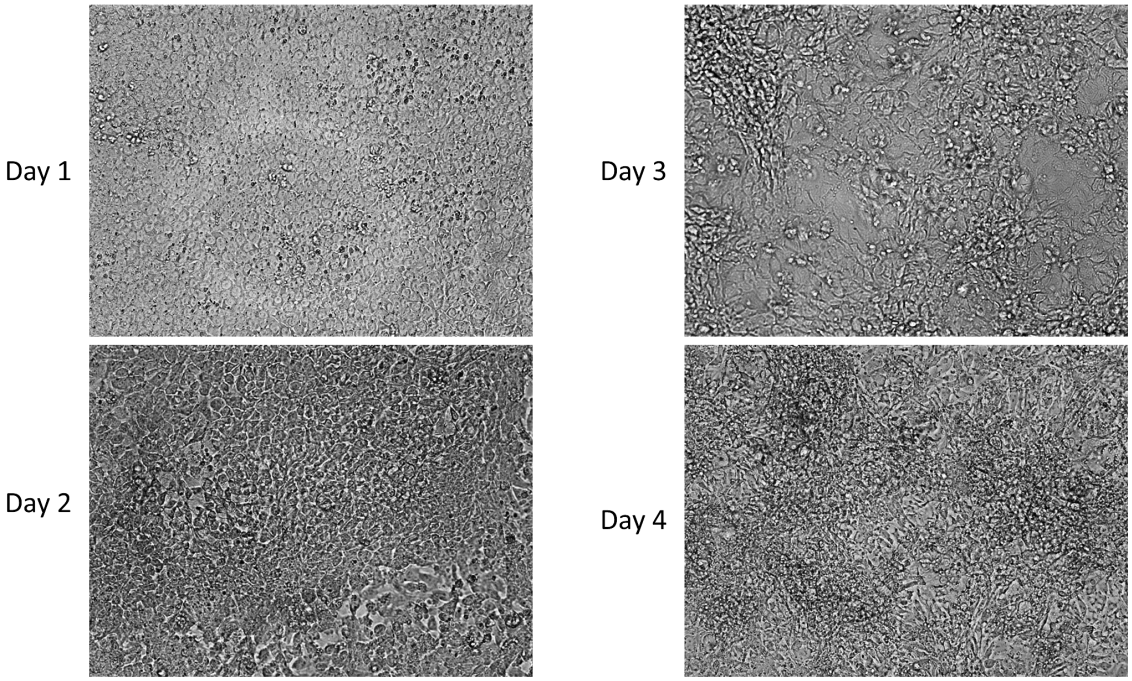

Figure 5-3. Visual appearance of the differentiating cells in 6-well plates. Note that the cells elongate and become more opaque during the transition.

Representative cTNT, WGA and DAPI immunostaining images of CMs derived from iPSCs, on cECM (Figure 5-5.A) and on vitronectin-coated well plates (Figure 5-5.B) shows improved arrangement and organization in position of the cells.

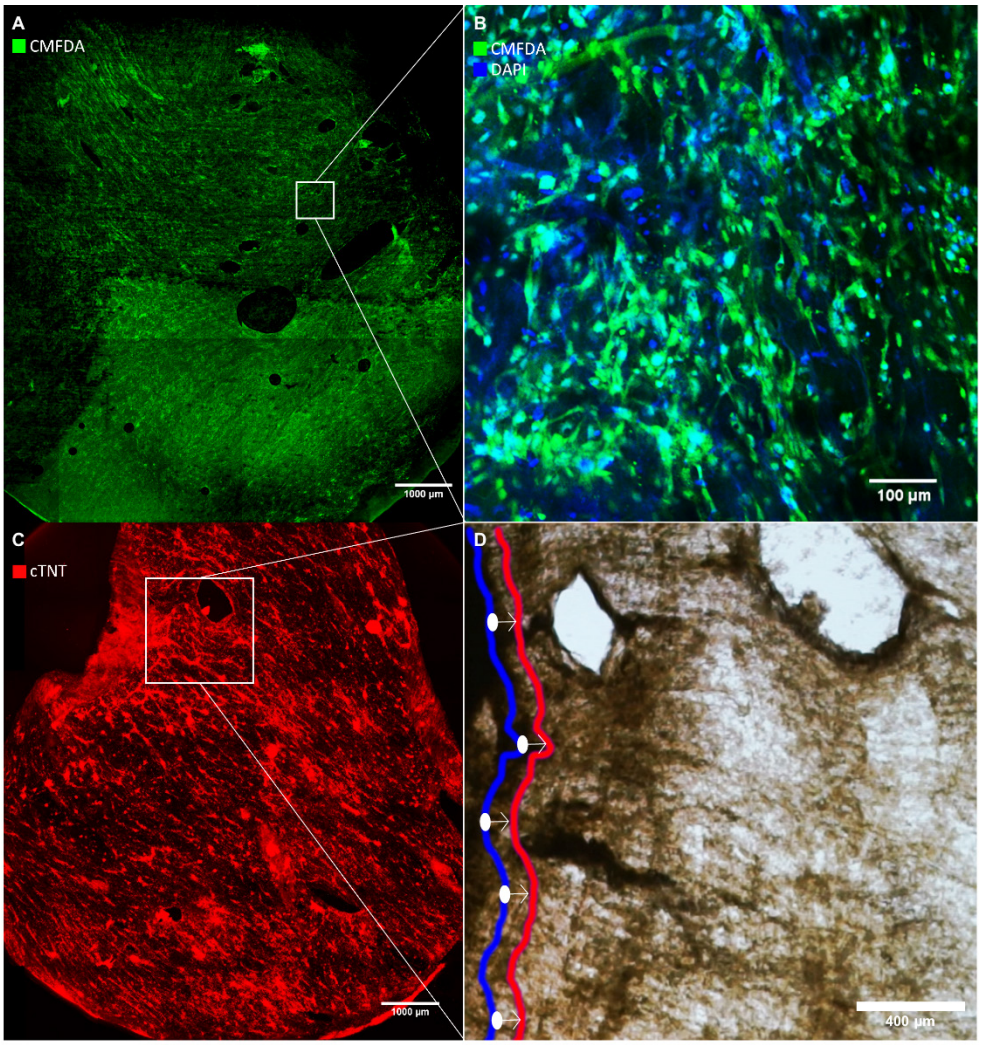

Figure 5-4. A representative stitched image from a recellularized sample with a scale bar of 1 mm (A) and a 10 times higher magnification on the same sample (B) illustrating a confluent presence of reseeded cells on the cECM 2 days after reseeding. A representative stitched image acquired with cTNT immunostaining of a beating cECM (C) shows presence of differentiated CMs throughout the cECM. Contraction of the same sample is shown with relaxed and contracted phases, marked with a blue and a red line respectively from a representative zone (D).

Representative videos of beating CMs, 20 days after reseeding, on the cECM sheets (Supplementary Video-3, accessible online: https://goo.gl/FkznlV) and vitronectin-coated plated (Supplementary Video-4, accessible online: https://goo.gl/HzqMNd) shows the effect of cECM in preserving the CM phenotype and improving the beating function. A rotating 3D confocal

image (Supplementary Video-5 accessible online: https://goo.gl/2VffY4) from a representative recellularized sample is also available showing the 3D structure of CMs on cECM.

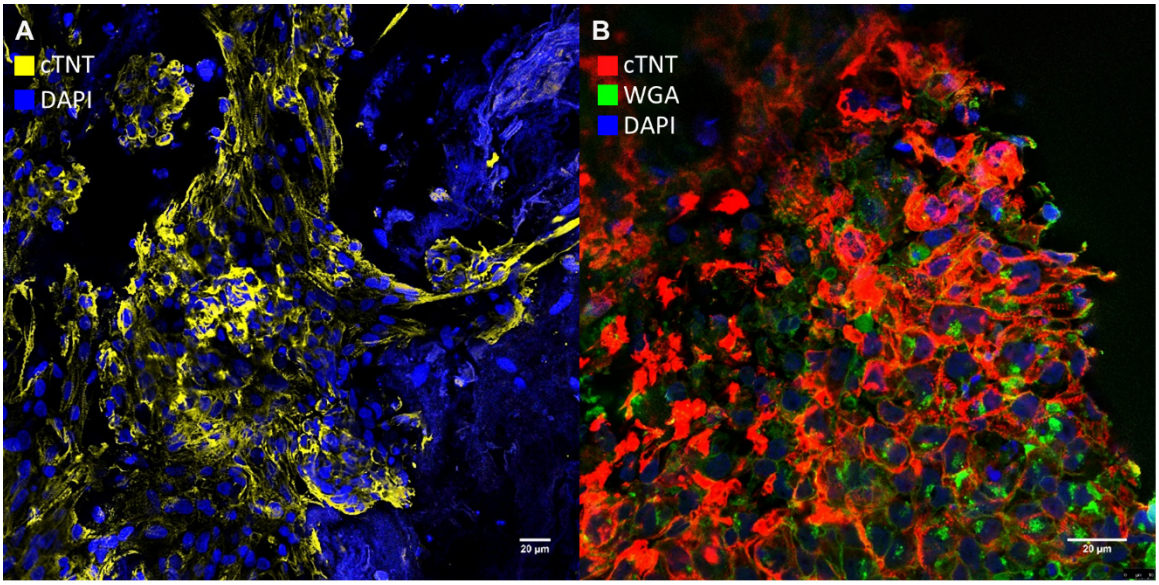

Figure 5-5. Representative cTNT, WGA and DAPI immunostaining images of CMs derived from iPSCs, on cECM (A) and on vitronectin-coated well plates (B) shows improved arrangement and organization of the cells.

5.3.4 VIABILITY ASSAY

Based on the assay manufacturer's instructions, a calibration curve for the fluorescence intensity of samples versus the number of live cells was made using known amounts of cells in vitronectin-coated 48 well plates and the regression R square was observed to be 0.99 (Figure 5-6.A). The number of live cells were measured in the recellularized samples (N=3) 1, 2, 4, 10 and 14 days after reseeding. As shown in Figure 5-6.B, the average number of live cells on the cECM started from $(7.48 \pm 0.82) \times 10^5$ live cells on day 1, increased slightly to $(7.56 \pm 0.99) \times 10^5$ live cells by day 4 and then declined to $(6.80 \pm 0.73) \times 10^5$ live cells 14 days after reseeding.

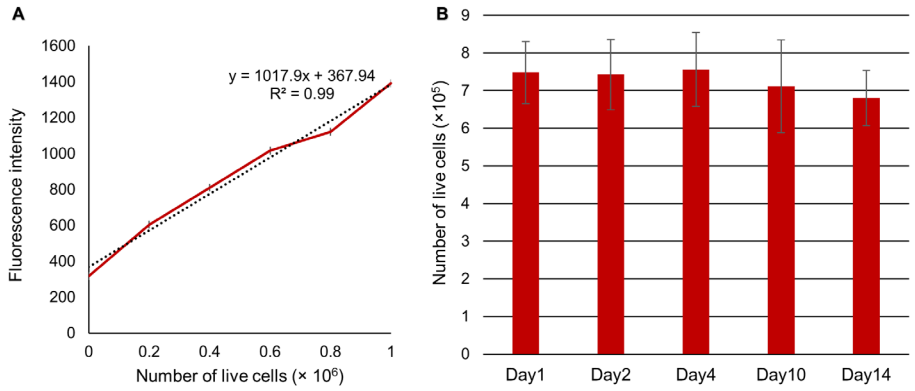

Figure 5-6. Viability assay for calculating the number of live cells on the cECM. A calibration curve was made according to the manufacturer's protocol (A) and the number of live cells on the cECM was calculated on day 1 to day 14 after reseeding (B).

5.4 DISCUSSION

The pioneering work by Ott *et al*. brought attention to the potential of using natural ECM obtained by decellularization, as a scaffold for recellularization and tissue engineering [2]. Since then the decellularization process has been extensively explored [158] especially in search of protocols for human-sized organ decellularization. Many different decellularization approaches have been introduced for hearts [21-23, 25, 123, 194, 210], kidneys [123, 145, 148], lungs [123, 135, 162] and livers [123, 142]. As described in this chapter 3 of this dissertation, for whole porcine heart decellularization, coronary retrograde perfusion combined with automated pressure-controlled systems improves the decellularization efficiency.

In this study, decellularization was accomplished with 6 hours of SDS exposure resulting in residual DNA content lower than the accepted standard for successful decellularization [23]. Due to the denaturing aspect of using SDS in the decellularization process [8], the concentration of SDS used in this study was lower than other suggested protocols [123] resulting in enhanced retention of collagen and glycosaminoglycans as shown in chapter 3, Figure 3-4. In addition to

the biocompatibility, porosity of the scaffolds produced for tissue engineering is an important design factor [211]. Acquired SEM images from the decellularized samples in this study demonstrate high porosity as a result of complete cell removal and therefore cECM can be used as an appropriate scaffold, naturally designed for cell support.

Derivation of embryonic stem cell lines from human sources [212] is very significant in cardiac tissue engineering because of their ability to proliferate indefinitely *in vitro* and giving rise to any tissue. However use of these cells has major drawbacks including requirement of human embryos for development, raising ethical issues, and immunogenicity difficulties due to the heterologous source of these cells. Introduction of human iPSCs could largely overcome the limitations of embryonic stem cells [213]. So far, development of human iPSCs has mostly been through fibroblast cells and although a skin biopsy might be considered negligibly invasive, a blood draw is simpler and more acceptable particularly in the infant population [209]. It has been shown that PBMC-derived human iPSCs can be differentiated into cardiomyocytes with high efficiency [214] and therefore is useful for myocardial tissue engineering [155]. Nevertheless, there are limitations for the use of these cells in clinical therapeutics. Limitations such as the lack of an established method for separating the atrial and ventricular CMs and variability of differentiation between the iPSC cell lines, should be addressed by further studies and experimentation. Atrial and ventricular CMs are district in functions and have different expression of genes. Atrial CMs have shorter duration of action potentials and faster tension generation/ relaxation rates but create less active tension than the ventricular CMs.

It has been shown that whole heart decellularization can also be used to generate human cECM [123, 215]. However, due to the variabilities in the hearts from different donors [123], human hearts might not be a reliable source for cardiac tissue engineering. In contrast, it is

possible to obtain a controlled population as a source for creating porcine cECM. As demonstrated in this chapter, slices of porcine cECM were reseeded with CMs derived from human iPSCs and it was shown that cECM aids in preserving the CM phenotype over time (Supplementary video 3 and 4, accessible online: https://goo.gl/FkznlV and https://goo.gl/HzqMNd). CMs attached to the cECM showed arrangement in direction of the cECM fibers (Figure 5-4 and Figure 5-5.A) which was not observed in the CM samples without cECM (Figure 5-5.B).

The protocol developed in this study can be used for perfusion recellularization of large portions of decellularized hearts (e.g. left ventricle) in order to obtain a 3D recellularized working model. The ultimate goal of cardiac tissue engineering is to create a transplantable tissue with autologous cells to eliminate immunogenicity and provide enough function to replenish the loss due to cardiac disease. Many challenges however must be confronted in order to achieve the ultimate goal. The scaffolds must be repopulated with all of the necessary cell types in the myocardium including CMs, endothelial cells, vascular smooth muscle cells and stromal cells such as fibroblasts and pericytes. Robertson *et al.* [3] showed that addition of endothelial cells with CMs improves the function of recellularized rat hearts by a factor of 4 and prevents thrombosis in the transplanted engineered hearts. Appropriate placement of various cell types into their native positions is also very critical in creating engineered functional tissues suitable for transplantation [7, 155, 174].

Data from the viability assays indicated that from 10^6 Stage-2 cells that were reseeded on the cECM, 0.75×10^6 cells were attached to the scaffold by day 1 resulting in a 75% reseeding success which is significantly higher than the perfusion reseeding success reported by Lu *et al.* [20]. The number of live cells did not change drastically in 14 days demonstrating the limited

proliferation ability of terminally differentiated CMs which is a well-known characteristic of these cells [59, 174].

The heart contains dense tissues and a 1 cm^2 slice, with 100 µm thickness of an adult left ventricle, contains approximately 10^6 CMs [7]. The main challenges involved with culturing a more dense cardiac tissue are increasing the number of cells on the cECM, and overcoming the oxygenation and nutrient requirements. Culturing human iPSCs on the cECM and taking advantage of the highly proliferative stage of the stem cells to confluently repopulate the scaffold might be a viable approach to achieve a dense tissue. However, in our experiments with culturing undifferentiated iPSCs on cECM, the adherence of stem cells to the scaffold was very insignificant (data not shown). The reason for this observation might be the lack of iPSCs' integrin repertoire involved with adherence to collagen-I, which is the main component of ECM [126, 128, 216].

6 DISSERTATION SYNOPSIS

6.1 CONCLUSIONS

As discussed in chapter 1, the strategy of whole heart decellularization followed by recellularization with autologous cells has significant advantages in cardiac tissue engineering and regenerative medicine therapies. Although rodent models are beneficial in providing initial results and proof of concept for cardiac tissue engineering, a scale-up is necessary to make the strategy useful for mankind. In this research I found that generally, decellularization of porcine hearts is more challenging than murine hearts and can take much longer which is due to the larger size and structural complexity of porcine hearts.

In this study, porcine hearts were harvested fresh from a local abattoir and a protocol was developed for effective preparation of the hearts for decellularization. The developed protocol (section 3.2.1) enables an inexpensive source for obtaining organs for tissue engineering research and contains important details such as the necessary wash of the heart with 10 Units/mL heparinized PBS, and antibiotics. I found that the successful decellularization most likely fails if the hearts are not washed with heparinized PBS thoroughly after harvesting.

The automated pressure controlled apparatus that was described in section 3.2.2 provides accurate control on the flow pressure on the heart during the decellularization process. The gradual pressure increase that is added to the computer programming of the controller also plays an important role in maintaining the vasculature and the aortic valve of the hearts intact. I

observed that a sudden increase in the pressure on the heart damages the aortic valve and results in unsuccessful decellularization.

The resulting acellular cECM contained 11 ng of DNA per mg of lyophilized tissue which is well below 50 ng/mg established criteria for successful decellularization and demonstrating 98% cell removal. In the macrophage stimulation assay, cECM samples demonstrated limited potential for causing an immune response. I found that culturing macrophages is more challenging than most other mammalian cells because they don't adhere to the plates and as stated in section 3.2.6, it's important to use DMEM without phenol red to avoid interferences in the Griess assay.

As shown in Figure 3-4, the developed decellularization assay demonstrated retention of the GAGs particularly in the left heart and collagen proteins almost throughout the heart. Although the Sircol® assay for collagen quantification produced reliable results, I found the hydroxyproline assay described in section 4.2.5 more user friendly and accurate.

The cECM samples exhibited a high capacity for recellularization. I designed and created a perfusion bioreactor and recellularized the decellularized right ventricle of the hearts with human fibroblasts and endothelial cells. Perfusion of the endothelial cells through the vasculature was effective in the attachment of endothelial cells to the lumen of the blood vessels throughout the vasculature. Fibroblast cells were injected in particular areas of the tissue and as shown in Figure 3-8, they have less dispersion through the tissue. Major challenges that I had in this part of research were preventing bacterial contamination of the cell culture medium during recellularization as well as proper aeration of the medium. Due to foaming, the use of a bubble

aerator is not possible; therefore I used sterile gas flow in the bioreactor and added stir bars to agitate the medium.

In chapter 4 of this dissertation, I demonstrated the novel use of a hemolysis assay for determining the cytotoxicity of decellularized heart tissues due to residual chemicals used in the decellularization process. I showed that the removal of SDS was accelerated by a factor of 4 by introducing an additional 2 h of TX-100 wash in the decellularization process. The cytotoxicity of the cECM samples was eliminated in the TX-100 group after 10 h of PBS wash compared to 40 h when not including TX-100 in the process. The results from the hemolysis assay were shown to be consistent with the established cell viability live/dead assay on endothelial cells in contact with cECM specimens.

In addition, SEM images of the cECM showed the adverse effects of prolonged (up to 100 h) exposure to SDS and TX100 on collagen and the tissue structure. The preparation method that I developed and described in section 4.2.6 for SEM sample preparation includes flash freezing the sample in a frozen ethanol slurry and is much faster and less destructive compared to standard fixation and dehydration methods. However, the tissue samples still needed to be coated with conductive elements and the coating process, and if not performed carefully can alter the surface characteristics of cECM.

I was trained on how to maintain and expand cultures of human induced pluripotent stem cells and human peripheral blood monocyte derived iPSCs were obtained from Dr. Tristani-Firouzi at the University of Utah. Although the stem cell research has advanced significantly during the past couple of years, methods and strategies for maintaining a healthy population of iPSCs and differentiating them into cardiomyocytes are still imperfect and improving. Human

iPSCs need very special care. Requirements such as the need for renewing the iPSC's medium every day due to denaturation of bFGF and auto differentiating colonies in culture flasks are challenges in working with human iPS cells.

As described in chapter 5, the cells were successfully differentiated into beating cardiomyocytes in a directed differentiation pathway. The cells were directed to differentiate into a mesodermal cell type followed by cardiac progenitor and fetal cardiomyocyte phenotypes. Figure 5-2 shows the pathway protocol that was developed for differentiation of human iPSCs into CMs and reseeding them onto cECM. SOX2 and OCT4 genes were used as markers for pluripotency and CDH1 and CDH2 were used for mesoderm stage verification of the cells. Finally, differentiated CMs expressed cardiac troponin T which is shown in Figure 5-4 and Figure 5-5.

I decellularized whole porcine hearts in the automated, pressure-controlled apparatus as described in chapter 3, and prepared 300 µm slices of cECM for recellularization. A cryostat at -20 °C was used for making slices and because the 300 µm required thickness for the recellularization slices was relatively higher than standard cryostat sectioning thickness; frozen cECM samples could not be sliced without breakage. In order to solve that problem a subsequent step of 5% ethanol perfusion was added to the decellularization process and as a result the frozen cECM samples became less brittle and intact slices of 300 µm could be created. Another issue was that reseeded cECM slices curled up after one day, creating a spherical-shaped tissue not suitable for filming and imaging. In order to solve the problem, cECM slices were mounted on glass cover slips with the corners folded over and pressed against the glass.

The protocol that was developed for differentiating iPSCs into CMs and reseeding them on cECM slices was described in sections 5.2.3 and 5.2.4. Using that protocol acellular cECM slices were recellularized with human CMs. After 10 days the scaffolds started to beat and it was shown that cECM improves the overall function of the CMs by preserving the CM phenotype and arrangement of the cells.

In this study, slices of cECM were recellularized with CMs differentiated from human iPSCs. In the developed protocol, differentiation started in cell culture plates and differentiating cells at cardiac progenitor stage were reseeded onto the cECM. It was shown that the number of viable cells decreased after reseeding and did not increase during 14 days of culture. My preliminary results from culturing human iPSCs on cECM before initiating the differentiation were not successful and the cells that attached to the cECM did not survive.

The described methods in this dissertation enable the combination of human iPSCs as an autologous cell source with porcine acellular cECM as the scaffold for mechanical and biochemical cell support in order to create a functional cardiac tissue. This method can be used for tissue engineering and regenerative medicine therapies in the future.

6.2 RECOMMENDATIONS FOR FUTURE STUDIES

In this study a decellularization process was optimized based on using SDS as the main surfactant to remove the cellular debris. Although the decellularization process was shown to be effective in creating cECM acceptable for cardiac tissue engineering, downsides such as the necessary prolonged washes to remove cytotoxicity still exist. I therefore suggest additional research on decellularization with various materials.

As an example, my preliminary results from decellularization with a 0.1 N solution of sodium hydroxide instead of SDS, showed a decrease in the overall decellularization time. The concentration of NaOH that I used for decellularization was 25 times lower than that for vascular corrosion casting and the decellularization was performed at room temperature. Sodium hydroxide creates a very corrosive base at high concentrations (>1 N). On the other hand, for centuries people have been making soap by mixing fat and caustic soda in a process called saponification. Cellular membranes mostly consist of phospholipid layers and it is possible that caustic soda reacts with the phospholipids, creating surfactants that help in decellularization of the organ without damaging extracellular proteins.

This hypothesis can be tested and analyzed by decellularizing hearts with various concentrations of NaOH, measuring the remnant DNA contents as well as collagen and GAGs. SEM imaging and recellularizing capacity of the decellularized cECM must also be studied to ensure that the basic solutions do not adversely alter the cECM protein structures.

Although decellularization with NaOH might be advantageous in ways, many challenges are involved with using basic solutions that need to be dealt with. These challenges are large disposal volumes of basic solutions and optimizing the decellularization process to enhance cell attachment to the cECM in the recellularization process.

In order to perform 3D recellularization of the cECM, special bioreactors need to be designed to overcome challenges such as aeration of the growth medium, maintaining the sterility and optimizing the amount of required medium in the bioreactor. The designed bioreactors can consist of several chambers for purposes like aeration or decontamination,

reservoirs for holding the growth medium and a main chamber that is large enough for whole heart recellularization.

For future studies, I recommend designing a bioreactor with a larger chamber for whole heart recellularization and advanced control systems. A similar control system as described in section 3.2.2 can be created to control the environment during recellularization. Concentration of CO_2 and pH of the medium can be monitored with special sensors and the data can be used to control the flow rate of the perfusion and determine when the media needs to be renewed. This bioreactor can be used for recellularization of whole hearts or portions of the heart with various cell types such as HUVECs, HCFs and eventually iPSCs differentiated into CMs.

Engineering the cECM in order to enhance the non-differentiated iPSCs attachment to the scaffolds has also great importance and I recommend performing studies in this regard. Having the iPSCs attached to the cECM eliminates the need for expanding the cells in cell culture flasks and improves the overall viability of the differentiated cells by avoiding the dissociation step. Methods such as coating the cECM with vitronectin, laminin or fibronectin can be studied for engineering the cECM. Human iPSCs can then be reseeded onto the coated cECM and after 24 h, the cells can be fluorescently labeled with calcein and imaged with confocal laser scanning microscopy. Resazurin based assays similar to section 5.2.5 can also be used to check the viability of the cells on the cECM.

Another recommendation for future studies is 3D recellularization of the cECM in a perfusion bioreactor. However, for recellularizing large portions of the hearts such as the right ventricle, great numbers of cells are needed (1 billion cells) which makes it expensive and labor intensive. Therefore I suggest starting with smaller areas of the heart that can be cannulated and

used for 3D recellularization. CMs or iPSCs can be injected or perfused into the cECM in a similar way to section 3.2.12 and cultured for 10 days. Histology and immunofluorescence staining can be used to determine the efficiency of the recellularization and cell types that repopulate the cECM.

In addition, co-cultures of various cell types such as human endothelial cells and cardiac fibroblasts on cECM can be explored. Multiple cell types can be added together and the function and survival rate of the CMs can be studied.

Addition of mechanical and electrical stimulation has been shown that can improve the alignment and maturation of the differentiated CMs. For future studies, mechanical machines that are able to stretch the cECM can be created and combined with electrical stimulators to exercise and pace the cells. The use of mechanical and electrical stimulation can be studied in order to obtain more mature cardiomyocytes. The alignment of CMs on the cECM can be studied by fluorescently staining the cells and using confocal laser scanning microscopy. Also the maturation level of the CMs can be studied by performing gene expression measurements of relative genes such as cTNT, SCN5A, KIR2, RYR2, BNP and ANP.

7 References

1. http://www.cdc.gov/dhdsp/data_statistics/fact_sheets/fs_heart_disease.htm.

2. Ott, H.C., et al., *Perfusion-decellularized matrix: using nature's platform to engineer a bioartificial heart.* Nat Med, 2008. **14**(2): p. 213-21.

3. Robertson, M.J., et al., *Optimizing Recellularization of Whole Decellularized Heart Extracellular Matrix.* PloS one, 2014. **9**(2): p. e90406.

4. Vacanti, J.P., *Tissue engineering and the road to whole organs.* Br J Surg, 2012. **99**(4): p. 451-3.

5. Song, J.J. and H.C. Ott, *Organ engineering based on decellularized matrix scaffolds.* Trends Mol. Med., 2011. **17**(8): p. 424-432.

6. Gilbert, T.W., T.L. Sellaro, and S.F. Badylak, *Decellularization of tissues and organs.* Biomaterials, 2006. **27**(19): p. 3675-3683.

7. Badylak, S.F., D. Taylor, and K. Uygun, *Whole-Organ Tissue Engineering: Decellularization and Recellularization of Three-Dimensional Matrix Scaffolds.* Annual Review of Biomedical Engineering, Vol 13, 2011. **13**: p. 27-53.

8. Crapo, P.M., T.W. Gilbert, and S.F. Badylak, *An overview of tissue and whole organ decellularization processes.* Biomaterials, 2011. **32**(12): p. 3233-3243.

9. Gilbert, T.W., *Strategies for tissue and organ decellularization.* Journal of Cellular Biochemistry, 2012. **113**(7): p. 2217-2222.

10. Soto-Gutierrez, A., et al., *Perspectives on whole-organ assembly: moving toward transplantation on demand.* Journal of Clinical Investigation, 2012. **122**(11): p. 3817-3823.

11. He, M. and A. Callanan, *Comparison of Methods for Whole-Organ Decellularization in Tissue Engineering of Bioartificial Organs.* Tissue Eng Part B, 2013. **19**(3): p. 194-208.

12. Arenas-Herrera, J.E., et al., *Decellularization for whole organ bioengineering.* Biomed. Mater. (Bristol, U. K.), 2013. **8**(1): p. 014106, 9 pp.

13. Badylak, S.F., et al., *Engineered whole organs and complex tissues.* Lancet, 2012. **379**(9819): p. 943-952.

14. Lin, B., T.-Y. Lu, and L. Yang, *Hear the beat: decellularized mouse heart regenerated with human induced pluripotent stem cells.* Expert Rev. Cardiovasc. Ther., 2014. **12**(2): p. 135-137.

15. Gui, L., et al., *Novel Utilization of Serum in Tissue Decellularization.* Tissue Eng Part C, 2010. **16**(2): p. 173-184.

16. Witzenburg, C., et al., *Mechanical changes in the rat right ventricle with decellularization.* Journal of Biomechanics, 2012. **45**(5): p. 842-849.

17. Akhyari, P., et al., *The Quest for an Optimized Protocol for Whole-Heart Decellularization: A Comparison of Three Popular and a Novel Decellularization Technique and Their Diverse Effects on Crucial Extracellular Matrix Qualities.* Tissue Eng Part C, 2011. **17**(9): p. 915-926.

18. Crawford, B., et al., *Cardiac decellularisation with long-term storage and repopulation with canine peripheral blood progenitor cells.* Can. J. Chem. Eng., 2012. **90**(6): p. 1457-1464.

19. Ng, S.L.J., et al., *Lineage restricted progenitors for the repopulation of decellularized heart.* Biomaterials, 2011. **32**(30): p. 7571-7580.

20. Lu, T.-Y., et al., *Repopulation of decellularized mouse heart with human induced pluripotent stem cell-derived cardiovascular progenitor cells.* Nat. Commun., 2013. **4**: p. 3307/1-3307/11.

21. Wainwright, J.M., et al., *Preparation of Cardiac Extracellular Matrix from an Intact Porcine Heart.* Tissue Eng Part C, 2010. **16**(3): p. 525-532.

22. Eitan, Y., et al., *Acellular Cardiac Extracellular Matrix as a Scaffold for Tissue Engineering: In Vitro Cell Support, Remodeling, and Biocompatibility.* Tissue Eng Part C, 2010. **16**(4): p. 671-683.

23. Remlinger, N.T., P.D. Wearden, and T.W. Gilbert, *Procedure for Decellularization of Porcine Heart by Retrograde Coronary Perfusion.* J Vis Exp, 2012(70): p. e50059.

24. Wang, B., et al., *Myocardial Scaffold-Based Cardiac Tissue Engineering: Application of Coordinated Mechanical and Electrical Stimulations.* Langmuir, 2013: p. Ahead of Print.

25. Merna, N., et al., *Optical Imaging Predicts Mechanical Properties During Decellularization of Cardiac Tissue.* Tissue Eng Part C, 2013. **19**(10): p. 802-809.

26. Momtahan, N.S., Sivaprasad; Roeder, Beverly L; Barrow, Jeffery R; Pitt, William G; Cook, Alonzo D. *Novel Thrombogenicity Analysis of Decellularized Cardiac Organs*. in *TERMIS-AM*. 2013. Atlanta, GA.

27. Guyette, J.P., et al., *Decellularizing Human Hearts: Characterizing Native Cardiac Matrix for Clinical Translation.* The Journal of Heart and Lung Transplantation, 2013. **32**(4, Supplement): p. S45.

28. Sanchez, P.L., et al., *Characterization and Biocompatibility of Perfusion-Decellularized Human Heart Matrix: Toward Bioengineering Perfusable Human Heart Grafts.* Journal of the American College of Cardiology, 2012. **59**(13, Supplement): p. E857.

29. Guyette, J.P., et al., *Perfusion decellularization of whole organs.* Nat. Protoc., 2014: p. Ahead of Print.

30. Lee, L.T., J.E. Deas, and C. Howe, *Removal of unbound sodium dodecyl sulfate (SDS) from proteins in solution by electrophoresis through Triton X-100-agarose.* J. Immunol. Methods, 1978. **19**(1): p. 69-75.

31. Huelsmann, J., et al., *A novel customizable modular bioreactor system for whole-heart cultivation under controlled 3D biomechanical stimulation.* J. Artif. Organs, 2013. **16**(3): p. 294-304.

32. Assmann, A., et al., *Development of a growing rat model for the in vivo assessment of engineered aortic conduits.* J Surg Res, 2012. **176**(2): p. 367-75.

33. Badylak, S.F. and T.W. Gilbert, *Immune response to biologic scaffold materials.* Semin. Immunol., 2008. **20**(2): p. 109-116.

34. Akhyari, P., et al., *In vivo functional performance and structural maturation of decellularised allogenic aortic valves in the subcoronary position.* Eur J Cardiothorac Surg, 2010. **38**(5): p. 539-46.

35. Gilbert, T.W., J.M. Freund, and S.F. Badylak, *Quantification of DNA in Biologic Scaffold Materials.* Journal of Surgical Research, 2009. **152**(1): p. 135-139.

36. Keane, T.J., et al., *Consequences of ineffective decellularization of biologic scaffolds on the host response.* Biomaterials, 2012. **33**(6): p. 1771-1781.

37. Ieda, M., et al., *Direct reprogramming of fibroblasts into functional cardiomyocytes by defined factors.* Cell (Cambridge, MA, U. S.), 2010. **142**(3): p. 375-386.

38. Pearl, J.I., et al., *Short-Term Immunosuppression Promotes Engraftment of Embryonic and Induced Pluripotent Stem Cells.* Cell Stem Cell, 2011. **8**(3): p. 309-317.

39. Chen, J.X., et al., *Inefficient reprogramming of fibroblasts into cardiomyocytes using Gata4, Mef2c, and Tbx5.* Circ. Res., 2012. **111**(1): p. 50-55.

40. Ohno, Y., et al., *Distinct iPS Cells Show Different Cardiac Differentiation Efficiency.* Stem Cells Int, 2013. **2013**: p. 659739.

41. Obokata, H., et al., *Bidirectional developmental potential in reprogrammed cells with acquired pluripotency.* Nature (London, U. K.), 2014. **505**(7485): p. 676-680.

42. Obokata, H., et al., *Stimulus-triggered fate conversion of somatic cells into pluripotency.* Nature (London, U. K.), 2014. **505**(7485): p. 641-647.

43. Zhao, B., et al., *Cardiac telocytes were decreased during myocardial infarction and their therapeutic effects for ischaemic heart in rat.* J. Cell. Mol. Med., 2013. **17**(1): p. 123-133.

44. Maherali, N. and K. Hochedlinger, *Induced pluripotency of mouse and human somatic cells.* Cold Spring Harbor Symp. Quant. Biol., 2008. **73**(Control and Regulation of Stem Cells): p. 157-162.

45. Turner, W.S., et al., *Engineering natural matrices: patterning cells derived from embryonic stem cells into implantable carriers that are designed to support cardiac tissue regeneration.* Journal of Tissue Engineering and Regenerative Medicine, 2012. **6**: p. 109-109.

46. Bertipaglia, B., et al., *Cell characterization of porcine aortic valve and decellularized leaflets repopulated with aortic valve interstitial cells: the VESALIO Project (Vitalitate Exornatum Succedaneum Aorticum Labore Ingenioso Obtenibitur).* Ann Thorac Surg, 2003. **75**(4): p. 1274-82.

47. Rieder, E., et al., *Decellularization protocols of porcine heart valves differ importantly in efficiency of cell removal and susceptibility of the matrix to recellularization with human vascular cells.* J Thorac Cardiovasc Surg, 2004. **127**(2): p. 399-405.

48. Weiss, M.L. and D.L. Troyer, *Stem cells in the umbilical cord.* Stem Cell Rev., 2006. **2**(2): p. 155-162.

49. Fusaki, N., et al., *Efficient induction of transgene-free human pluripotent stem cells using a vector based on Sendai virus, an RNA virus that does not integrate into the host genome.* Proc. Jpn. Acad., Ser. B, 2009. **85**(8): p. 348-362.

50. Lengner, C.J., *iPS cell technology in regenerative medicine.* Ann. N. Y. Acad. Sci., 2010. **1192**: p. 38-44.

51. Wu, S.M. and K. Hochedlinger, *Harnessing the potential of induced pluripotent stem cells for regenerative medicine.* Nat. Cell Biol., 2011. **13**(5): p. 497-505.

52. Lin, B., et al., *High-purity enrichment of functional cardiovascular cells from human iPS cells.* Cardiovasc. Res., 2012. **95**(3): p. 327-335.

53. Lan, F., et al., *Safe Genetic Modification of Cardiac Stem Cells Using a Site-Specific Integration Technique.* Circulation, 2012. **126**(11, Suppl. 1): p. S20-S28.

54. Mordwinkin, N.M., P.W. Burridge, and J.C. Wu, *A review of human pluripotent stem cell-derived cardiomyocytes for high-throughput drug discovery, cardiotoxicity screening, and publication standards.* J Cardiovasc Transl Res, 2013. **6**(1): p. 22-30.

55. Lambert, J.M., E.F. Lopez, and M.L. Lindsey, *Macrophage roles following myocardial infarction.* Int J Cardiol, 2008. **130**(2): p. 147-58.

56. Chen, W. and N.G. Frangogiannis, *Fibroblasts in post-infarction inflammation and cardiac repair.* Biochim. Biophys. Acta, Mol. Cell Res., 2013. **1833**(4): p. 945-953.

57. McGuigan, A.P. and M.V. Sefton, *The thrombogenicity of human umbilical vein endothelial cell seeded collagen modules.* Biomaterials, 2008. **29**(16): p. 2453-2463.

58. Bajpai, V.K. and S.T. Andreadis, *Stem Cell Sources for Vascular Tissue Engineering and Regeneration.* Tissue Eng Part B, 2012. **18**(5): p. 405-425.

59. Vunjak-Novakovic, G., et al., *Challenges in cardiac tissue engineering.* Tissue Eng Part B, 2010. **16**(2): p. 169-87.

60. Jing, D., et al., *Stem cells for heart cell therapies.* Tissue Eng Part B, 2008. **14**(4): p. 393-406.

61. Robinton, D.A. and G.Q. Daley, *The promise of induced pluripotent stem cells in research and therapy.* Nature (London, U. K.), 2012. **481**(7381): p. 295-305.

62. Liu, Y., et al., *Generation of functional organs from stem cells.* Cell Regener., 2013. **2**: p. 1.

63. Le, X., et al., *Engineering a biocompatible scaffold with either micrometre or nanometre scale surface topography for promoting protein adsorption and cellular response.* Int. J. Biomater., 2013: p. 782549, 16 pp.

64. Higuchi, S., et al., *Heart extracellular matrix supports cardiomyocyte differentiation of mouse embryonic stem cells.* J. Biosci. Bioeng., 2013. **115**(3): p. 320-325.

65. Tosun, Z. and P.S. McFetridge, *Improved recellularization of ex vivo vascular scaffolds using directed transport gradients to modulate ECM remodeling.* Biotechnol. Bioeng., 2013: p. Ahead of Print.

66. Daly, A.B., et al., *Initial Binding and Recellularization of Decellularized Mouse Lung Scaffolds with Bone Marrow-Derived Mesenchymal Stromal Cells.* Tissue Eng Part A, 2012. **18**(1 and 2): p. 1-16.

67. Gherghiceanu, M. and L.M. Popescu, *Heterocellular communication in the heart: electron tomography of telocyte-myocyte junctions.* J. Cell. Mol. Med., 2011. **15**(4): p. 1005-1011.

68. Popescu, L.M. and M.-S. Faussone-Pellegrini, *TELOCYTES - a case of serendipity: the winding way from Interstitial Cells of Cajal (ICC), via Interstitial Cajal-Like Cells (ICLC) to TELOCYTES.* J Cell Mol Med, 2010. **14**(4): p. 729-40.

69. Perets, A., et al., *Enhancing the vascularization of three-dimensional porous alginate scaffolds by incorporating controlled release basic fibroblast growth factor microspheres.* J. Biomed. Mater. Res., Part A, 2003. **65A**(4): p. 489-497.

70. Dobaczewski, M., W. Chen, and N.G. Frangogiannis, *Transforming growth factor (TGF)-β signaling in cardiac remodeling.* J. Mol. Cell. Cardiol., 2011. **51**(4): p. 600-606.

71. Bujak, M. and N.G. Frangogiannis, *The role of TGF-β signaling in myocardial infarction and cardiac remodeling.* Cardiovasc. Res., 2007. **74**(2): p. 184-195.

72. Zisch, A.H., et al., *Cell-demanded release of VEGF from synthetic, biointeractive cell-ingrowth matrices for vascularized tissue growth.* FASEB J., 2003. **17**(15): p. 2260-2262, 10.1096/fj.02-1041fje.

73. Kitajima, T., H. Terai, and Y. Ito, *A fusion protein of hepatocyte growth factor for immobilization to collagen.* Biomaterials, 2007. **28**(11): p. 1989-1997.

74. Andrae, J., R. Gallini, and C. Betsholtz, *Role of platelet-derived growth factors in physiology and medicine.* Genes Dev., 2008. **22**(10): p. 1276-1312.

75. Lin, H., et al., *The effect of collagen-targeting platelet-derived growth factor on cellularization and vascularization of collagen scaffolds.* Biomaterials, 2006. **27**(33): p. 5708-5714.

76. Van Wijk, B., A.F.M. Moorman, and M.J.B. Van den Hoff, *Role of bone morphogenetic proteins in cardiac differentiation.* Cardiovasc. Res., 2007. **74**(2): p. 244-255.

77. Fiedler, U. and H.G. Augustin, *Angiopoietins: a link between angiogenesis and inflammation.* Trends Immunol., 2006. **27**(12): p. 552-558.

78. D'Amore, P.A. and S.R. Smith, *Growth factor effects on cells of the vascular wall: a survey.* Growth Factors, 1993. **8**(1): p. 61-75.

79. Lee, K.Y., et al., *Controlled growth factor release from synthetic extracellular matrices.* Nature (London), 2000. **408**(6815): p. 998-1000.

80. Freeman, I., A. Kedem, and S. Cohen, *The effect of sulfation of alginate hydrogels on the specific binding and controlled release of heparin-binding proteins.* Biomaterials, 2008. **29**(22): p. 3260-3268.

81. Harel-Adar, T., et al., *Modulation of cardiac macrophages by phosphatidylserine-presenting liposomes improves infarct repair.* Proc. Natl. Acad. Sci. U. S. A., 2011. **108**(5): p. 1827-1832, S1827/1-S1827/4.

82. Ratcliffe, A. and L.E. Niklason, *Bioreactors and bioprocessing for tissue engineering.* Ann. N. Y. Acad. Sci., 2002. **961**(Reparative Medicine): p. 210-215.

83. Foster, E., *Echocardiographic evaluation of the atria and appendages*, in *UpToDate*. 2014: accessed online at www.uptodate.com ©.

84. Al-Saady, N.M., O.A. Obel, and A.J. Camm, *Left atrial appendage: structure, function, and role in thromboembolism.* Heart, 1999. **82**(5): p. 547-54.

85. Bursac, N., et al., *Cultivation in rotating bioreactors promotes maintenance of cardiac myocyte electrophysiology and molecular properties.* Tissue Eng., 2003. **9**(6): p. 1243-1253.

86. Matthew G. Geeslin, G.J.C., Stefan M. Kren, Ephraim M. Sparrow, David A. Hultman, Doris A. Taylor *Bioreactor for the reconstitution of a decellularized vascular matrix of biological origin.* Journal of Biomedical Science and Engineering, 2011. **Vol.4** (No.6): p. 8.

87. Avci-Adali, M., et al., *Application of a rotating bioreactor consisting of low-cost and ready-to-use medical disposables for in vitro evaluation of the endothelialization efficiency of small-caliber vascular prostheses.* J Biomed Mater Res B Appl Biomater, 2013. **101**(6): p. 1061-8.

88. Jungebluth, P., et al., *Verification of cell viability in bioengineered tissues and organs before clinical transplantation.* Biomaterials, 2013. **34**(16): p. 4057-4067.

89. Kasimir, M.-T., et al., *The decellularized porcine heart valve matrix in tissue engineering: Platelet adhesion and activation.* Thromb. Haemostasis, 2005. **94**(3): p. 562-567.

90. Kasimir, M.-T., et al., *Decellularization does not eliminate thrombogenicity and inflammatory stimulation in tissue-engineered porcine heart valves.* J Heart Valve Dis, 2006. **15**(2): p. 278-86; discussion 286.

91. Lichtenberg, A., et al., *Preclinical testing of tissue-engineered heart valves re-endothelialized under simulated physiological conditions.* Circulation, 2006. **114**(1 Suppl): p. I559-65.

92. Ye, X., et al., *Polyelectrolyte multilayer film on decellularized porcine aortic valve can reduce the adhesion of blood cells without affecting the growth of human circulating progenitor cells.* Acta Biomater., 2012. **8**(3): p. 1057-1067.

93. Bellis, S.L., *Advantages of RGD peptides for directing cell association with biomaterials.* Biomaterials, 2011. **32**(18): p. 4205-4210.

94. McLane, L.T., et al., *Spatial Organization and Mechanical Properties of the Pericellular Matrix on Chondrocytes.* Biophys. J., 2013. **104**(5): p. 986-996.

95. Kader, K.N., et al., *eNOS-overexpressing endothelial cells inhibit platelet aggregation and smooth muscle cell proliferation in vitro.* Tissue Eng., 2000. **6**(3): p. 241-251.

96. Deutsch, M., et al., *In vitro endothelialization of expanded polytetrafluoroethylene grafts: a clinical case report after 41 months of implantation.* J Vasc Surg, 1997. **25**(4): p. 757-63.

97. Assmann, A., et al., *Acceleration of autologous in vivo recellularization of decellularized aortic conduits by fibronectin surface coating.* Biomaterials, 2013. **34**(25): p. 6015-6026.

98. Wissink, M.J.B., et al., *Endothelial Cell Seeding on Crosslinked Collagen: Effects of Crosslinking on Endothelial Cell Proliferation and Functional Parameters.* Thrombosis and Haemostasis, 2000. **84**(8): p. 325-331.

99. Begovac, P.C., et al., *Improvements in GORE-TEX vascular graft performance by Carmeda BioActive surface heparin immobilization.* Eur J Vasc Endovasc Surg, 2003. **25**(5): p. 432-7.

100. Lord, M.S., et al., *The modulation of platelet and endothelial cell adhesion to vascular graft materials by perlecan.* Biomaterials, 2009. **30**(28): p. 4898-4906.

101. Waterhouse, A., et al., *Elastin as a Nonthrombogenic Biomaterial.* Tissue Eng Part B, 2011. **17**(2): p. 93-99.

102. Desai, N.P. and J.A. Hubbell, *Surface modifications of polymeric biomaterials for reduced thrombogenicity.* Polym. Mater. Sci. Eng., 1990. **62**: p. 731-5.

103. Smith, R.S., et al., *Vascular catheters with a nonleaching poly-sulfobetaine surface modification reduce thrombus formation and microbial attachment.* Sci. Transl. Med., 2012. **4**(153): p. 132, 11 pp.

104. Barrera, D.A., et al., *Synthesis and RGD peptide modification of a new biodegradable copolymer: poly(lactic acid-co-lysine).* J. Am. Chem. Soc., 1993. **115**(23): p. 11010-11.

105. Brandley, B.K. and R.L. Schnaar, *Covalent attachment of an Arg-Gly-Asp sequence peptide to derivatizable polyacrylamide surfaces: support of fibroblast adhesion and long-term growth.* Anal. Biochem., 1988. **172**(1): p. 270-8.

106. Cook, A.D., et al., *Characterization and development of RGD-peptide-modified poly(lactic acid-co-lysine) as an interactive, resorbable biomaterial.* J Biomed Mater Res, 1997. **35**(4): p. 513-23.

107. Lin, H.B., et al., *Synthesis, surface, and cell-adhesion properties of polyurethanes containing covalently grafted RGD-peptides.* J. Biomed. Mater. Res., 1994. **28**(3): p. 329-42.

108. Massia, S.P. and J.A. Hubbell, *Covalent surface immobilization of Arg-Gly-Asp- and Tyr-Ile-Gly-Ser-Arg-containing peptides to obtain well-defined cell-adhesive substrates.* Anal. Biochem., 1990. **187**(2): p. 292-301.

109. Massia, S.P. and J.A. Hubbell, *An RGD spacing of 440 nm is sufficient for integrin αvβ3-mediated fibroblast spreading and 140 nm for focal contact and stress fiber formation.* J. Cell Biol., 1991. **114**(5): p. 1089-100.

110. Seyfert, U.T., V. Biehl, and J. Schenk, *In vitro hemocompatibility testing of biomaterials according to the ISO 10993-4.* Biomol. Eng., 2002. **19**(2-6): p. 91-96.

111. Sinn, S., et al., *A novel in vitro model for preclinical testing of the hemocompatibility of intravascular stents according to ISO 10993-4.* J. Mater. Sci.: Mater. Med., 2011. **22**(6): p. 1521-1528.

112. Sukavaneshvar, S., K.A. Solen, and S.F. Mohammad, *An In-vitro Model to Study Device-induced Thrombosis and Embolism: Evaluation of the Efficacy of Tirofiban, Aspirin, and Dipyridamole.* Thrombosis and Haemostasis, 2000. **83**(2): p. 322-326.

113. Gorbet, M.B. and M.V. Sefton, *Biomaterial-associated thrombosis: roles of coagulation factors, complement, platelets and leukocytes.* Biomaterials, 2004. **25**(26): p. 5681-703.

114. Hanson, S.R. and K.S. Sakariassen, *Blood flow and antithrombotic drug effects.* American Heart Journal, 1998. **135**(5, Supplement): p. S132-S145.

115. Shankarraman, V., et al., *Standardized methods to quantify thrombogenicity of blood-contacting materials via thromboelastography.* J. Biomed. Mater. Res., Part B, 2012. **100B**(1): p. 230-238.

116. Swier, P., et al., *An in vitro test model to study the performance and thrombogenicity of cardiovascular devices.* ASAIO Trans, 1989. **35**(3): p. 683-7.

117. Paul, R., et al., *In vitro thrombogenicity testing of artificial organs.* Int J Artif Organs, 1998. **21**(9): p. 548-52.

118. Ensley, A.E., et al., *Fluid Shear Stress Alters the Hemostatic Properties of Endothelial Outgrowth Cells.* Tissue Eng Part A, 2012. **18**(1 and 2): p. 127-136.

119. Sukavaneshvar, S., *Assessment and management of vascular implant thrombogenecity.* Thrombus and Stroke, 2008: p. 57-77.

120. van Oeveren , W., *Obstacles in haemocompatibility testing.* Scientifica (Cairo), 2013. **2013**: p. 392584.

121. Ratner, B.D., *The catastrophe revisited: Blood compatibility in the 21st Century.* Biomaterials, 2007. **28**(34): p. 5144-5147.

122. Bloch, O., et al., *Immune Response in Patients Receiving a Bioprosthetic Heart Valve: Lack of Response with Decellularized Valves.* Tissue Eng Part A, 2011. **17**(19 and 20): p. 2399-2405.

123. Guyette, J.P., et al., *Perfusion decellularization of whole organs.* Nat Protoc, 2014. **9**(6): p. 1451-68.

124. Dobaczewski, M., C. Gonzalez-Quesada, and N.G. Frangogiannis, *The extracellular matrix as a modulator of the inflammatory and reparative response following myocardial infarction.* J. Mol. Cell. Cardiol., 2010. **48**(3): p. 504-511.

125. Badylak, S.F., B.N. Brown, and T.W. Gilbert, *Chapter II.6.16 - Tissue Engineering with Decellularized Tissues*, in *Biomaterials Science (Third Edition)*, D.R. Buddy, et al., Editors. 2013, Academic Press. p. 1316-1331.

126. Badylak, S.F., D.O. Freytes, and T.W. Gilbert, *Extracellular matrix as a biological scaffold material: Structure and function.* Acta Biomaterialia, 2009. **5**(1): p. 1-13.

127. Badylak, S.F.B., Bryan N; Gilbert, Thomas W; Daly, Kerry A; Huber, Alexander; Turner, Neill J, *Snapshot: Biologic Scaffolds For Constructive Tissue Remodeling.* Biomaterials, 2011. **32**(1): p. 316-319.

128. Badylak, S.F., *The extracellular matrix as a scaffold for tissue reconstruction.* Semin. Cell Dev. Biol., 2002. **13**(5): p. 377-383.

129. Schwartz, S.D., et al., *Embryonic stem cell trials for macular degeneration: a preliminary report.* Lancet, 2012. **379**(9817): p. 713-720.

130. Harley, C.B., A.B. Futcher, and C.W. Greider, *Telomeres shorten during ageing of human fibroblasts.* Nature (London), 1990. **345**(6274): p. 458-60.

131. Shimizu, T., et al., *Cell sheet engineering for myocardial tissue reconstruction.* Biomaterials, 2003. **24**(13): p. 2309-2316.

132. L'Heureux, N., et al., *A completely biological tissue-engineered human blood vessel.* FASEB J., 1998. **12**(1): p. 47-56.

133. Haykal, S., et al., *The effect of decellularization of tracheal allografts on leukocyte infiltration and of recellularization on regulatory T cell recruitment.* Biomaterials, 2013. **34**(23): p. 5821-5832.

134. Bonenfant, N.R., et al., *The effects of storage and sterilization on de-cellularized and re-cellularized whole lung.* Biomaterials, 2013. **34**(13): p. 3231-3245.

135. Bonvillain, R.W., et al., *A Nonhuman Primate Model of Lung Regeneration: Detergent-Mediated Decellularization and Initial In Vitro Recellularization with Mesenchymal Stem Cells.* Tissue Eng Part A, 2012. **18**(23-24): p. 2437-2452.

136. Calle, E.A., T.H. Petersen, and L.E. Niklason, *Procedure for Lung Engineering.* J Vis Exp, 2011(49): p. e2651.

137. Jensen, T., et al., *A Rapid Lung De-cellularization Protocol Supports Embryonic Stem Cell Differentiation In Vitro and Following Implantation.* Tissue Eng Part C, 2012. **18**(8): p. 632-646.

138. Nonaka, P.N., et al., *Effects of freezing/thawing on the mechanical properties of decellularized lungs.* J Biomed Mater Res A, 2013.

139. Ott, H.C., et al., *Regeneration and orthotopic transplantation of a bioartificial lung.* Nat. Med. (N. Y., NY, U. S.), 2010. **16**(8): p. 927-933.

140. Petersen, T.H., et al., *Tissue-Engineered Lungs for in Vivo Implantation.* Science (Washington, DC, U. S.), 2010. **329**(5991): p. 538-541.

141. Baptista, P.M., et al., *Whole organ decellularization - a tool for bioscaffold fabrication and organ bioengineering.* Conf Proc IEEE Eng Med Biol Soc, 2009. **2009**: p. 6526-9.

142. Kajbafzadeh, A.-M., et al., *Determining the Optimal Decellularization and Sterilization Protocol for Preparing a Tissue Scaffold of a Human-Sized Liver Tissue.* Tissue Eng Part C, 2013. **19**(8): p. 642-651.

143. Mirmalek-Sani, S.-H., et al., *Porcine pancreas extracellular matrix as a platform for endocrine pancreas bioengineering.* Biomaterials, 2013. **34**(22): p. 5488-5495.

144. Conklin, B.S., et al., *Development and evaluation of a novel decellularized vascular xenograft.* Med Eng Phys, 2002. **24**(3): p. 173-83.

145. Orlando, G., et al., *Discarded human kidneys as a source of ECM scaffold for kidney regeneration technologies.* Biomaterials, 2013. **34**(24): p. 5915-5925.

146. Orlando, G., et al., *A rapid decellularization technique for the recellularization of renal organ tissue.* Trans. Annu. Meet. Soc. Biomater., 2010. **32**(Annual Meeting of the Society for Biomaterials: Giving Life to a World of Materials, 2010, Volume 2): p. 527.

147. Song, J.J., et al., *Regeneration and experimental orthotopic transplantation of a bioengineered kidney.* Nat. Med. (N. Y., NY, U. S.), 2013: p. Ahead of Print.

148. Sullivan, D.C., et al., *Decellularization methods of porcine kidneys for whole organ engineering using a high-throughput system.* Biomaterials, 2012. **33**(31): p. 7756-7764.

149. Hodde, J. and M. Hiles, *Virus safety of a porcine-derived medical device: evaluation of a viral inactivation method.* Biotechnol. Bioeng., 2002. **79**(2): p. 211-216.

150. Hodde, J., et al., *Effects of sterilization on an extracellular matrix scaffold: Part I. Composition and matrix architecture.* J. Mater. Sci.: Mater. Med., 2007. **18**(4): p. 537-543.

151. Hodde, J., A. Janis, and M. Hiles, *Effects of sterilization on an extracellular matrix scaffold: Part II. Bioactivity and matrix interaction.* J. Mater. Sci.: Mater. Med., 2007. **18**(4): p. 545-550.

152. Timms, D., *A review of clinical ventricular assist devices.* Medical Engineering & Physics, 2011. **33**(9): p. 1041-1047.

153. Loforte, A., et al., *Use of Mechanical Circulatory Support Devices in End-Stage Heart Failure Patients.* Journal of cardiac surgery, 2014. **29**(5): p. 717-722.

154. Samson, R., R. Ramachandran, and T.H. Le Jemtel, *Systolic Heart Failure: Knowledge Gaps, Misconceptions, and Future Directions.* The Ochsner Journal, 2014. **14**(4): p. 569-575.

155. Coulombe, K.L.K., et al., *Heart regeneration with engineered myocardial tissue.* Annu. Rev. Biomed. Eng., 2014. **16**: p. 1-28.

156. Bajaj, P., et al., *3D Biofabrication Strategies for Tissue Engineering and Regenerative Medicine.* Annual Review of Biomedical Engineering, 2014. **16**(1).

157. Hanson, K.P., et al., *Spatial and Temporal Analysis of Extracellular Matrix Proteins in the Developing Murine Heart: A Blueprint for Regeneration.* Tissue Eng., Part A, 2013. **19**(9-10): p. 1132-1143.

158. Momtahan, N., et al., *Strategies and Processes to Decellularize and Recellularize Hearts to Generate Functional Organs and Reduce the Risk of Thrombosis.* Tissue Eng Part B Rev, 2015. **21**(1): p. 115-132.

159. Araki, R., et al., *Negligible immunogenicity of terminally differentiated cells derived from induced pluripotent or embryonic stem cells.* Nature, 2013.

160. Zhang, C., S.V. Murphy, and A. Atala, *Regenerative medicine in urology.* Seminars in Pediatric Surgery, 2014. **23**(3): p. 106-111.

161. Faulk, D.M., et al., *The effect of detergents on the basement membrane complex of a biologic scaffold material.* Acta Biomaterialia, 2014. **10**(1): p. 183-193.

162. Price, A.P., et al., *Automated Decellularization of Intact, Human-Sized Lungs for Tissue Engineering.* Tissue Eng Part C Methods, 2014.

163. Zhang, Z., et al., *Polybetaine modification of PDMS microfluidic devices to resist thrombus formation in whole blood.* Lab on a Chip, 2013. **13**(10): p. 1963-1968.

164. Badylak, S.F., et al., *Macrophage Phenotype as a Determinant of Biologic Scaffold Remodeling.* Tissue Eng., Part A, 2008. **14**(11): p. 1835-1842.

165. Brown, B.N., et al., *Macrophage phenotype and remodeling outcomes in response to biologic scaffolds with and without a cellular component.* Biomaterials, 2009. **30**(8): p. 1482-1491.

166. Sukavaneshvar, S., K.A. Solen, and S.F. Mohammad, *Device induced thromboembolism in a bovine in vitro coronary stent model.* ASAIO journal, 1998. **44**(5): p. M393-M396.

167. Mirmalek-Sani, S.-H., et al., *Immunogenicity of Decellularized Porcine Liver for Bioengineered Hepatic Tissue.* The American Journal of Pathology, 2013. **183**(2): p. 558-565.

168. Badylak, S.F., *Xenogeneic extracellular matrix as a scaffold for tissue reconstruction.* Transplant Immunol., 2004. **12**(3-4): p. 367-377.

169. Naugle, J.E., et al., *Type VI collagen induces cardiac myofibroblast differentiation: implications for postinfarction remodeling.* American Journal of Physiology-Heart and Circulatory Physiology, 2006. **290**(1): p. H323-H330.

170. Schenke-Layland, K., et al., *Impact of decellularization of xenogeneic tissue on extracellular matrix integrity for tissue engineering of heart valves.* Journal of structural biology, 2003. **143**(3): p. 201-208.

171. Lutolf, M.P., P.M. Gilbert, and H.M. Blau, *Designing materials to direct stem-cell fate.* Nature, 2009. **462**(7272): p. 433-441.

172. Kilian, K.A., et al., *Geometric cues for directing the differentiation of mesenchymal stem cells.* Proceedings of the National Academy of Sciences, 2010. **107**(11): p. 4872-4877.

173. Pek, Y.S., A.C. Wan, and J.Y. Ying, *The effect of matrix stiffness on mesenchymal stem cell differentiation in a 3D thixotropic gel.* Biomaterials, 2010. **31**(3): p. 385-391.

174. Taylor, D., L. Sampaio, and A. Gobin, *Building New Hearts: A Review of Trends in Cardiac Tissue Engineering.* American Journal of Transplantation, 2014. **14**(11): p. 2448-2459.

175. Wang, B., et al., *Fabrication of cardiac patch with decellularized porcine myocardial scaffold and bone marrow mononuclear cells.* Journal of Biomedical Materials Research Part A, 2010. **94**(4): p. 1100-1110.

176. Bronshtein, T., et al., *A Mathematical Model for Analyzing the Elasticity, Viscosity, and Failure of Soft Tissue: Comparison of Native and Decellularized Porcine Cardiac Extracellular Matrix for Tissue Engineering.* Tissue Eng., Part C, 2013. **19**(8): p. 620-630.

177. Sarig, U., et al., *Thick Acellular Heart Extracellular Matrix with Inherent Vasculature: A Potential Platform for Myocardial Tissue Regeneration.* Tissue Eng., Part A, 2012. **18**(19-20): p. 2125-2137.

178. Aubin, H., et al., *Decellularized whole heart for bioartificial heart.* Methods Mol Biol, 2013. **1036**: p. 163-78.

179. Cebotari, S., et al., *Detergent decellularization of heart valves for tissue engineering: toxicological effects of residual detergents on human endothelial cells.* Artificial organs, 2010. **34**(3): p. 206-210.

180. Krzyzaniak, J.F., D.M. Raymond, and S.H. Yalkowsky, *Lysis of human red blood cells 1: effect of contact time on water induced hemolysis.* PDA Journal of Pharmaceutical Science and Technology, 1996. **50**(4): p. 223-226.

181. Krzyzaniak, J.F., et al., *Lysis of human red blood cells. 4. Comparison of in vitro and in vivo hemolysis data.* Journal of pharmaceutical sciences, 1997. **86**(11): p. 1215-1217.

182. Ricard-Blum, S., *The collagen family.* Cold Spring Harbor perspectives in biology, 2011. **3**(1): p. a004978.

183. Parpart, A.K., et al., *The osmotic resistance (fragility) of human red cells.* Journal of Clinical Investigation, 1947. **26**(4): p. 636.

184. Zhao, W., W.-T.T. Ho, and Z.J. Zhao, *Quantitative analyses of myelofibrosis by determining hydroxyproline.* Stem Cell Investigation, 2015. **2**(1).

185. Boyde, A. and C. Wood, *Preparation of animal tissues for surface-scanning electron microscopy.* Journal of Microscopy, 1969. **90**(3): p. 221-249.

186. Worthen, D. and M. Wickham, *Scanning electron microscopy tissue preparation.* Investigative ophthalmology, 1972. **11**(3): p. 133.

187. Jurado, E., et al., *Simplified spectrophotometric method using methylene blue for determining anionic surfactants: Applications to the study of primary biodegradation in aerobic screening tests.* Chemosphere, 2006. **65**(2): p. 278-285.

188. Rusconi, F., et al., *Quantification of sodium dodecyl sulfate in microliter-volume biochemical samples by visible light spectroscopy.* Analytical biochemistry, 2001. **295**(1): p. 31-37.

189. Krzyzaniak, J.F. and S.H. Yalkowsky, *Lysis of human red blood cells 3: effect of contact time on surfactant-induced hemolysis.* PDA Journal of Pharmaceutical Science and Technology, 1998. **52**(2): p. 66-69.

190. Uygun, B.E., et al., *Organ reengineering through development of a transplantable recellularized liver graft using decellularized liver matrix.* Nat. Med. (N. Y., NY, U. S.), 2010. **16**(7): p. 814-820.

191. Weber, B., et al., *Off-the-shelf human decellularized tissue-engineered heart valves in a non-human primate model.* Biomaterials, 2013. **34**(30): p. 269-280.

192. Ott, H.C., et al., *Perfusion-decellularized matrix: using nature's platform to engineer a bioartificial heart.* Nature Medicine, 2008. **14**(2): p. 213-221.

193. Wainwright, J.M., et al., *Preparation of Cardiac Extracellular Matrix from an Intact Porcine Heart.* Tissue Engineering Part C-Methods, 2010. **16**(3): p. 525-532.

194. Momtahan, N., et al., *Automation of Pressure Control Improves Whole Porcine Heart Decellularization.* Tissue Engineering Part C: Methods, 2015. **21**(11): p. 1148-1161.

195. Lu, T.-Y., et al., *Repopulation of decellularized mouse heart with human induced pluripotent stem cell-derived cardiovascular progenitor cells.* Nature communications, 2013. **4**.

196. Andersen, K.K., et al., *The Role of Decorated SDS Micelles in Sub-CMC Protein Denaturation and Association.* Journal of Molecular Biology, 2009. **391**(1): p. 207-226.

197. Michaux, C., et al., *Protecting role of cosolvents in protein denaturation by SDS: a structural study.* BMC structural biology, 2008. **8**(1): p. 29.

198. de la Maza, A. and J.L. Parra, *Vesicle-micelle structural transitions of phospholipid bilayers and sodium dodecyl sulfate.* Langmuir, 1995. **11**(7): p. 2435-2441.

199. Gratzer, P.F., R.D. Harrison, and T. Woods, *Matrix alteration and not residual sodium dodecyl sulfate cytotoxicity affects the cellular repopulation of a decellularized matrix.* Tissue engineering, 2006. **12**(10): p. 2975-2983.

200. Campbell, R., M.A. Winkler, and H. Wu, *Quantification of sodium dodecyl sulfate in microliter biochemical samples by gas chromatography.* Analytical biochemistry, 2004. **335**(1): p. 98-102.

201. Song, J.J.G., Jacques P; Gilpin, Sarah E; Gonzalez, Gabriel; Vacanti, Joseph P; Ott, Harald C, *Regeneration and experimental orthotopic transplantation of bioengineered kidney.* Nature Medicine, 2013. **19**(5): p. 9.

202. Faulk, D., et al., *The effect of detergents on the basement membrane complex of a biologic scaffold material.* Acta biomaterialia, 2014. **10**(1): p. 183-193.

203. Langer, R. and J.P. Vacanti, *Tissue engineering.* Science (Washington, D. C., 1883-), 1993. **260**(5110): p. 920-6.

204. Takahashi, K., et al., *Induction of Pluripotent Stem Cells from Adult Human Fibroblasts by Defined Factors.* Cell, 2007. **131**(5): p. 861-872.

205. Lee, K., et al. *Natural Cardiac Extracellular Matrix Sheet as a Biomaterial for Cardiomyocyte Transplantation*. in *Transplantation proceedings*. 2015. Elsevier.

206. Sirabella, D., E. Cimetta, and G. Vunjak-Novakovic, *"The state of the heart": Recent advances in engineering human cardiac tissue from pluripotent stem cells.* Experimental Biology and Medicine, 2015: p. 1535370215589910.

207. Parsa, H., K. Ronaldson, and G. Vunjak-Novakovic, *Bioengineering methods for myocardial regeneration.* Advanced drug delivery reviews, 2015.

208. Cimetta, E., A. Godier-Furnémont, and G. Vunjak-Novakovic, *Bioengineering heart tissue for in vitro testing.* Current opinion in biotechnology, 2013. **24**(5): p. 926-932.

209. Riedel, M., et al., *Functional and Pharmacological Analysis of Cardiomyocytes Differentiated from Human Peripheral Blood Mononuclear-Derived Pluripotent Stem Cells.* Stem Cell Rep., 2014. **3**(1): p. 131-141.

210. Weymann, A., et al., *Development and evaluation of a perfusion decellularization porcine heart model--generation of 3-dimensional myocardial neoscaffolds.* Circ J, 2011. **75**(4): p. 852-60.

211. Chen, G., T. Ushida, and T. Tateishi, *Scaffold design for tissue engineering.* Macromolecular Bioscience, 2002. **2**(2): p. 67-77.

212. Thomson, J.A., et al., *Embryonic stem cell lines derived from human blastocysts.* science, 1998. **282**(5391): p. 1145-1147.

213. Martins, A.M., G. Vunjak-Novakovic, and R.L. Reis, *The Current Status of iPS Cells in Cardiac Research and Their Potential for Tissue Engineering and Regenerative Medicine.* Stem Cell Reviews and Reports, 2014. **10**(2): p. 177-190.

214. Fuerstenau-Sharp, M., et al., *Generation of Highly Purified Human Cardiomyocytes from Peripheral Blood Mononuclear Cell-Derived Induced Pluripotent Stem Cells.* 2015.

215. Taylor, D. and H. Ott, *Decellularization and Recellularization of Organs and Tissues*, M. Regents Of The University Of, D. Taylor, and H. Ott, Editors. 2010.

216. Rowland, T.J., et al., *Roles of integrins in human induced pluripotent stem cell growth on Matrigel and vitronectin.* Stem cells and development, 2009. **19**(8): p. 1231-1240.